UNIVERSITÀ DEGLI STUDI DI PADOVA

Dipartimento di Fisica e Astronomia "Galileo Galilei"

Master Degree in Physics

Final Dissertation

Role of dynamic metabolic strategies in species coexistence patterns

Thesis supervisor
Prof. Amos Maritan

Candidate
Sofia Moschin

Thesis co-supervisor
Prof. Samir Simon Suweis

Academic Year 2022/2023

ABSTRACT

The local coexistence of species in large ecosystems has traditionally been explained within the framework of niche theory. However, this theory struggles to justify the observed rich biodiversity in nearly homogeneous environments. Surprisingly, there is evidence suggesting that the presence of species-specific pathogens can significantly increase biodiversity compared to their absence.

The first objective of this thesis is to introduce the well-known consumer-resource model proposed by MacArthur which incorporates the dynamics of species and resources, highlighting their competitive and metabolic interactions. The thesis presents the innovative Adaptive Interactive Model in which the metabolic strategies of species will not be treated as adjustable parameters, but will be promoted to dynamic variables with their own dynamics. The dynamics will be designed so that the fitness of the species evolves to increase as much as possible under physiological constraints. Moreover, the time evolution of the populations will also include a coarse-grained term that represents the interactions among species, allowing for relaxation of energy limitations. This deterministic model not only predicts the violation of the well-known Competition Exclusion Principle but also manages to relax certain unnatural fine-tuned constraints that characterise previous models.

Furthermore, stochasticity is incorporated into the dynamics of metabolic strategies to explore the effects of annealed noises on species survival. This new stochastic model is able to predict coexistence as a consequence of the interplay between the variability of the metabolic strategies and the characteristic time of the annealed noise.

These original deterministic and stochastic models, presented to address the "Paradox of the Plankton", are analyzed using various numerical and analytical methods, focusing on the role of metabolic strategies in promoting species coexistence.

ACKNOWLEDGEMENTS

I would like to sincerely thank Prof. Maritan and Prof. Suweis for their constant guidance and invaluable mentorship throughout this thesis work.

I thank the team of the Laboratory of Interdisciplinary Physics for their daily advice in entering this field.

I am grateful to my friends, who have been by my side every single step of the way, always rooting for me.

Thank you, my three musketeers, for being with me since the very beginning. Your presence and support meant the world.

Contents

List of Tables

List of Figures

PREFACE

An ecological community consists of sympatric species' populations, i.e. living in the same area at the same time and interacting with one another. It is influenced by both the environment and the relationships between species. For the purpose of this thesis, which specifically examines the temporal evolution of populations' dynamics, we adopt the following definition of population as proposed by Turchin:

> I define a population as a group of individuals of the same species that live together in a defined area of sufficient size to permit normal dispersal and migration behaviors. Thus, temporal changes in population abundance are primarily determined by birth and death processes, and emigration/immigration processes can be neglected without a serious loss of predictability. [1]

Community ecology is a subfield of ecology that investigates factors affecting species' population distribution and abundance, community structure and ultimately biodiversity. This domain focuses on species interactions, such as competition, predation, herbivory, parasitism, and mutualism. Important questions include understanding feeding relationships, identifying competitive interactions and resource competition, and determining if the presence of certain species benefits others.

> In any study of evolutionary ecology, food relations appear as one of the most important aspects of the system of animate nature. There is quite obviously much more to living communities than the raw dictum "eat or be eaten", but in order to understand the higher intricacies of any ecological system, it is most easy to start from this crudely simple point of view. [2]

In the context of ecological studies, G. E. Hutchinson posed a fundamental question in his work "Homage to Santa Rosalia": Why does the natural world exhibit such a remarkable abundance of plant and animal species? Hutchinson put forth the notion that trophic interactions, i.e. feeding relationships among organisms in an ecosystem, play a primary role in shaping diversity patterns. The fundamental premise of this argumentation is that a significant portion of community structure can be comprehended by understanding the food web among populations belonging to different species. Originally termed "food relations" by Hutchinson, these processes are now commonly referred to as "consumer-resource interactions" and "resource competition." [26] This thesis investigates the influence of consumer-resource interactions on species composition and diversity within communities. These interactions, which encompass both species-to-species interactions and interactions between species and their environment, are assumed to play a significant role in shaping major patterns observed in ecological systems. To examine the long-term effects of the consumer-resource process, an equilibrium approach is employed. The choice to adopt an equilibrium framework is rooted in its inherent simplicity compared to assuming that every observation can only be explained by non-equilibrium processes. All the models examined in this thesis concentrate on the idealized scenario of infinite temporal coexistence, thereby

[1] P. TURCHIN, *Complex Population Dynamics: A Theoretical/Empirical Synthesis*, Series: MPB-35 (Monographs in Population Biology), Princeton University Pres, (2003), pp. 402.

[2] G. E. HUTCHINSON, *Homage to Santa Rosalia or Why Are There So Many Kinds of Animals?*, The American Naturalist, Vol. 93, No. 870 (1959), pp. 145-159.

avoiding the incorporation of multiple finite temporal scales that would arise when considering the inevitable perturbations on the communities, which could undermine their coexistence. According to Hardin's principle of competitive exclusion, proposed in 1960 [21], when there is a single nutrient present, it is predicted that one species alone would outcompete all the others so that in a final equilibrium situation the assemblage would reduce to a population of a single species. From a broader standpoint, a straightforward mathematical demonstration supports the conclusion that in an ecosystem with p resources, the number of distinct species capable of persisting in the stationary state cannot exceed p.

The mathematical procedure used to demonstrate the principle is indeed robust. However, paradoxically, it appears to be violated in several natural situations.

One prominent example that challenges the principle is the Paradox of the Plankton, initially introduced by Hutchinson [27]. This paradox revolves around the coexistence of a considerable number of phytoplankton species in a relatively uniform and unstructured environment, where they compete for a limited set of resources. Despite the competitive pressures, these species manage to persist and maintain biodiversity, defying the predictions set by the Competitive Exclusion Principle.

Numerous ecological theoretical models have been put forward to elucidate the remarkable biodiversity observed in real ecosystems and its impact on stability. However, the contrasting perspectives on species coexistence presented by the Competition Exclusion Principle and the Paradox of the Plankton continue to be the central focus of research in the field of Statistical Physics of Complex Systems applied to ecology.

This thesis focuses on understanding how competition influences and propel biodiversity through the role of the metabolic strategies, meaning the diverse approaches and adaptations that organisms employ to acquire, store and utilize resources in their environment for growth, reproduction, and survival.

This work introduces two original models: a deterministic model and a stochastic model. Both models prove the role of dynamic metabolic strategies on promoting species coexistence patterns.

After conducting a comprehensive review of the Consumer-Resource Model, the first chapter presents its expanded version, renamed as the Static Model [48], which incorporates fine-tuned metabolic strategies and it's able to violate the Competition Exclusion Principle under certain limiting conditions.

The second chapter of this thesis focuses on the Adaptive Model [46], while the third chapter explores the Interactive Model [20]. These two models are of significant interest as they introduce two important concepts, dynamic metabolic adaptation and inter-species interaction, that can predict the survival of all initial species. The main findings of these models are replicated. Several original results are presented, particularly in the case of the Adaptive Model (Figures 2.5, 2.7,2.8, 2.10 and Appendix A) where metabolic strategies are elevated from static parameters to dynamic variables. The fundamental role of the speed of degradation of the resources in the evolution of metabolic strategies is unveiled.

In the fourth chapter, the thesis introduces the original Adaptive Interactive Model, which represents a new formulation capable of violating the Competition Exclusion Principle. This model offers increased flexibility and reduces the necessity for precise fine-tuning of energy budgets, which was a requirement in earlier models. As a result, it provides a more realistic description of the natural ecological dynamics.

The Stochastic Model as an extension to the deterministic model is the new theoretical framework which is presented in the fifth chapter of this thesis. This innovative model incorporates the influence of colored noise in the evolution of metabolic strategies, demonstrating the role of stochasticity in promoting biodiversity.

It is important to note that all the results presented in the last two chapters are original contributions.

THE STATIC MODEL

In this chapter, we will begin by introducing the Chemostat Model, which offers valuable insights into the dynamics of a controlled environment where the growth of microorganisms is limited by a single nutrient.

Subsequently, we will delve into the MacArthur's Model, which enables us to track the temporal evolution of multiple competing species as they contend for multiple resources [38]. At stationarity the equations for the concentrations of the nutrients form a system of m equations in p variables, which is solvable only for $m \leq p$. According to the mathematical formulation of the Competition Exclusion Principle, in a system with m species and p resources, where $m > p$, $m - p$ species are predicted to go extinct [21]. Consequently, the MacArthur's Model is not able to justify the rich biodiversity observed in nearly homogeneous environments.

To address this limitation, we present the model proposed by Posfai, Taillefumier, and Wingreen [48], to which we will refer on Static Model. This model allows for the coexistence of numerous species, even when competing for limited resources, under carefully calibrated conditions. This model serves as a fundamental foundation for explaining for understanding why the Competition Exclusion Principle appears to be violated in certain plankton species. In this thesis, we build upon the Static Model as it highlights the significant role of metabolic strategies and the inherent trade-offs they entail in elucidating the observed biodiversity.

1.1 The Chemostat Model

Competition modeling is a challenging aspect of mathematical biology due to the various ways populations can compete, making it difficult to develop general models. In a ecosystem represented formally by ordinary differential equations, competition is typically represented by the condition that the growth rate of one population diminishes or remains unchanged when another population increases. For a system described by

$$\dot{y}_i = y_i f_i(y) \tag{1.1}$$

where $i = 1, 2, ...n$, f_i is the growth rate, a continuously differentiable function defined on R^n, and $y = (y_1, .., y_n)$, this competitive condition $i \neq j$ is expressed by

$$\frac{\partial f_i}{\partial y_j} \leq 0 \tag{1.2}$$

Exploitative competition, the simplest form of competition, occurs when multiple populations compete for the same resource, such as a common food supply. The chemostat is a laboratory device that offers a convenient and well-defined mathematical model for investigating this form of competition, while also creating effective comparisons with experimental data. It consists of three connected vessels: the feed bottle, the culture vessel where growth occurs, and the overflow or collection vessel. The feed bottle holds an abundant supply of all the essential nutrients required by microorganisms. However, there is a deliberate scarcity of one particular "limiting" nutrient, whose concentration is the only one that is going to affect the dynamics of the system. Nutrients from the feed bottle are continuously pumped into the culture vessel of volume V, where microorganisms grow and interact. The culture

vessel's contents, including the limiting nutrient, organisms, and possibly their byproducts, are then pumped into the collection vessel.

The chemostat model provides a simplified representation, through differential equations, of an ecosystem, where a single nutrient is the primary factor limiting the growth and survival of microorganisms [53]. For the sake of semplicity, the focus is on a single organism growing in the chemostat. The rate of change of the limiting nutrient concentration $S(t)$ at time t can be described using differential equations. The concentration of the input limiting nutrient is kept fixed at $S^{(0)}$. The rate of change of the nutrient in the culture vessel is described by

$$\text{rate of change= input - washout - consumption} \tag{1.3}$$

where the washout process simulates the emigration that naturally occurs within ecosystems and the consumption represents the depletion of resources as they are utilized by organisms. For organisms the rate of change is going to be indeed:

$$\text{rate of change = growth - washout} \tag{1.4}$$

By defining F as the volumetric flow rate for both inflow and outflow, we can describe the change over time in the amount of nutrients $VS(t)$. The equation can be written as:

$$\frac{d}{dt}(VS) = S^{(0)}F - S(t)F - \text{consumption} \tag{1.5}$$

Here, $S^{(0)}F$ and $S(t)F$ represent the contributions from nutrient input and output, respectively.

V is a constant quantity, both sides of the Equation can be divided by V. Denoting $D = F/V$ as the washout rate, we obtain

$$\frac{d}{dt}(S) = S^{(0)}D - S(t)D - \text{consumption} \tag{1.6}$$

The consumption term takes the following form:

$$\text{consumption} = \frac{mS(t)\ x(t)}{a + S(t)} \tag{1.7}$$

In this equation, $x(t)$ represents the concentration of the organism, m denotes the maximal growth rate, and a is the half-saturation constant, expressed in concentration units. Although a simple monotonic relationship in S is mathematically sufficient, this formulation, which includes the experimentally measurable parameters m and a is commonly used for the uptake function.

The relationship between the growth of a species and the utilization of nutrients is proved to be further constrained by the yield constant, denoted as γ:

$$\frac{dx}{dt} = -\gamma \frac{dS}{dt}_{|cons} \tag{1.8}$$

being $\frac{dx}{dt}$ the growth rate of the species and $\frac{dS}{dt}_{|cons}$ the consumption of the resource. In batch culture the dimensionless γ can be determined by

$$\gamma = \frac{\text{mass of the organism formed}}{\text{mass of the substrate used}} \tag{1.9}$$

Evidently the assumption that the reproduction is proportional to nutrient uptake is a vast simplification. The yield constant we defined indicates the efficiency of the conversion of the nutrient into population. Therefore, under these assumptions, the consumption term acquires the form

$$\text{consumption} = -\frac{x(t)}{\gamma}\frac{mS(t)}{a + S(t)} \tag{1.10}$$

Assuming that growth is proportional to consumption, we obtain the equation for the evolution of x over time:

$$\frac{dx}{dt} = x(t)\left(\frac{mS(t)}{a+S(t)} - D\right) \tag{1.11}$$

The evolution in time of $S(t)$ is determined by:

$$\frac{dS}{dt} = D(S^{(0)} - S(t)) - \frac{x(t)}{\gamma}\frac{mS(t)}{a+S(t)} \tag{1.12}$$

Proceeding with the following re-scaling:

$$t \to tD \quad S \to \frac{S}{S^{(0)}} \quad a \to \frac{a}{S^{(0)}} \quad x \to \frac{x}{S^{(0)}} \tag{1.13}$$

Equations 1.11 and 1.12 take an adimensional expression

$$\frac{dx}{dt} = x\left(\frac{m}{a+S} - 1\right) \tag{1.14}$$

$$\frac{dS}{dt} = (1-S) - \frac{x}{\gamma}\frac{mS}{a+S} \tag{1.15}$$

The chemostat model is primarily designed to investigate the dynamics of a single nutrient in a controlled laboratory setting. However, in order to explore more complex ecological interactions and resource constraints, we turn to the MacArthur's consumer-resource model. This model extends the understanding of population dynamics by considering the dynamic interplay between consumers and their shared resources. In the following sections, we will delve into the mathematical formulation and key concepts of the MacArthur's consumer-resource model to study how different species compete for limited resources and how this competition shapes their population dynamics.

1.2 The MacArthur's consumer-resource model

We consider an ecological community composed of m different species competing for p different resources [38]. Given $\sigma = 1, ..., m$ and $i = 1, ..., p$, n_σ represents the population's density of the species σ and c_i is the concentration of the resource i. Every of σ species possesses a distinct metabolic strategy $\alpha_{\sigma i}$, which represents the maximum consumption rate at which the species uptakes the resource i and converts it into its biomass.

We assume that resources are uniformly distributed in space and that they are supplied with a specific rate $\vec{s} = (s_1, ..., s_p)$, which is constant in time in this model. $S = \sum_{i=1}^{p} s_i$ represents the total nutrient supply rate.
Nutrients can be affected by some chemical processes of degradation, so $\vec{\mu} = (\mu_1, ..., \mu_p)$ embodies the fact that resources degrade in time with a rate μ_i.
The populations of the species σ decay with intrinsic mortality rate δ_σ.
The function $r_i(c_i)$ represents the per-enzyme uptake rate of the resource i. In general the dependence of a species' growth rate on a nutrient concentration saturates as c_i increases. Any monotone increasing and continuously differentiable function of the concentration of the i resource, such that $r_0(c_0)$, could work, however typically $r_i(c_i)$ takes the form of a Monod function [53]

$$r_i(c_i) = \frac{c_i}{c_i + k_i}, \tag{1.16}$$

where $k_i > 0$ is the half saturation constant, so that $r_i < 1 \ \forall \ c_i$. The Monod functions saturates quickly for small k_i: the nutrients are used at the maximum rate possible, even in a ecosystem with a small number of individuals per species. It is important to note that the half-saturation constant is

strongly influenced by the specific characteristics of the medium in which the species exist.
The parameter $v_i < 1$, often called resource value, measures the efficiency of the conversion of the resource to biomass: the more valuable the resource is the larger the growth rate of the population is going to be, keeping the uptake rate fixed.

The metabolic strategies of this ecosystem are represented by the matrix A, composed by the $\alpha_{\sigma i}$ elements,

$$A = \begin{pmatrix} \alpha_{11} & \dots & \alpha_{1p} \\ \vdots & & \vdots \\ \alpha_{m1} & \dots & \alpha_{mp} \end{pmatrix}. \tag{1.17}$$

The MacArthur's consumer-resource model focuses on the competition among species for shared resources. However, it does not take into account dynamic metabolic adaptation. In fact, one of the basic assumptions of this model is that the maximum resource uptake rates don't change in time.
The consumption rate of the nutrient i by the σ species depends only on the concentration of that given resource and not on the presence of other species or the concentration of other resources.

With these assumptions, a community of m species competing for p resources evolves according to these equations:

$$\dot{n}_\sigma = n_\sigma(t) \left(\sum_{i=1}^{p} v_i r_i(c_i(t)) \, \alpha_{\sigma i} - \delta_\sigma \right) \tag{1.18}$$

$$\dot{c}_i = s_i(t) - \sum_{\sigma=1}^{m} n_\sigma \alpha_{\sigma i} r_i(c_i(t)) - \mu_i c_i(t) \tag{1.19}$$

Considering a scenario involving a single species and a single resource, it is possible to draw parallels with the previously presented Chemostat Model. Equations 1.43 and 1.44 for $m = 1$ and $p = 1$ become

$$\dot{n} = n \left(v \, \alpha \frac{c(t)}{c(t) + k} - \delta \right) \tag{1.20}$$

$$\dot{c} = s(t) - n \, \alpha \frac{c(t)}{c(t) + k} - \mu c(t) \tag{1.21}$$

Considering a constant supply rate $s(t) = s$, it is possible to prove that this system of equations is equivalent to the one that composes the Chemostat Model:

$$\frac{dx}{dt} = x \left(\frac{mS}{a + S} - D \right) \tag{1.22}$$

$$\frac{dS}{dt} = D \left(S^{(0)} - S\,(t) \right) - \frac{x(t)}{\gamma} \frac{mS(t)}{a + S(t)} \tag{1.23}$$

Upon comparing the two sets of equations, we observe that γ can be identified with v. Additionally, we can establish the following correspondences:

$$x(t) \to n(t) \quad S(t) \to c(t) \quad m \to v\alpha \quad a \to k \quad D \to \delta \quad 1/\gamma \to \alpha \quad s \to DS^{(0)} \tag{1.24}$$

It is important to note that these identifications are valid assuming that μ in the MacArthur's Model is equal to δ. Consequently, xD corresponds to $n\delta$, and $DS(t)$ corresponds to $\mu c(t)$.

1.2.1 The MacArthur's consumer-resource model and the Competition Exclusion Principle

The Competition Exclusion Principle (CEP) states that the number of coexisting species competing for the same set of nutrients is bounded by the number of resources itself [21] [23]. The theoretical work done on the MacArthur's consumer resource model predicts the validity of the Competition Exclusion Principle.

It is straightforward to study the stationary solutions $\dot{n}_\sigma = 0$ of the MacArthur's model in the case in which the degradation rate vector $\vec{\mu}$ is absent. Equation 1.18 becomes

$$n_\sigma \left(\sum_{i=1}^{p} v_i r_i(c_i)\ \alpha_{\sigma i}\ - \delta_\sigma \right) = 0 \tag{1.25}$$

The first set of stationary solutions is given by $n^*_\sigma = 0\ \forall\ \sigma$, which represents the extinction of all the species. The second set ends up giving $\sum_{i=1}^{p} v_i r_i\ \alpha_{\sigma i}\ = \delta_\sigma$ which represents a system of m equations in p variables. For $m > p$ the system has no solution, so that at most p particles can survive. The Competition Exclusion Principle finds its mathematical correspondence in the MacArthur's system of m equations which is solvable only for $m \leq p$.

This theoretical prediction is extremely violated by the scenario of the Paradox of the Plankton [34] [27]. It has been shown experimentally that some hundred of different microbial species of phytoplankton coexist in close-by regions characterised by a few dozen of abiotic nutrients [7].

Numerous attempts have been made to harmonize theory and experiments, yet no explanation has been obtained to fill the gap between the predictions of the CEP and the observed species' coexistence [48] [49].

This challenge could be overcome in different ways. Firstly, within the resource-competition models, oscillatory or chaotic dynamics could determine the emergence of different coexisting populations. However, the long-term evolution of those solutions presentes issues in terms of stability [25] [1] [52].

1.2.2 Half saturation constant in the MacArthur's Model

The choice of the Monod function as the functional response of the consumer to the resource is based on its mathematical properties and its ability to capture certain ecological dynamics. The Monod function is a commonly used mathematical function that describes the rate at which a consumer species consumes a given resource as a function of the resource concentration. In particular, the Monod function is able to captures the saturation effect. The consumption rate increases as the resource concentration increases but saturates at high resource concentrations, taking in account that there is a maximum rate at which the consumer can metabolize the resource. The half-saturation constant allows for the consideration of different consumer-resource relationships. Higher values of k indicate a lower affinity of the consumer for the resource, resulting in slower consumption rates at lower resource concentrations. Finally, the non-linear relationship between resource concentration and consumption rate, which is provided by the Monod function, can lead to a variety of dynamic behaviors in the consumer-resource system, such as oscillations, stable coexistence, or competitive exclusion.

The role of the half-saturation constant is investigated considering a system with just one resource for the sake of simplicity. The dimensional analysis of Equation 1.19 suggests that the dimensions of resource concentration $[s]$ can be inferred as $[c]/[t]$ and $[\mu]$ as $1/[t]$. Dividing the equation by the

half saturation constant, k we get:

$$\begin{aligned}\dot{c} &= s(t) - \sum_{\sigma=1}^{m} n_\sigma \alpha_\sigma r(c(t)) - \mu c \\ &= s(t) - \sum_{\sigma=1}^{m} n_\sigma \alpha_\sigma \frac{c(t)}{k\left(\frac{c(t)}{k}+1\right)} - \mu c\end{aligned} \tag{1.26}$$

By introducing the rescaled variables $\tilde{c} \to \frac{c}{k}$, $\tilde{s} \to \frac{s}{k}$ and $t \to k \cdot \tau$, we incorporate the half saturation constant into the resources' concentrations and supply rates. We consequently get:

$$\dot{\tilde{c}} = \tilde{s}(\tau) - \sum_{\sigma=1}^{m} n_\sigma \alpha_\sigma \frac{\tilde{c}}{\tilde{c}+1} - \mu \tilde{c} \tag{1.27}$$

This rescaling allows to account for the influence of the half saturation constant on the timescale of the dynamics. However it is important to note that the fundamental physics of the Static model remains unchanged. Figure 1.1 shows how the behaviour of the population densities in terms of stationary coexistence is the same for different k just on a different timescale (results are presented in arbitrary units). For this reason the updated models of the following chapters, which have been designed with the objective of portraying a dynamic able to violate the Competition Exclusion Principle, don't act significantly on the half-saturation constant.

1.3 The Posfai, Taillefumier and Wingreen's Model

In the context of phytoplankton, it has been highlighted that trade-offs between different abilities could play a central role in maintaining diversity [35]. This is the starting point of the Static Model proposed by Posfai, Taillefumier and Wingreen, which is a competition-resource model where the species are constraint to use their different abilities of using the different resources within a trade-off [48]. Every species has a fixed number of enzymes that can be used for metabolism. The rate $\alpha_{\sigma i}$ is proportional to the number of enzymes that the species σ assigns to the process of importing and metabolising the resource i. Considering that the assimilation of a given resource might be easier or more difficult, the model assumes that there are different costs ν_i. However, all organisms have the same energy budget E thus $\sum_{i=1}^{p} \nu_i \, \alpha_{\sigma i} = E \ \forall \sigma$.

The original paper of Posfai, Taillefumier and Wingreen, characterised by fixed metabolic strategies, considers the death rate δ and the energy budget E to be equal for all the species. On top of these constraints, the time evolution of the system looks like the MacArtur's one:

$$\dot{n}_\sigma \ = n_\sigma(t) \ \left(\sum_{i=1}^{p} \nu_i r_i(c_i(t)) \ \alpha_{\sigma i} \ - \delta_\sigma \right) \tag{1.28}$$

$$\dot{c}_i = s_i - \sum_{\sigma=1}^{m} n_\sigma \alpha_{\sigma i} r_i(c_i(t)) - \mu_i c_i(t) \tag{1.29}$$

It is possible to observe a violation of the CEP only if

- $\sum_{i=1}^{p} \alpha_{\sigma i} \ = E \ \forall \sigma$, where E is the maximum resource uptake rate which is the same for all the species,
- $\delta_\sigma = \delta \ \forall \sigma$, where δ is the death rate which is the same for all the species,
- $\vec{s} = (s_1, ..., s_p)$ belongs to the convex hull of the metabolic strategies $\vec{\alpha}_\sigma = (\alpha_{\sigma 1}, ..., \alpha_{\sigma p})$.

Whenever one of those constrains is not satisfied (for example if $\sum_{i=1}^{p} \alpha_{\sigma i} \leq E_\sigma$ with E_σ which differ for every species), at least $m - p$ species are going to die. It is evident that this kind of fine-tuned constraints do not satisfy the need to portray the variety of behaviours in natural communities.

1.3.1 Rescaling the Static Model

In this section we we move away from the assumption of species independence characterising both the energy budget and the death rates, to develop a general formalism that it is going to be used also in the following chapters.

The model that we present in this work considers a specific δ_σ and E_σ for each species σ, which will be correlated by a factor Q independent on the species. The death rate of the system is then represented by the vector $\vec{\delta} = (\delta_1, ..., \delta_m)$.

The energy budget then becomes:

$$E_\sigma = \sum_{i=1}^{p} v_i \, \alpha_{\sigma i} \tag{1.30}$$

Considering that in physically relevant cases, the order of magnitude of the degradation rates μ_i is much smaller than the supply rate of the nutrients, we set $\mu_i = 0$ in this preliminary analysis.

At stationary(*), we have $\dot{n}_\sigma$ and $\dot{c}_i$ so that equation 1.28 and 1.29 become

$$\sum_{i=1}^{p} v_i \alpha_{\sigma i} r_i^* = \delta_\sigma \tag{1.31}$$

$$r_i^* = \frac{s_i}{\sum_{\sigma=1}^{m} n_\sigma^* \alpha_{\sigma i}} \tag{1.32}$$

Equation 1.31 can be written as a system of m equations in p unknown r_i^*:

$$\begin{cases} \alpha_{11} v_1 r_1^* + \ldots + \alpha_{1p} v_p r_p^* = \delta_1 \\ \vdots \\ \alpha_{m1} v_1 r_1^* + \ldots + \alpha_{mp} v_p r_p^* = \delta_m. \end{cases} \tag{1.33}$$

Imposing the energy constraint $\sum_{i=1}^{p} \alpha_{\sigma i} = E_\sigma^*$, can get non trivial solutions for $m > p$ which is

$$r_i^* = \frac{1}{v_i} \cdot \frac{\delta_\sigma}{E_\sigma^*}. \tag{1.34}$$

In the Equation 1.34 the right-hand side depends only on the index i whereas the right-hand side displays a dependence on σ and i, which means that it is impossible to find all species existing in a stationary state.

However we can introduce the condition $E_\sigma^* = Q\delta_\sigma$ to make the equation solvable. This is possible if we establish a connection between our model and the metabolic theory of ecology.

Considering the characteristic mass $\mathcal{M}_\sigma$ of an individual belonging to the species σ, we can recover the total biomass density M_σ through the population density n_σ: $M_\sigma = \mathcal{M}_\sigma n_\sigma$. It is possible then to

rescale the Equations 1.18 and 1.19, to get a new set of equations which is not identical with respect to the previous one but it keeps the main physical insights.

$$\dot{M}_\sigma = M_\sigma \left(\sum_{i=1}^{p} v_i \ \alpha_{\sigma i} \ r_i(c_i) \ - \delta_\sigma \right) \tag{1.35}$$

$$\dot{c}_i = s_i - \sum_{\sigma=1}^{m} M_\sigma \alpha_{\sigma i} r_i(c_i) - \mu_i c_i. \tag{1.36}$$

Given the universal exponent λ, the metabolic theory of ecology states that

$$\alpha_{\sigma i} \propto M_\sigma^{-\lambda} \text{ and } \delta_\sigma \propto M_\sigma^{-\lambda} \tag{1.37}$$

Due to the fact that $\sum_{i=1}^{p} \alpha_{\sigma i}(t) = E^*_\sigma$, we infer that $E^*_\sigma \propto M_\sigma^{-\lambda}$. For this reason the Characteristic Timescale Ratio (CTR) is $E^*_\sigma \backslash \delta_\sigma = Q$, where Q doesn't depend on the species' identity. We are going to show that, at this stage of the model, this is the condition for which coexistence of $m > p$ species is possible.

Introducing the assumption $E^*_\sigma = Q\delta_\sigma$, we can find a suitable solution for the stationary state.

$$r_i^* = \frac{1}{v_i} \cdot \frac{1}{Q} \tag{1.38}$$

Recalling the fact that $r_i^* < 1$, we underline the constraint $1 \backslash v_i < Q \ \forall i$. Having $v_i > Q^{-1} \ \forall i$ means that the energy available for growth coming from a resource would be insufficient for growth.

We introduce a parameterised notation

$$\hat{n} \coloneqq \sum_{\sigma=1}^{m} n_\sigma \delta_\sigma \quad \text{and} \quad n \coloneqq \sum_{\sigma=1}^{m} n_\sigma. \tag{1.39}$$

Summing every side of 1.18 over σ,

$$\dot{n} = \sum_{\sigma=1}^{m} \dot{n}_\sigma = \sum_{\sigma=1}^{m} \sum_{i=1}^{p} n_\sigma v_i r_i \ \alpha_{\sigma i} \ - \sum_{\sigma=1}^{m} \delta_\sigma = \sum_{\sigma=1}^{m} \sum_{i=1}^{p} n_\sigma v_i r_i \ \alpha_{\sigma i} \ - \hat{n}. \tag{1.40}$$

In the stationary state, Equation 1.29 gives $s_i = \sum_{\sigma=1}^{m} n^*_\sigma \alpha_{\sigma i} r_i^*$.

For $\dot{n}_\sigma = 0$ we get $\hat{n}^* = \sum_{\sigma=1}^{m} \sum_{i=1}^{p} n^*_\sigma v_i r_i^* \ \alpha_{\sigma i}$.

Recalling the definition of $\hat{n}$, we note that at stationarity this quantity is given by $\hat{n}^* \coloneqq \sum_{\sigma=1}^{m} n^*_\sigma \delta_\sigma$. Putting these two equations together, we get

$$\hat{n}^* = \sum_{i=1}^{p} v_i s_i \tag{1.41}$$

We define now the new quantities

$$x^*_\sigma \ \coloneqq \ \frac{n^*_\sigma \delta_\sigma}{\sum_{\rho=1}^{p} n^*_\rho \delta_\rho} \qquad \hat{s}_i \coloneqq \frac{v_i s_i}{\sum_{j=1}^{p} v_j s_j} \qquad \hat{\alpha}_{\sigma i} \coloneqq \frac{\alpha_{\sigma i}}{Q \delta_\sigma} \tag{1.42}$$

so that the following normalisations hold

$$\sum_{\sigma=1}^{m} x_\sigma^* = 1 \qquad \sum_{i=1}^{p} \hat{s}_i = 1 \qquad \sum_{i=1}^{p} \hat{\alpha}_{\sigma i} = 1 \ \forall \sigma. \tag{1.43}$$

Using Equations 1.43, 1.41 and 1.42 and the fact that $\sum_{\sigma=1}^{m} = n_\sigma^* \delta_\sigma = \sum_{i=1}^{p} = v_i s_i$, is possible to find out that

$$\hat{s}_i = \sum_{\sigma=1}^{m} x_\sigma^* \hat{\alpha}_{\sigma i} \tag{1.44}$$

because

$$\hat{s}_i = \frac{v_i s_i}{\sum_{j=1}^{p} v_j s_j} = \frac{s_i}{\sum_{j=1}^{p} v_j s_j \ v_i^{-1}} = \frac{\sum_{\sigma=1}^{m} n_\sigma^* \alpha_{\sigma i}}{\sum_{j=1}^{p} v_j s_j} \frac{r_i^*}{Q r_i^*} = \frac{\sum_{\sigma=1}^{m} n_\sigma^* \delta_\sigma}{\sum_{\rho=1}^{m} n_\rho^* \delta_\rho} \frac{\alpha_{\sigma i}}{Q \delta_\sigma} = \sum_{\sigma=1}^{m} x_\sigma^* \hat{\alpha}_{\sigma i} \tag{1.45}$$

This is equivalent to a system of p equations in m unknowns x_σ^*, so for $m < p$ it will admit infinite positive solutions.

However the coexistence at stationarity for an arbitrary number of species (violation of the CEP) is achieved when Equation 1.44 has a positive solution $x_1^* > 0 \ \forall \sigma$. Thus the steady state that we are searching will exists if the set

$$\left\{ x_1^* > 0, \ ..., \ x_m^* > 0 \ : \ x_1^* \vec{\alpha}_1 + ... + x_m^* \vec{\alpha}_m \ = \vec{s} \right\} \tag{1.46}$$

is non-empty. This requirement coincides with the definition of convex hull. In fact a vector $\vec{y} = (y_1, ..., \ y_p)$ belongs to the convex hull of a series of points $\vec{x} = (x_1, ..., \ x_{p)}$ if it can been written as a convex combination of them, meaning that

$$\vec{y} = \sum_{i=1}^{z} a_i \vec{x}_i \tag{1.47}$$

where the coefficients $(a_1, ..., a_z)$ are built such that

$$a_i > 0 \ \forall i \text{ and } \sum_{i=1}^{z} a_i = 1 \tag{1.48}$$

Considering the definition of x_σ^* and the normalisation $\sum_{\sigma=1}^{m} x_\sigma^* = 1$ that follows, we can state that the species coexistence that allows the violation of the CEP is possible when $\vec{\hat{s}}$ is a convex combination of the rescaled metabolic strategies $\vec{\hat{\alpha}}_{\sigma i}$.

We want to understand how an initial mixed population of species evolve and how the community is going to be diverse at infinite times.

The case for which $p = 1$ and $m > 1$ is peculiar because

$$\hat{s} = \sum_{\sigma=1}^{m} x_\sigma^* \hat{\alpha}_\sigma \tag{1.49}$$

where $\hat{\alpha}_\sigma > 0 \ \forall \sigma$ and $\hat{s} = 1$. This means that in the presence of multiple nutrients, the coexistence of competing species becomes possible as infinite solutions are possible.

When just one resource is available, all the species will coexist at the stationary state. On the other hand, for $p > 1$ resources if the vector $\vec{\hat{s}}$ does not lie within the convex hull of the metabolic strategies, the system follows the Competition Exclusion Principle.

When the consider non-zero degradation rates $\mu_i \neq 0$, at stationarity Equation 1.29 becomes:

$$s_i^* = \sum_{\sigma=1}^{m} n_\sigma^* \alpha_{\sigma i} r_i^* - \mu_i c_i^*. \tag{1.50}$$

In this condition we can define

$$\tilde{s}_i \coloneqq \frac{v_i \left(s_i - \mu_i c_i^*\right)}{\sum_{j=1}^{p} v_j \left(s_j - \mu_j c_j^*\right)}. \tag{1.51}$$

which is equivalent to

$$\tilde{s}_i = \sum_{\sigma=1}^{m} x_\sigma^* \hat{\alpha}_{\sigma i}. \tag{1.52}$$

In general, when the rescaled vector supply lies within the convex hull of the rescaled metabolic strategies, an environment equally favorable for all the species is created, violating the Competition Exclusion Principle, as can be seen in Figure 1.2.

1.4 Numerical Results

In this section, we will present the most relevant simulations related to the ecosystem dynamics in both the MacArthur's model and the Static model. Parameters and initial conditions are presented in arbitrary units.

Figure 1.1 illustrates the influence of the half-saturation constant in modifying the the transient dynamics observed in the MacArthur's model. The half saturation constant has no impact on the stationary state. As expected, only $m - p$ species will persist at the stationarity out of m species and p resources.

Figure 1.2 presents the violation of the Competition Exclusion Principle, thanks to the constraints concerning the supply rate, the death rate and the energy budget introduced in the Static Model. In the presence of species independent death rates and energy budgets, coexistence of all the initial species is observed if the rescaled supply rate lies within the convex hull of the rescaled metabolic strategies. We selected $p = 3$ resources as it allows the metabolic strategies to be confined within a 2-dimensional simplex, specifically a triangle whose vertex represemt the nutrients. This choice facilitates the visualization and representation of the system dynamics.

Figure 1.1: Time evolution of the population densities (left column) and the concentration of resources (right column) within the MacArthur's framework for different values of the half saturation constant. The system evolves according to 1.43 and 1.44 with $m = 3$, $p = 1$, $\mu = 0$, $s = U[0.5, 1.5]$ (with U uniform distribution), $\delta_\sigma = \delta = 1$, $v = 1$, $\vec{\alpha} = [2, 7, 12]$. The simulations are performed for (1) k=1, (2) k=10 and (3) k=30.

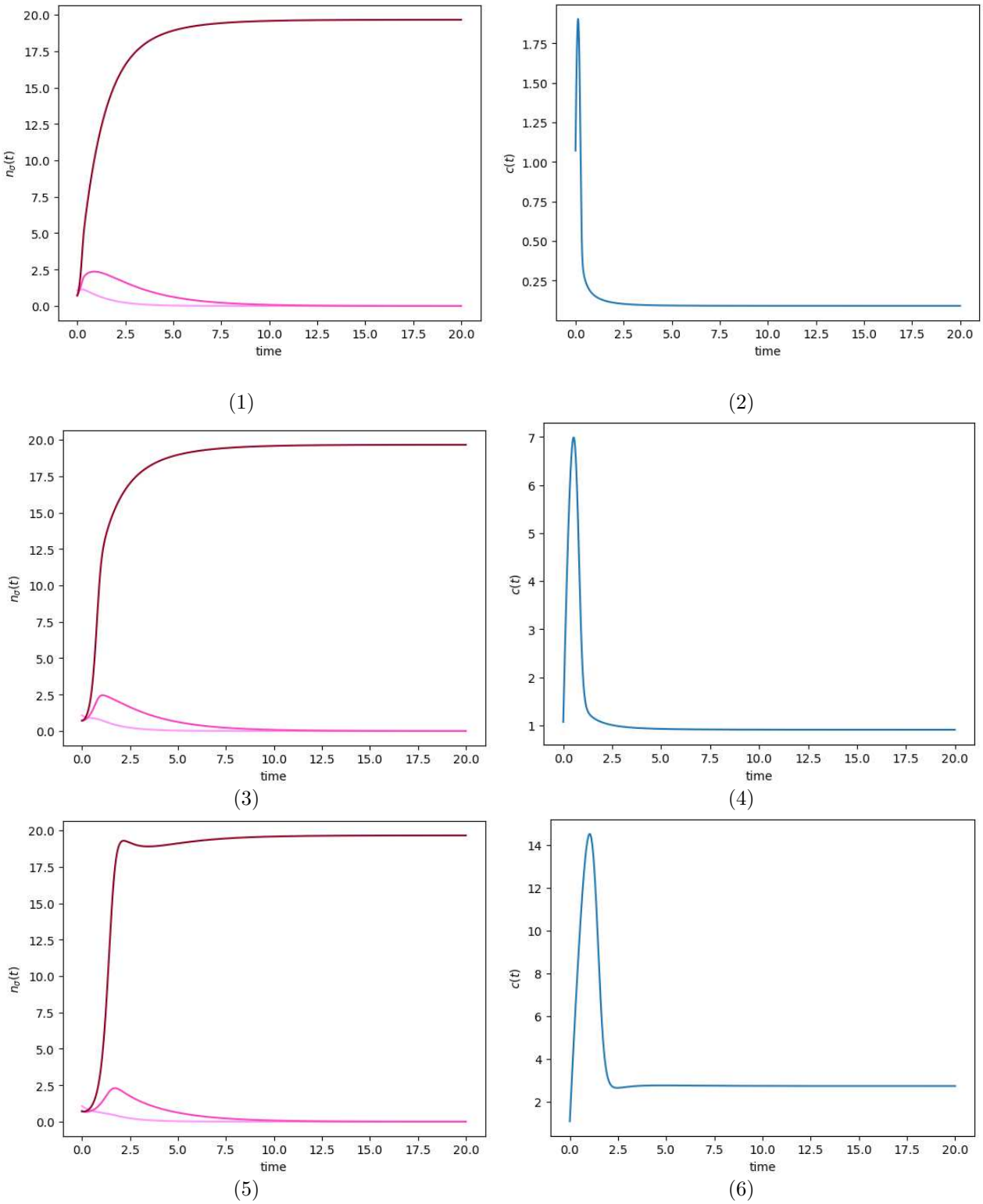

Figure 1.2: Time evolution of the convex hull of the rescaled metabolic strategies (left column) and of the population densities (right column) within the Static Model framework. The system evolves according to $m = 10$, $p = 3$, $\mu = 0$, $s = U[10^{-3}, 10^{-2}]$ (with U uniform distribution), $\delta_\sigma = \delta = 0.05$, $v = U[10^8, 5 \cdot 10^9]$, $Q = U[10^{-7}, 5 \cdot 10^{-5}]$, $\sum_{i=1}^{p} \alpha_{\sigma i} = E = Q\delta \ \forall \sigma$. The initial conditions are $n_i(0) = U[10^6, 5 \cdot 10^6]$ and $c_i(0) = U[10^{-3}, 10^{-2}]$. The supply rates are such: (1) $\vec{\hat{s}}$ is inside the convex hull of the rescaled metabolic strategies, allowing the coexistence of all the initial species, (2) $\vec{\hat{s}}$ lies outside of the convex hull, determining the extinction of $m - p$ species.

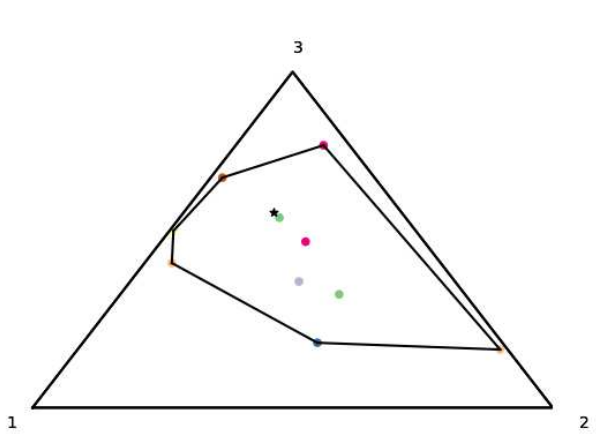

(1)

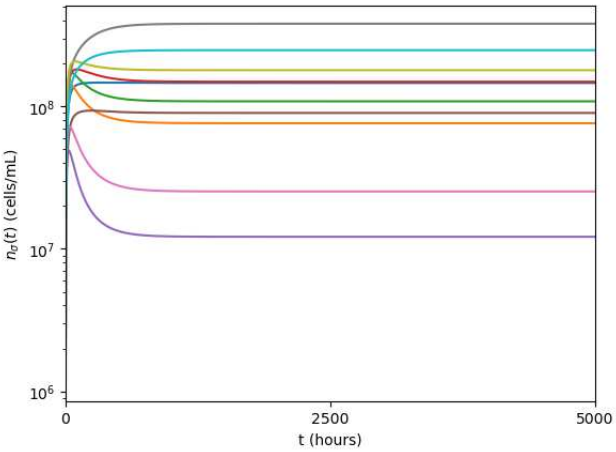

(2)

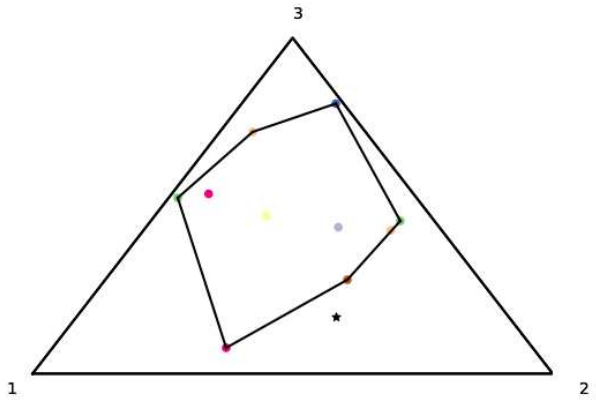

(3)

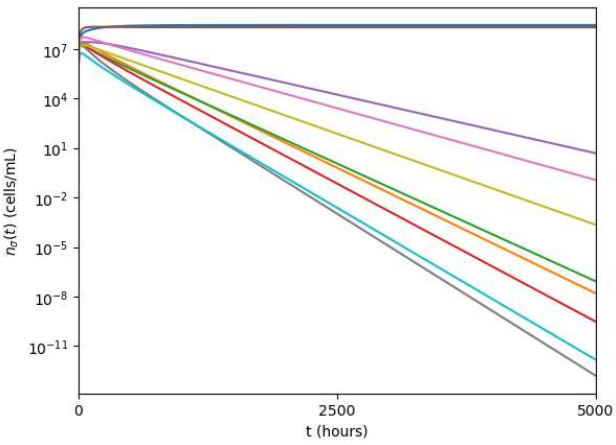

(4)

THE ADAPTIVE MODEL

In this chapter we are going to study the model developed by Pacciani-Mori, Giometto, Suweis, and Maritan, which we will refer to as the Adaptive Model [46].

Experimentally it is proved that microbes can adapt to different environmental conditions both by recycling resources and by varying the rates at which they assume them over time. Already in the 1940s, it has been proved that *Escherichia Coli* and *Bacilius Subtilis* show a biphasic growth curve, i.e. diauxie curve, when in a culture with two different sugars [43] [42] [29], [5], [44], [54]. They don't use the two nutrients at the same time, but first the one with the highest growth rate and, when they run out of it, they start to use the other resource after a lag phase.
Actually it has been showed that this metabolic dynamic adaptation occurs among several different microbial species [36], [32], [15]. The rate of consumption of the nutrients can be varied by the species depending on presence of other microbial species and the abundance of different nutrients. In this complex system, species are agents that interact with each other and with the environment giving rise to emergent properties.

The Adaptive Model is able to reproduce correctly the experimental diauxic curve of growth of *E. coli* on two different resources, by incorporating a time-dependent constrained optimized dynamics of the metabolic strategies. The metabolic strategies evolve to maximize the growth rate of the species respecting a total energy constraint.

This chapter delves into various facets of the dynamics, particularly in relation to the supply of resources in the environment and their metabolic utilization by the species. In particular, special attention is given to the velocity of resource degradation and its impact on species behavior. This thesis has proved that when the degradation rates of resources exceed a certain threshold, species undergo a sharp transition and cease to utilize those resources.

2.1 Adaptive dynamic of the metabolic strategies

The Adaptive Model, introduces a novel feature by allowing the metabolic strategies, defined as the maximum resource uptake rates, to vary with time [46]. This extension enables the model to capture the dynamic nature of species' interactions and adaptability in response to changing environmental conditions. The temporal dynamics of each metabolic strategy $\vec{\alpha}_\sigma = (\alpha_{\sigma 1}, \ ..., \ \alpha_{\sigma p})^T$ is meant to maximise the fitness of each species.
The fitness is defined as the growth rate of the species σ as $g_\sigma = \sum_{i=1}^{p} v_i r_i \ \alpha_{\sigma i}$ [33] [45].

We impose that each $\vec{\alpha}_\sigma$ changes in time following the gradient ascent dynamics:

$$\dot{\alpha}_{\sigma i} = d\delta_\sigma \frac{\partial g_\sigma}{\partial \alpha_{\sigma i}} = v_i r_i d\delta_\sigma > 0 \tag{2.1}$$

Conceptually this is a huge improvement of the Static Model, because the metabolic strategies are promoted from parameters to dynamical variables, creating a matrix $m \times p$ that changes in time. However, this is just the starting point, because species have a limited amount of energy that can be used to assimilate the resources whereas formally the metabolic strategies can grow indefinitely

in Equation 2.1. The total energy that can be used is the same as in the Static Model but the alphas can change their values: energy constraint becomes softer with respect to the previous model, $\sum_{i=1}^{p} \alpha_{\sigma i}(t) \coloneqq E_\sigma(t) \leqslant E^*_\sigma$. This upper bound constraint has been experimentally proven to be the key element to make the agreement between the Flux Balance Model of *E.coli* and experiment data better. [4]

2.2 Constrained dynamics for the metabolic strategies

We are going now to present a general formalism aimed to introduce some constraints in a differential equation, where the temporal evolution of a variable coincides with the spacial gradient of a quantity dependent on the variable.
$Q(\vec{x})$ is the quantity to be maximised with the temporal evolution of a variable $\vec{x}(t) \in \mathbb{R}^q$. We assume the variable $\vec{x}(t)$ is subjected to a constraint $\varphi(\vec{x}) = 0$.

We want to keep the constraint $\varphi(\vec{x})$ constant, so we get rid of the component of $\vec{\nabla}Q$ parallel to $\vec{\nabla}\varphi$, i.e.

$$\dot{\vec{x}} = \vec{\nabla}Q(\vec{x}) - \frac{\vec{\nabla}\varphi(\vec{x})}{|\vec{\nabla}\varphi(\vec{x})|}\left(\frac{\vec{\nabla}\varphi(\vec{x})}{|\vec{\nabla}\varphi(\vec{x})|}\cdot\vec{\nabla}Q(\vec{x})\right) \tag{2.2}$$

The Equation 2.2 is suitable because Q increases with time due to the Schwartz's inequality :

$$\dot{Q} = \vec{\nabla}Q(\vec{x})\cdot\dot{\vec{x}} = \dot{\vec{x}}^2 = |\vec{\nabla}Q|^2 - \left(\frac{\vec{\nabla}\varphi}{\vec{\nabla}\varphi|}\cdot\vec{\nabla}Q\right)^2 \geqslant 0 \tag{2.3}$$

and φ is constant along the trajectories:

$$\dot{\varphi} = \vec{\nabla}\varphi\cdot\dot{\vec{x}} = \vec{\nabla}\varphi\cdot\vec{\nabla}Q - \frac{|\vec{\nabla}\varphi|^2}{|\vec{\nabla}\varphi|^2}\vec{\nabla}\varphi\cdot\vec{\nabla}Q = 0. \tag{2.4}$$

If the constraint is softer than the strict equality is means that we have to introduce an Heaviside function.

$$\dot{\vec{x}} = \vec{\nabla}Q(\vec{x}) - \theta(\varphi(\vec{x}))\frac{\vec{\nabla}\varphi(\vec{x})}{|\vec{\nabla}\varphi(\vec{x})|}\left(\frac{\vec{\nabla}\varphi(\vec{x})}{|\vec{\nabla}\varphi(\vec{x})|}\cdot\vec{\nabla}Q(\vec{x})\right) \tag{2.5}$$

Considering just one species, substituting $\vec{x}$ with $\vec{\alpha}$ and Q with$d\delta g$ and neglecting the Heaviside function for now, we obtain by components

$$\dot{\alpha_i} = d\delta\ \frac{\partial g}{\partial\alpha_i} - \frac{\partial\varphi(\vec{\alpha})/\partial\alpha_i}{\sum_{i=1}^{p}(\partial\varphi(\vec{\alpha})/\partial\alpha_i)^2}\ \sum_{i=1}^{p}\frac{\partial\varphi(\vec{\alpha})}{\partial\alpha_i}d\delta\ \frac{\partial g}{\partial\alpha_i} \tag{2.6}$$

We introduce some auxiliary variables η_i of which the metabolic strategies are non-neagtive functions:

$$\alpha_i \coloneqq F(\eta_i) \text{ with } F(x) \geq 0 \quad \forall\ x \tag{2.7}$$

Now we use the Equation 2.6 of α_i for η_i, to obtain

$$\dot{\eta_i} = d\delta\ \frac{\partial g}{\partial\eta_i} - \frac{\partial\varphi(\vec{\eta})/\partial\eta_i}{\sum_{i=1}^{p}(\partial\varphi(\vec{\eta})/\partial\eta_i)^2}\ \sum_{i=1}^{p}\frac{\partial\varphi(\vec{\eta})}{\partial\eta_i}d\delta\ \frac{\partial g}{\partial\eta_i} \tag{2.8}$$

Considering that $\alpha_i = F(\eta_i)$, the time derivative is $\dot{\alpha_i} = F'(\eta_i)\ \dot{\eta_i}$ and the partial derivative is $\frac{\partial}{\partial\alpha_i} = \frac{\partial}{\partial\eta_i}\ \frac{1}{F'(\eta_i)}$.

We proceed now to a change of variables using the time and partial derivatives, to write the Equation 2.8 in terms of α_i

$$\dot{\eta_i} = \frac{1}{\mathcal{F}'(\eta_i)}\ \dot{\alpha_i} \ = \ d\delta \frac{\partial g}{\partial \alpha_i}\mathcal{F}'(\eta_i) - \frac{\partial \varphi(\vec{\alpha})/\partial \alpha_i \mathcal{F}'(\eta_i)}{\sum_{i=1}^{p}(\partial \varphi(\vec{\eta})/\partial \alpha_i)^2\ (\mathcal{F}'(\eta_i))^2}\ \sum_{i=1}^{p}\frac{\partial \varphi(\vec{\alpha})}{\partial \alpha_i}\mathcal{F}'(\eta_i)\ d\delta\ \frac{\partial g}{\partial \alpha_i}\mathcal{F}'(\eta_i) \quad (2.9)$$

Multiplying both sides of Equation 2.9 by $F'(\eta_i)$ we get the equation for the dynamic of the time derivative of $\dot{\alpha_i}$:

$$\dot{\alpha_i} = \ [\mathcal{F}'(\eta_i)]^2 \left[d\delta \frac{\partial g}{\partial \alpha_i} - \frac{\partial \varphi(\vec{\alpha})/\partial \alpha_i}{\sum_{i=1}^{p}(\partial \varphi(\vec{\eta})/\partial \alpha_i)^2\ (\mathcal{F}'(\eta_i))^2}\ \sum_{i=1}^{p}\frac{\partial \varphi(\vec{\alpha})}{\partial \alpha_i}\ d\delta\ \frac{\partial g}{\partial \alpha_i}(\mathcal{F}'(\eta_i))^2 \right] \quad (2.10)$$

We don't have constraints on the form of F. Considering for example $F(\eta_i) = \eta_i^2/4$ we have that the squared derivative of the function gives back the metabolic strategy's component. In fact,

$F'(\eta_i) = \ 2\eta_i/4$ and $[F'(\eta_i)]^2 = 4\eta_i^2\ /16 = \ F(\eta_i) = \ \alpha_i$

$$\begin{aligned} \dot{\alpha_i} \ &= \ [\mathcal{F}'(\eta_i)]^2 \left[d\delta \frac{\partial g}{\partial \alpha_i} - \frac{\partial \varphi(\vec{\alpha})/\partial \alpha_i}{\sum_{i=1}^{p}(\partial \varphi(\vec{\eta})/\partial \alpha_i)^2\ (\mathcal{F}'(\eta_i))^2}\ \sum_{i=1}^{p}\frac{\partial \varphi(\vec{\alpha})}{\partial \alpha_i}\ d\delta\ \frac{\partial g}{\partial \alpha_i}(\mathcal{F}'(\eta_i))^2 \right] \\ &= \alpha_i \left[d\delta \frac{\partial g}{\partial \alpha_i} - \frac{\partial \varphi(\vec{\alpha})/\partial \alpha_i}{\sum_{i=1}^{p}(\partial \varphi(\vec{\eta})/\partial \alpha_i)^2\ \alpha_i}\ \sum_{i=1}^{p}\frac{\partial \varphi(\vec{\alpha})}{\partial \alpha_i}\ d\delta\ \frac{\partial g}{\partial \alpha_i}\alpha_i \right] \end{aligned} \quad (2.11)$$

Continuing in a framework with only one species, we recall $g = \sum_{i=1}^{p} v_i \alpha_i r_i - \delta$.

The energy budget constraint $\varphi(\vec{\alpha}) = \sum_{i=1}^{p}\frac{\alpha_i}{E^*} - 1$ is rearranged in order to make it nondimensional.

Therefore we have $\frac{\partial g}{\partial \alpha_i} = v_i r_i$ and $\frac{\partial \varphi(\vec{\alpha})}{\partial \alpha_i} = \frac{1}{E^*}$ so that

$$\dot{\alpha_i} = d\delta\ \alpha_i \left[v_i r_i - \frac{1/E^*}{(1/E^*)^2 \sum_{i=1}^{p}\alpha_i}\ 1/E^* \sum_{i=1}^{p}\ v_i r_i\ \alpha_i \right] \quad (2.12)$$

The total energy budget E disappears in the Equation 2.12. Inserting again the Heaviside function we obtain the i-th component metabolic strategy's dynamic

$$\dot{\alpha_i} \ = d\delta\ \alpha_i \left[v_i r_i - \frac{\theta(\varphi(\vec{\alpha}))}{\sum_{i=1}^{p}\alpha_i}\ \sum_{i=1}^{p}\ v_i r_i\ \alpha_i \right] \quad (2.13)$$

The Heaviside function prevents the metabolic strategies from growing indefinitely.

Expanding Equation 2.13 to an ecosystem with multiple species, we define so that we obtain

$$\dot{\alpha}_{\sigma i} = d\delta_\sigma\ \alpha_{\sigma i} \left[v_i r_i - \frac{\theta_\sigma(\varphi(\vec{\alpha}_\sigma))}{\sum_{i=1}^{p}\alpha_{\sigma i}}\ \sum_{i=1}^{p}\ v_i r_i\ \alpha_{\sigma i} \right] \quad (2.14)$$

Figure 2.1: Effect of the constraint present in Equation 2.2: $\vec{x}(t)$ is bounded to move in the manifold defined by the constraint $\varphi(\vec{x}) = 0$. Qualitative example for a system with $p = 2$ resources.

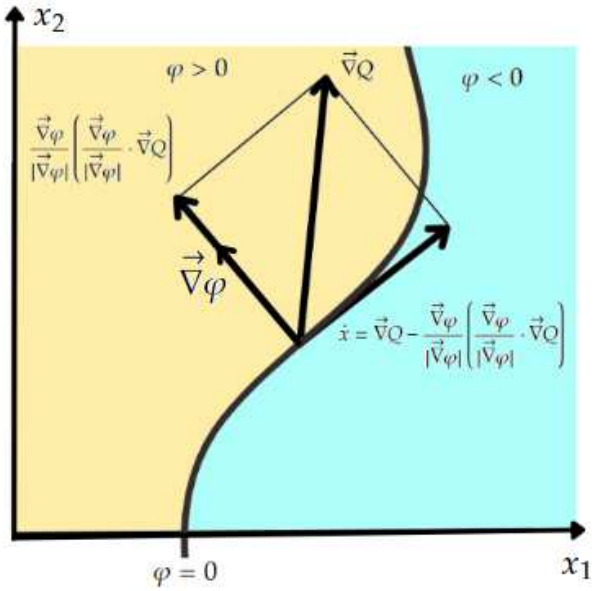

2.3 The Adaptive Model

In the framework of the Adaptive Model, a community of m species and p resources evolves according to the following equations:

$$\dot{n}_\sigma = n_\sigma \left(\sum_{i=1}^{p} v_i r_i(c_i)\ \alpha_{\sigma i} - \delta_\sigma \right) \tag{2.15}$$

$$\dot{c}_i = s_i(t) - \sum_{\sigma=1}^{m} n_\sigma \alpha_{\sigma i} r_i(c_i) - \mu_i c_i \tag{2.16}$$

$$\dot{\alpha}_{\sigma i} = d\delta_\sigma\ \alpha_{\sigma i} \left[v_i r_i - \frac{\theta_\sigma(\varphi(\vec{\alpha}_\sigma))}{\sum_{i=1}^{p} \alpha_{\sigma i}} \sum_{i=1}^{p} v_i r_i\ \alpha_{\sigma i} \right] \tag{2.17}$$

Allowing the metabolic strategies to adapt means that Equation 1.44 becomes

$$\hat{s} = \sum_{\sigma=1}^{m} x^*_\sigma \hat{\alpha}^*_\sigma \text{where } \hat{\alpha}^*_\sigma > 0\ \forall\sigma \tag{2.18}$$

in the absence of degradation rates.

In the Adaptive Model, when we consider non-zero degradation rates $\mu_i \neq 0$, at stationarity Equation 1.19 becomes:

$$s^*_i = \sum_{\sigma=1}^{m} n^*_\sigma \alpha^*_{\sigma i} r^*_i - \mu_i c^*_i. \tag{2.19}$$

Considering the definition of $\tilde{s}_i$, which has been already introduced and has a strong dependence on the concentration of resources at stationarity,:

$$\tilde{s}_i := \frac{v_i \left(s_i - \mu_i c^*_i\right)}{\sum_{j=1}^{p} v_j \left(s_j - \mu_j c^*_j\right)}. \tag{2.20}$$

Table 2.1: Parameters used in the Adaptive Model, with their definition and units of measure.

Parameter	**Definition**	**Units**
n_σ	Population density of species σ	cell
c_i	Density of resource i	g of resource/(cell $\cdot h$)
μ_i	Degradation rate of resource i	1/h
δ_σ	Death rate of species σ	1/h
k_i	Half-saturation constant of resource i	g of resource/mL
s_i	Supply rate of resource i	g of resource/(mL $\cdot h$)
v_i	Conversion efficiency of resource i	cell/g of resource
$\alpha_{\sigma i}$	Metabolic strategies	g of resource/(cell $\cdot h$)
E^*_σ	Total uptake rate of species σ	g of resource/(cell $\cdot h$)

it is possible to infer that

$$\tilde{s}_i = \sum_{\sigma=1}^{m} x^*_\sigma \hat{\alpha}^*_{\sigma i} \tag{2.21}$$

The rescaled metabolic strategies at stationarity have changed in order to include $\vec{\tilde{s}}_i$ inside their convex hull.

2.4 Dimensional Analysis of the Adaptive Model

Equations 2.15 and 2.16 can be studied to derive the dimensions of all the variables and parameters of the model: this is essential to be able to draw a link between the experimental results and the theoretical model.
We start by the population densities $[n_\sigma]$ = population/volume = cell/mL and the concentrations of the resources $[c_i]$ = resource/volume = g of resource/mL. Considering that we are dealing with a time derivative, we infer that $[1/\delta_\sigma]$ = 1/time = 1/h from Equation 2.16 and that $[s_i]$ = g of resource/mL/h from 2.17. The Monod function $r_i = \frac{ci}{ki+ci}$ is dimensionless because the half-saturation constant has the dimensions of a concentration.
From Equation 2.16 we can infer that

$$\frac{[c_i]}{\text{time}} = [n_\sigma][\alpha_{\sigma i}] \tag{2.22}$$

so that the metabolic strategies' dimensions represent the rate of resources assimilation per hour and per cell

$$[\alpha_{\sigma i}] = \frac{\text{g of resource}}{\text{cell} \cdot \text{h}}. \tag{2.23}$$

The dimension of the resource value can be found from the Equation 2.15:

$$\frac{[n_\sigma]}{\text{time}} = [v_i][1][n_\sigma][\alpha_{\sigma i}] \tag{2.24}$$

to have

$$[v_i] = \frac{\text{cell}}{\text{g of resource}} \tag{2.25}$$

Furthermore, we recall the energy constraint $E^*_\sigma = Q\delta_\sigma$, which represents the maximum value that the sum over the the metabolic strategies can take at every instant of time.

$$\sum_{i=1}^{p} \alpha_{\sigma i} \coloneqq E_\sigma(t) \leqslant E^*_\sigma \tag{2.26}$$

Dimensionally, this translates into $[\alpha_{\sigma i}] = [Q][\delta_\sigma]$ so the Q parameter is described by

$$[Q] = \frac{[\alpha_{\sigma i}]}{[Q]} = \frac{\text{g of resource}}{\text{cell}} \tag{2.27}$$

Finally we can unveil the dimensions of the d parameter, the one responsible of the velocity of the alpha's dynamic (as we we are going to see):

$$[d] = \frac{[\alpha_{\sigma i}]}{\text{time}} \cdot \frac{1}{[\delta_\sigma][v_i][r_i]} = \frac{\text{g of resource}}{\text{cell}} \tag{2.28}$$

2.5 Numerical Results

In this section we present some numerical simulations describing the behaviour of the ecosystem described by the Adaptive Model, always in comparison with the Static one.

2.5.1 Diauxic curves

The dynamical metabolic adaptation successfully predicts the diauxic shifts and the existence of several species in a context with few resources. The main result of the Adaptive Model is the ability to reproduce the growth curves of the *S. cerevisiae* consuming different resources, while the Static Model would fail to, wrongly predicting the extinction of the species. *S. cerevisiae* uses primarily galactose, which is partially fermented, and from which yeast cells excrete ethanol. The system that we are going to simulate is composed by $m = 1$ species and $p = 2$ resources. It takes in account the fact that the second sugar is not present in the culture from the beginning but it is produced at a later time. The ethanol production is proportional to the galactose consumption rate through a factor Y which is included in the following equations.

$$\dot{n} = n \left(v_{gal}\alpha_{gal}\frac{c_{gal}}{K_{gal} + c_{gal}} + v_{eth}\alpha_{ethl}\frac{c_{eth}}{K_{eth} + c_{eth}} - \delta \right) \tag{2.29}$$

$$\dot{c}_{gal} = -n\alpha_{gal}\frac{c_{gal}}{K_{gal} + c_{gal}} \tag{2.30}$$

$$\dot{c}_{eth} = -n\alpha_{ethl}\frac{c_{eth}}{K_{eth} + c_{eth}} + Yn\alpha_{gal}\frac{c_{gal}}{K_{gal} + c_{gal}} \tag{2.31}$$

$$\dot{\alpha}_i = d\delta\, \alpha_i \left[v_i \frac{c_i}{K_i + c_i} - \theta \left(\frac{\alpha_{gal} + \alpha_{eth}}{Q\delta} - 1 \right) \frac{1}{\alpha_{gal} + \alpha_{eth}} \cdot \left(v_{gal}\alpha_{gal}\frac{c_{gal}}{K_{gal} + c_{gal}} + v_{eth}\alpha_{ethl}\frac{c_{eth}}{K_{eth} + c_{eth}} \right) \right] \tag{2.32}$$

$$\text{with } \frac{\alpha_{gal} + \alpha_{eth}}{Q\delta} \leq 1 \tag{2.33}$$

The parameters used are to simulate the dynamics are the ones described in the caption of Figure 2.2. [46]

2.5.2 Adaptive Non-Degradative Model with constant supply rate

We have chosen to portray in Figure 2.3 one of the several simulations performed to study the Adaptive Model, in the case in which the vector of degradation rates is zero $\vec{\mu}_i = 0$. The presence of $p = 3$ resources allow to use the graphical representation proposed by Posfai et al. [48]. The dynamics of the metabolic strategies play a crucial role in enabling the coexistence of all species. The convex hull of the rescaled metabolic strategies evolves in time to ensure that the rescaled supply rate remains within it at the stationary state.

2.5.3 Adaptive Non-Degradative Model with variable supply rate

Variability in the environment's conditions is a feature that can be added to the system. The supply rate vector becomes a function of time. In particular we have considered a periodic environment's variability, with a supply rate that shifts between two fixed values, one inside the convex hull and one outside of the convex hull of the rescaled metabolic strategies, at regular time intervals.
In the Static Model's framework the existence of all the species is determined by the quantity of time that the supply rate $\vec{s}(t)$ spends inside the convex hull. This dependence on the duration of the permanence inside the convex hull is not important anymore in the Adaptive Model: since metabolic strategies are allowed to adapt, populations can oscillate and so they are enabled to survive. Equations 2.15, 2.16 and 2.17 describe the system, whose environmental variability is mathematically expressed by:

$$\vec{s}(t) = \begin{cases} \vec{s}_{in} & 0 < t' \leqslant \tau_{in} \\ \vec{s}_{out} & \tau_{in} < t' \leqslant \tau_{out} \end{cases} \tag{2.34}$$

$\vec{s}_{in}$ and $\vec{s}_{out}$ are set as fixed values, such that the rescaled versions $\vec{\hat{s}}_{in}$ and $\vec{\hat{s}}_{out}$ are inside and outside of the convex hull of the initial rescaled metabolic strategies. The time is defined as $t' = t - \tau[t/\tau]$ with $\tau = \tau_{in} + \tau_{out}$. In the Static case, the difference between τ_{in} and τ_{out} is fundamental to determine extinctions or not: the Competition Exclusion principle holds if τ_{in} is large enough compared to τ_{out}. In the presence of a large τ_{in}, environmental variability allows to observe a variation of the CEP even when $d = 0$ (Static Model). In the simulations with variable supply rate that we present in Figure 2.4, the energy constraint is quite severe $E_\sigma(0) = Q\delta_\sigma$, because we want to be in the conditions in which the CEP can be violated theoretically also using fixed metabolic strategies.

2.5.4 Adaptation velocity in the Adaptive Non-Degradative Model with constant supply rate

The adaptation velocity, represented by the parameter d, is the speed of the dynamic metabolic adaptation for the metabolic strategies. The value of d is proven to be really impacting on the variability of the populations, as shown in Figure 2.5.

From Equation 2.17, it is straightforward to see that in the limit $d \to 0$, we recover the case of fixed metabolic strategies and so the dynamics of the population densities portrays the Competition Exclusion Principle.
The greater the adaptation velocity is the longest the time in which species will not end up experiencing extinction. On the contrary, when the adaptation velocity reaches higher values the dynamics is so speed up that the numerical simulations experience an excess of work.

2.5.5 Unfavorable resources in the Adaptive Non-Degradative Model with constant supply rate

If the j-th nutrient is characterised by $1/\nu_j > Q$, the resource is defined unfavorable, because its resource-to-biomass conversion efficiency is too low with respect to the total energy budget of the system. Under this condition, the Equation 1.38 does not have a feasible solution for $i = j$. Consequently it is possible to write Equation 1.31 as it follows

$$\delta_\sigma = v_j \alpha^*_{\sigma j} r^*_j + \sum_{i \neq j} v_i \alpha^*_{\sigma i} r^*_i = v_j \alpha^*_{\sigma j} r^*_j + \sum_{i \neq j} \alpha^*_{\sigma i} Q^{-1} = v_j \alpha^*_{\sigma j} r^*_j + Q^{-1} \left(\sum_{i=1}^{p} \alpha^*_{\sigma i} - \alpha^*_{\sigma j} \right) \ \forall \sigma \tag{2.35}$$

.

From $\sum_{i=1}^{p} \alpha^*_{\sigma i} = Q\delta_\sigma$ we get:

$$\alpha^*_{\sigma j} \left(v_j r_j - Q^{-1} \right) = 0 \ \forall \sigma \tag{2.36}$$

.

The only possible solution for Equation 2.36 is that at stationarity, all the species stop using the j-th resource, resulting in $\alpha^*_{\sigma j} = 0$ for all σ. Visually in the 2-dimensional simplex, it appears as if the metabolic strategies have moved away from the vertex associated with the unfavorable resource, clustering together on the opposite side of the triangle. This convergence indicates that none of the species are utilizing the j-th resource, and their metabolic strategies have shifted towards the other available resources.

In the Static framework, the absence of a dynamics on the metabolic strategies and the fact that $1/v_j > Q$ for the j-th resource determines that no possible steady solution can be found to Equation 1.31 which causes CEP to hold. in the Static contest, having just one unfavorable resource determines several extinctions if the metabolic strategies are fixed.

On the contrary, the Adaptive dynamics allows to observe coexistence of all the initial species at stationarity, despite of the presence of unfavorable resources. In the static model, the condition $1/v_j > Q$ can be observed in the time evolution of n_σ as multiple species die out. On the other hand, in the Adaptive model, it becomes more challenging to directly detect the presence of unfavorable resources solely based on the visualisation of the population's density dynamics. Species with the ability to adapt their metabolic strategies experience a minimization of the energy waste. In fact they can fine-tune their energy allocation based on the availability and quality of resources in their environment. The time evolution of the metabolic strategies of Figure 2.6 displays how species stop metabolising the resource which leads to a lower population growth rate per unit resource quantity. Equation 2.16 predicts the linear growth of the concentration of j-th resource: $\dot{c}_j = s_j(t)$ as, after a transient, $\alpha^*_{\sigma j} = 0$. In the presence of the degradation rates, the equation would turn out to be $\dot{c}_i = s_i(t) - \mu_i c_i$.

2.5.6 Adaptive Degradative model with constant supply rate

The introduction of a non zero vector of degradation rates $\vec{\mu} = (\mu_1, ..., \mu_p)$ allows to see some intriguing properties.

To comprehensively study the relationship between degradation rates and resource value, a methodical approach can be adopted in Figures 2.7 and 2.8.

Figure 2.7 presents a system with a predominant degradation rate over the others and a supply rate vector with comparable elements for each resource. The resources have a similar level of availability to the species. In such cases, the effect of the supply rates on the species' preferences may indeed be considered negligible. The final convex hull of the rescaled metabolic strategies shifts away from the vertex representing the resource that is most likely to undergo degradation.

On the other hand, in the ecosystem simulated in Figure 2.8 the first resource has a significantly higher supply rate compared to the others, while all nutrients have the same degradation rate. Being μ_1 markedly larger than $1\backslash v_1$, the species stop metabolising the first resource as can visually seen in the simplex presented in Figure 2.8: rescaled metabolic strategies squeeze onto the side in which $\tilde{\vec{s}}$ lie.

2.5.7 Degradation Rates in the Adaptive Degradative model with constant supply rate

Allowing the $\alpha_{\sigma i}$ to evolve accordingly to Equation 2.17, it is possible to delve the role of the degradation rates. In the presence of non-zero degradation rates in a system where one of the resources is volatile enough, characterized by μ_j being significantly larger than $1/v_j$, we observe the vanishing of the j-th components of the metabolic strategies. In this scenario, the final convex hull of the rescaled metabolic strategies undergoes a similar "smashing" process as a system with only one unfavorable resource and no degradation rates. The smashing process refers to the reduction or elimination of certain metabolic strategies as they become less advantageous. The relationship between $\vec{\mu}$ of the resources and the rescaled metabolic strategies at stationarity can be enquired in-depth by introducing a term λ, which regulates the magnitude of the degradation rates. Equation 2.16 becomes then:

$$\dot{c}_i = s_i(t) - \sum_{\sigma=1}^{m} n_\sigma \alpha_{\sigma i} r_i(c_i) - \lambda \mu_i c_i \tag{2.37}$$

The dynamics of the system is described then by the set of Equations 2.15, 2.37 and 2.17. Figure 2.9 shows how $\sum_{\sigma=1}^{m} \hat{\alpha}^*_{\sigma i}$, the total uptake of each resource i, varies according to the increasing value of λ while keeping all the parameters and initial conditions fixed across all the simulations. We indicate with p the resource with the higher degradation rate μ_p which corresponds to the lower resource value v_p by construction. Increasing the value of μ_p, through the parameter, making it become sufficiently larger than $1 \,/\, v_p$, determines how gradually the species stop using that resource p. For even greater λ the same will happen to the $p-1$ component of $\sum_{\sigma=1}^{m} \hat{\alpha}^*_{\sigma i}$. Species then minimize the energy needed to metabolize unfavorable or volatile resources, until only the first resource is used.

Moreover, this thesis presents a significant breakthrough by uncovering the "transition" related to the degradation rates vector of the system, which is shown in Figure 2.10. Through the manipulation of only the third component of $\vec{\mu}$ over time while keeping fixed $\mu_1 = \mu_2$ and the other parameters and initial conditions, it has been discovered that it exists a threshold for μ_3 above which all the species stop using the third resource. The area of the final convex hull of the rescaled metabolic strategies experiences an abrupt and peculiar "transition", which is one of the main finding of this thesis. The dynamic of the system for several different values of μ_3 has been studied and the convex hull's area demonstrates a remarkable collapse behavior dependent on $\Delta\mu = \mu_3 - \mu_1$, which is consequently elected to critical parameter. Species cease to utilize the resource once the degradation rate of that nutrient surpasses a specific threshold.

2.5.8 Angular Behaviour of the Metabolic strategies in the Adaptive Non-Degradative model with constant supply rate

This thesis aims to investigate the role of metabolic strategies from various perspectives. One of the main interests of this research is to examine whether metabolic strategies continue to grow in the direction initially taken. To facilitate this analysis, studying a system with $p = 2$ resources is highly advantageous because the corresponding $p-1$ dimensional simplex is a line. By studying the dynamics of the metabolic strategies within the simplex, we can observe how they evolve over time and whether they exhibit growth or convergence towards specific regions of the strategy space in a systematic way. This analysis of the angular behaviour of the metabolic strategies doesn't lead to any particular common pattern in augmenting the number of species under consideration. The absence of a clear energy distribution pattern observed in Figure A.2 dismisses the presence of any significant correlation between the initial and final proportions of resource uptake. The proportion with which species metabolize the two resources exhibits an intricate dynamic, which calls for further exploration from both analytical and computational perspectives. Thus to enhance the flow of reading, it was decided to present the detailed analysis in Appendix A.

Figure 2.2: Time evolution of the Adaptive Model with parameters $v_{gal} = 1.20 \cdot 10^{10}$ cell/g of resource, $v_{eth} = 1.25 \cdot 10^{10}$ cell/g of resource, $K_{gal} = 1.47 \cdot 10^{-3}$ g of resource/mL, $K_{gal} = 9.67 \cdot 10^{-3}$ g of resource/mL, $Y = 0.53$ g of ethanol/g of galactose, $Q = 2.18 \cdot 10^{-5}$ g of resource/cell, $\delta = 2.15 \cdot 10^{-6}$ 1/h, $d = 4.20 \cdot 10^{-6}$ g of resource/cell, , $d = 4.20 \cdot 10^{-6}$ g of resource/cell, $\alpha_{gal}(0) = 1.50 \cdot 10^{-11}$ g of resource/(cell $\cdot$ h), $\alpha_{eth}(0) = 7.75 \cdot 10^{-12}$ g of resource/(cell $\cdot$ h). (1) Time evolution of the population density: diauxic behaviour. (2) Time evolution of the concentration of the resources. Firstly galactose is consumed and sequentially, from its fermentation, ethanol is produced and used. (3) Time evolution of the metabolic strategies: they balance each other to maintain the total maximum uptake constant. (4) Time evolution of the constraint of Equation 2.29.

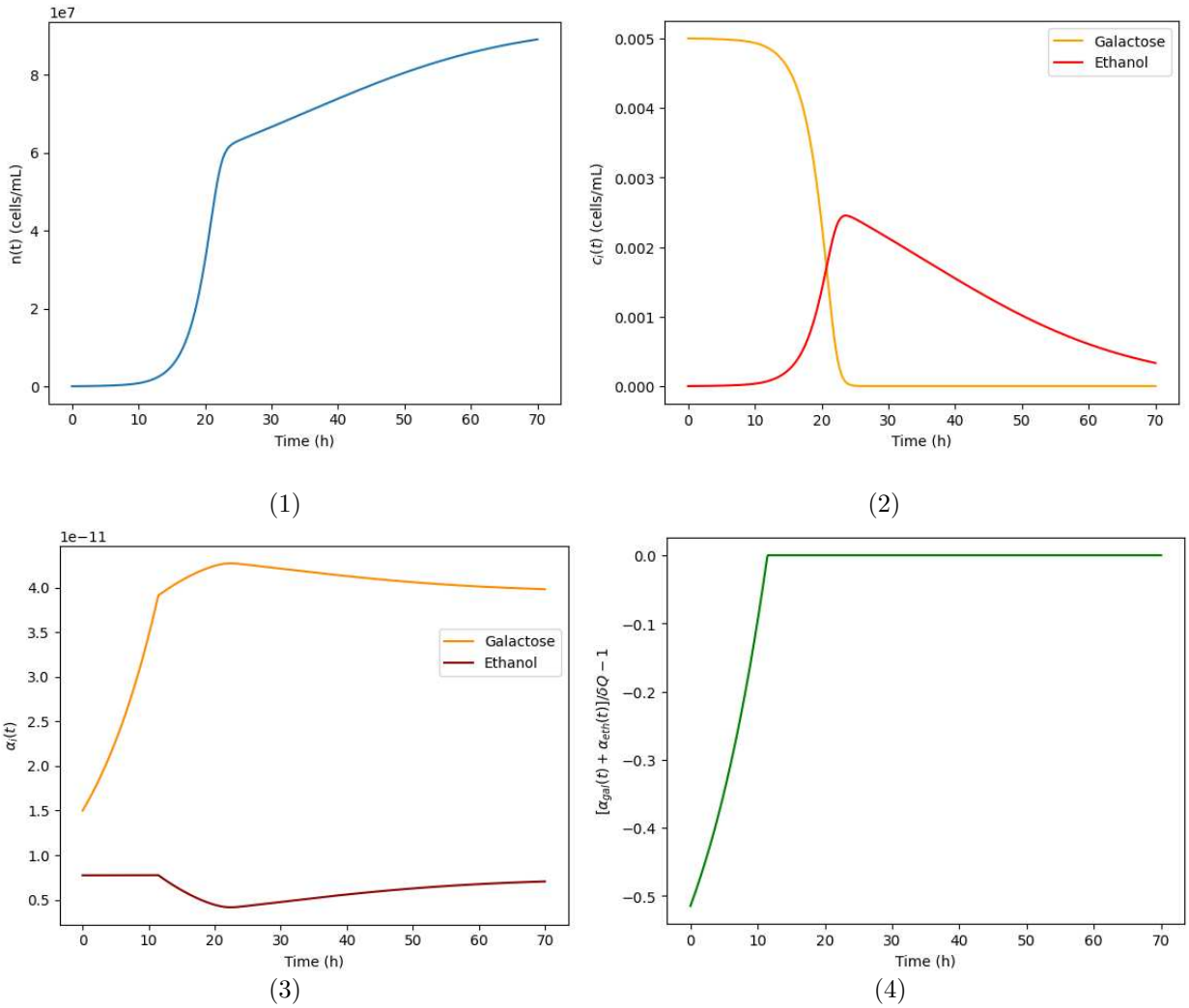

Figure 2.3: Time evolution in the Static and the Adaptive Model framework, with null degradation rates. In this simulation we consider $m = 10$ species, $p = 3$ resources, $Q \in U[10^{-7}, 5 \cdot 10^{-5}]$ g of resource/cell (with U the uniform distribution), $\delta_\sigma \in U[5 \cdot 10^{-3}, 5 \cdot 10^{-2}]$ 1/h, $E_\sigma(0) \in U[0, Q\delta_\sigma]$ g of resource/(cell · h), $v_i \in U[10^8, 5 \cdot 10^9]$ cell/g of resource, $n_\sigma(0) \in U[10^6, 5 \cdot 10^6]$ cell/mL, $c_i(0) \in U[10^{-3}, 10^{-2}]$ g of resource/mL, $k_i \in U[10^{-4}, 10^{-3}]$ g of resource/mL, $d = 4.20 \cdot 10^{-6}$ g of resource/cell, $s_i \in U[10^{-3}, 10^{-2}]$ g of resource/(mL·h) and $\alpha_{\sigma i}(0)$ such that $\sum_{i=1}^{p} \alpha_{\sigma i}(0) = E_\sigma(0)$. (1) and (2): Comparison of the time evolution of the species' density populations between the (1) Adaptive and (2) Static framework, with same initial conditions. (3) Time evolution of the rescaled metabolic strategies. (4) Time evolution of $E_\sigma(t)/Q\delta_\sigma$: as it should, the radius saturates for every species. (5) Initial simplex with the rescaled metabolic strategies $\hat{\alpha}_{\sigma i}$ and the rescaled supply vector of the nutrients $\overrightarrow{\hat{s}}$ (star). (6) Final simplex with the rescaled metabolic strategies that have evolved over time so that the supply vector is included.

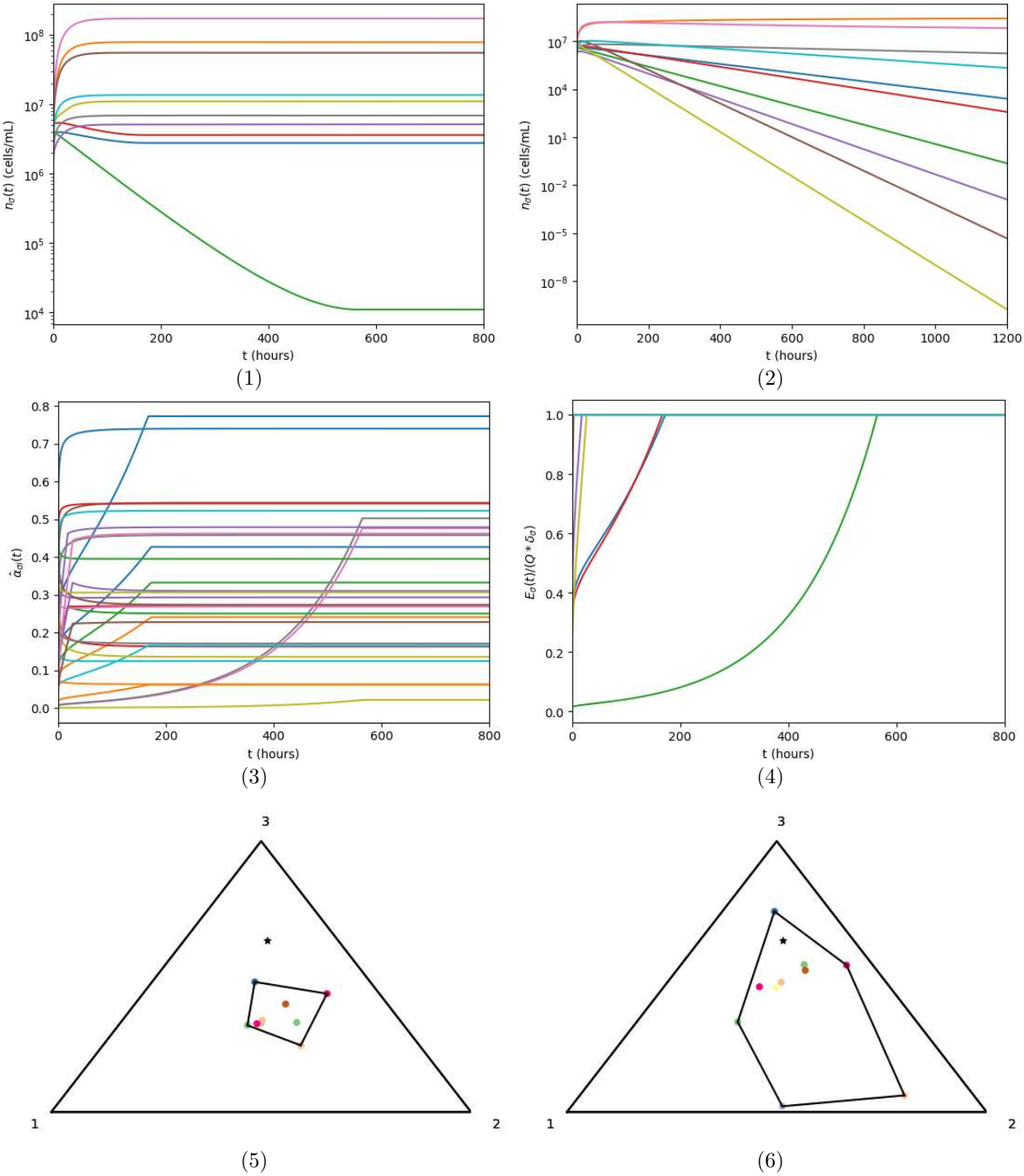

Figure 2.4: Time evolution in the Static and the Adaptive Model framework, with $\vec{s}(t)$ described by Equation 2.30. In this simulation we consider $m = 20$ species, $p = 3$ resources, $Q \in U[10^{-7}, 5 \cdot 10^{-6}]$ g of resource/cell (with U the uniform distribution), $\delta_\sigma \in U[5 \cdot 10^{-3}, 5 \cdot 10^{-2}]$ 1/h, $E_\sigma(0) = Q\delta_\sigma$ g of resource/(cell $\cdot$ h), $v_i \in U[10^8, 5 \cdot 10^9$ cell/g of resource, $n_\sigma(0) \in U[10^6, 5 \cdot 10^6]$ cell/mL, $c_i(0) \in U[10^{-3}, 10^{-2}]$ g of resource/mL, $k_i \in U[10^{-4}, 10^{-3}]$ g of resource/mL, $d = 4.20 \cdot 10^{-6}$ g of resource/cell. $s_i \in U[10^{-3}, 10^{-2}]$ g of resource/(mL $\cdot h$), $sothattherescaledversion_{in}$ lies inside the convex hull of $\vec{\alpha}_\sigma$, and $s_{out} \in U[10^{-3}, 10^{-2}]$ so that $\vec{s}_{out}$ is outside of the convex hull. $\alpha_{\sigma i}(0)$ such that $\sum_{i=1}^{p} \alpha_{\sigma i}(0) = E_\sigma(0)$.
(1) Initial simplex with the convex hull of the rescaled metabolic strategies, in the presence of $\vec{s}_{in}$ (red star) and $\vec{s}_{out}$ (red square). (2) Time evolution of the populations in the Adaptive framework, with τ_{in}=12h and τ_{out}=48h. (3) Time evolution of the populations in the Static framework, with τ_{in}=12h and τ_{out}=48 h. (4) Time evolution of the populations in the Adaptive framework, with τ_{in}=τ_{out}=12h (5) Time evolution of the populations in the Static framework, with τ_{in}=τ_{out}=12h: the duration of the stay of $\vec{s}_{in}$ inside of the convex hull destroys CEP even with fixed metabolic strategies.

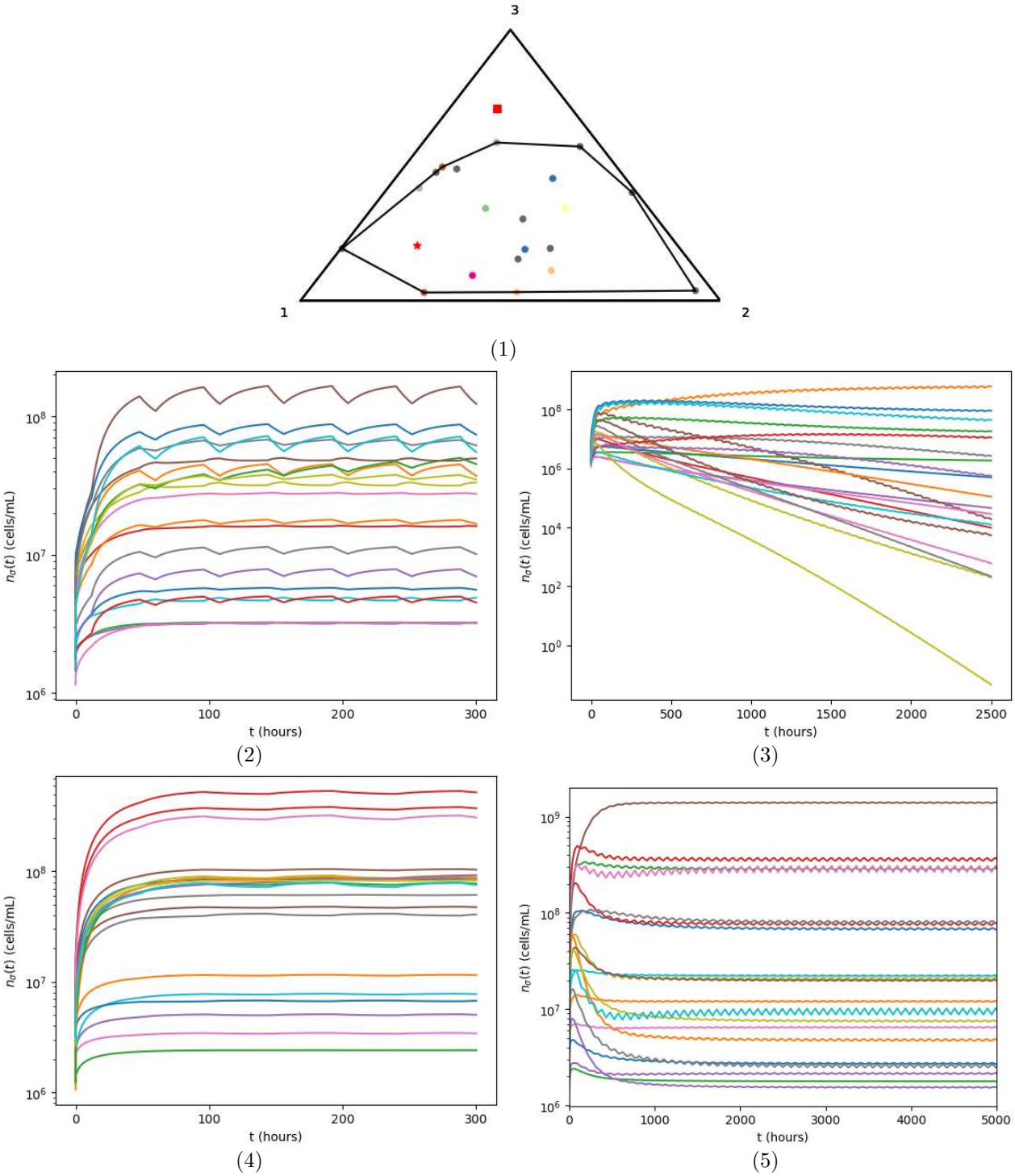

Figure 2.5: Time evolution of the population densities (left) and the energy constraints (right) in the case of an Adaptive Non Degenerating Model. The values of the parameters are chosen from the following distributions and then are kept fixed while performing all the simulations: $m = 10$ species, $p = 3$ resources, $Q \in U[10^{-7}, 5 \cdot 10^{-5}]$ g of resource/cell (with U the uniform distribution), $\delta_\sigma \in U[5 \cdot 10^{-3}, 5 \cdot 10^{-2}]$ 1/h, $E_\sigma(0) \in U[0, Q\delta_\sigma]$ g of resource/(cell $\cdot$ h), $v_i \in U[10^8, 5 \cdot 10^9$ cell/g of resource, $n_\sigma(0) \in U[10^6, 5 \cdot 10^6]$ cell/mL, $c_i(0) \in U[10^{-3}, 10^{-2}]$ g of resource/mL, $k_i \in U[10^{-4}, 10^{-3}]$ g of resource/mL, $d = 4.20 \cdot 10^{-6}$ g of resource/cell, $s_i \in U[10^{-3}, 10^{-2}]$ g of resource/(mL·h) and $\alpha_{\sigma i}(0)$ such that $\sum_{i=1}^{p} \alpha_{\sigma i}(0) = E_\sigma(0)$. d is the only parameter which is changed. (1) and (2): Typical most used value of $d = 4.20 \cdot 10^{-6}$ g of resource/cell. (3) and (4): At $d = 4.20 \cdot 10^{-7}$ g of resource/cell, we start to see the first extinctions and the timescale augments of at least a factor three. (5) and (6): For $d = 4.20 \cdot 10^{-8}$ g of resource/cell, the dynamic is extremely slow so that extremely high times the species don't reach the maximum value of the energy constraint.

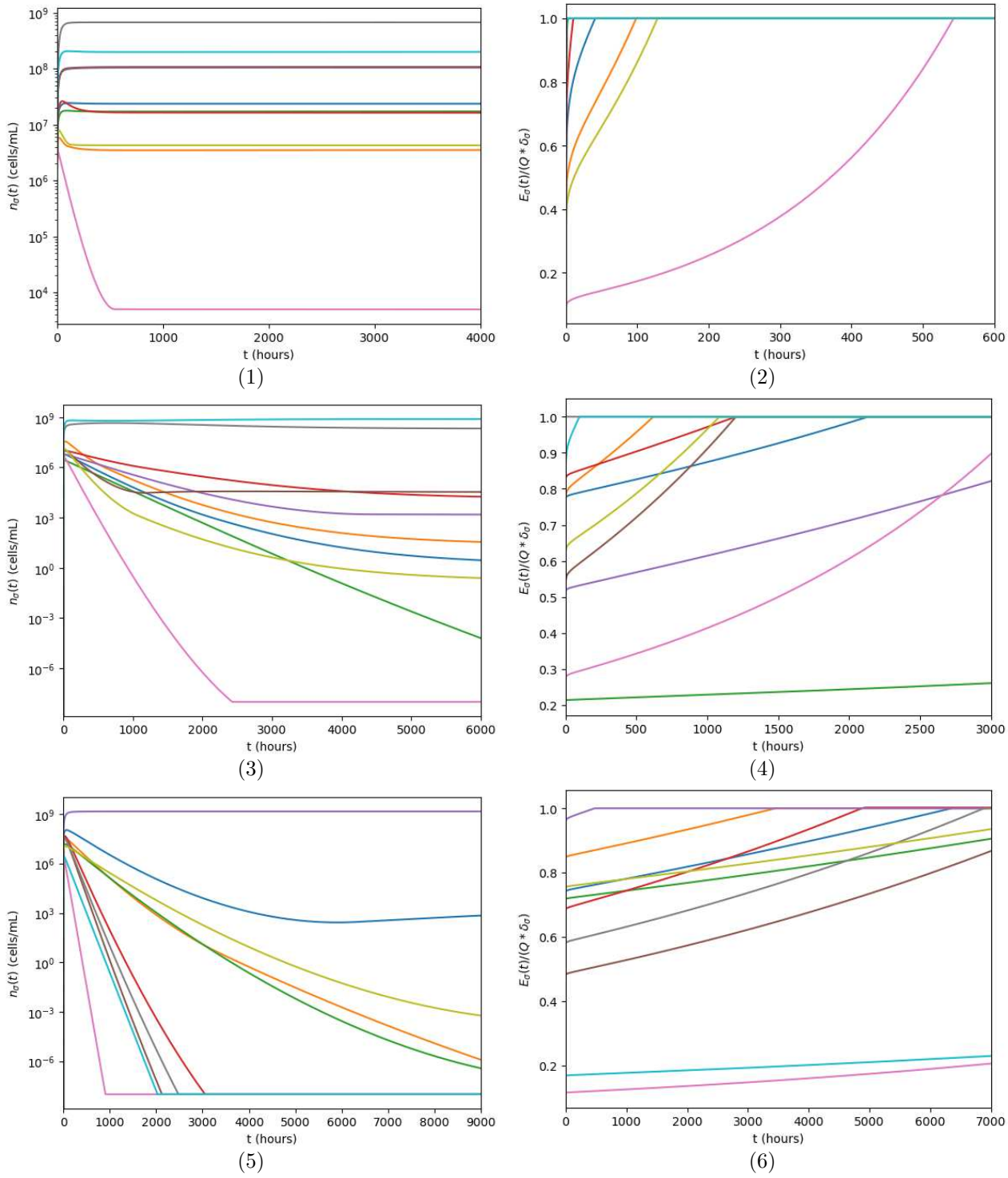

Figure 2.6: Time evolution in the Static and the Adaptive Model framework, in the presence of an unfavorable resource and in the absence of degradation rates. In this simulation we consider $m = 10$ species, $p = 3$ resources, $Q \in U[10^{-8}, 10^{-7}]$ g of resource/cell (with U the uniform distribution), $\delta_\sigma \in U[5 \cdot 10^{-3}, 5 \cdot 10^{-2}]$ 1/h, $E_\sigma(0) = Q\delta_\sigma$ g of resource/(cell $\cdot$ h), $n_\sigma(0) \in U[10^6, 5 \cdot 10^6]$ cell/mL, $c_i(0) \in U[10^{-3}, 10^{-2}]$ g of resource/mL, $k_i \in U[10^{-4}, 10^{-3}]$ g of resource/mL, $d = 4.20 \cdot 10^{-6}$ g of resource/cell. $s_i \in U[10^{-3}, 10^{-2}]$ g of resource/(mL·h), $\alpha_{\sigma i}(0)$ such that $\sum_{i=1}^{p} \alpha_{\sigma i}(0) = E_\sigma(0)$. The resource value is set $\vec{v} = (9 \cdot 10^6, 5.45 \cdot 10^8, 6.5 \cdot 10^7)$ cell/g of resource, so that $1/v_1 > Q$ and $1/v_2, 1/v_3 < Q$. Null degradation rates. (1) Adaptive evolution of the population's dynamics. (2) Time evolution of the rescaled metabolic strategies: the unfavorable resource is not used at stationarity. (3) Initial convex hull of the rescaled metabolic strategies. Present in the simplex the rescaled supply rate vector (star). (4) Final convex hull of the rescaled metabolic strategies. (5) Static evolution of the species. (6) Adaptive evolution of the nutrients' concentration: note the linear behaviour of the concentration of the unfavorable resource. (7) Evolution of the nutrients' concentration in the Static model.

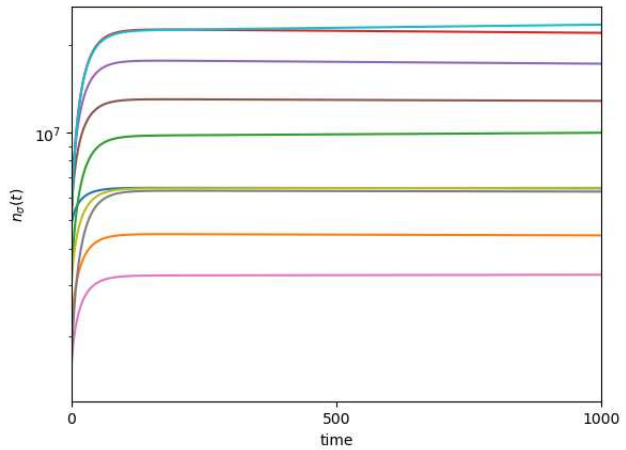

(1)

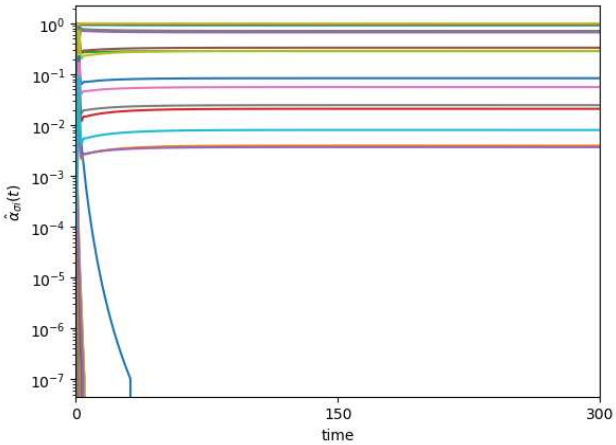

(2)

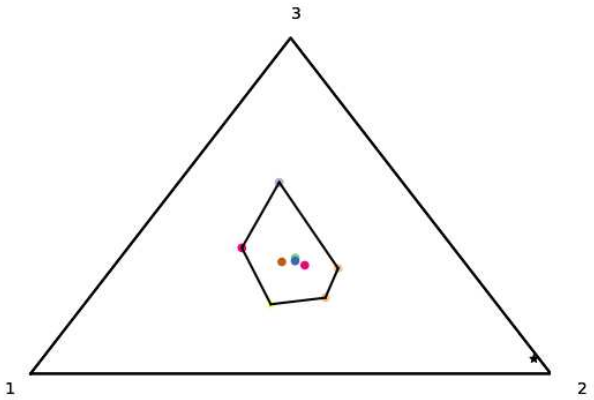

(3)

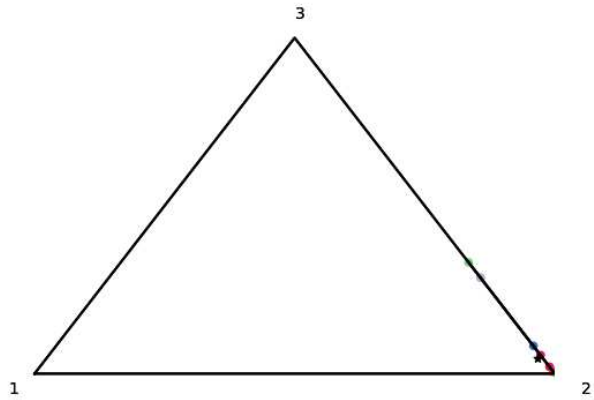

(4)

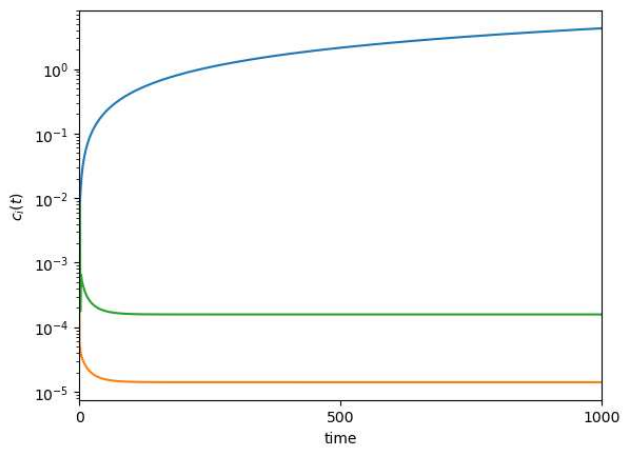

(5)

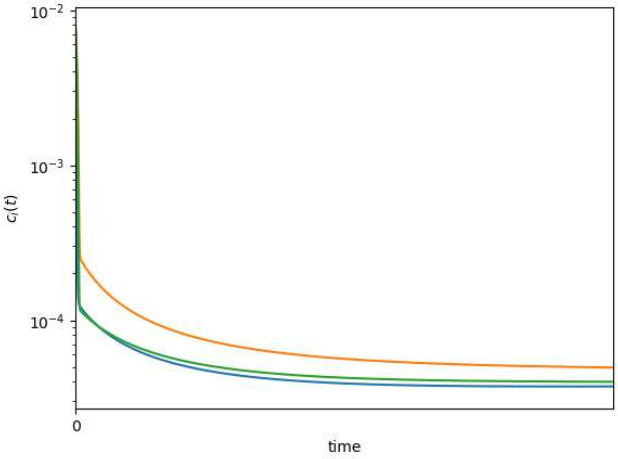

(6)

Figure 2.7: Time evolution in the Static and the Adaptive Model framework with non-null degradation rates. In this simulation we consider $m = 15$ species, $p = 3$ resources, $Q \in U[10^{-7}, 5 \cdot 10^{-7}]$ g of resource/cell (with U the uniform distribution), $\delta_\sigma \in U[5 \cdot 10^{-3}, 5 \cdot 10^{-2}]$ 1/h, $E_\sigma \in U[0, Q\delta_\sigma]$ g of resource/(cell · h), $n_\sigma(0) \in U[10^6, 5 \cdot 10^6]$ cell/mL, $c_i(0) \in U[10^{-3}, 10^{-2}]$ g of resource/mL, $k_i \in U[10^{-4}, 10^{-3}]$ g of resource/mL, $d = 4.20 \cdot 10^{-6}$ g of resource/cell, $\mu = [9000, 1000, 1000]$ $s_i \in U[10^{-3}, 10^{-2}]$ g of resource/(mL·h),$\alpha_{\sigma i}(0)$ such that $\sum_{i=1}^{p} \alpha_{\sigma i}(0) = E_\sigma(0)$. $v \in U[10^9, 5 \cdot 10^9]$. The resources values extracted are that such that $v_1 \approx v_2 \approx v_3$, so species don't have a preference for any specific resource. (1) Adaptive evolution of the population's dynamics. (2) Static evolution of the population's dynamic. (3) Time evolution of the rescaled metabolic strategies. (4) Time evolution of the energy constraint. (5) Initial convex hull of the rescaled metabolic strategies. Present in the simplex the rescaled supply rate vector (star). (6) Final convex hull of the rescaled metabolic strategies, which is slightly away from the vertex corresponding to the resource with the greatest degradation rate. $\tilde{\vec{s}}$ is represented by a triangle.

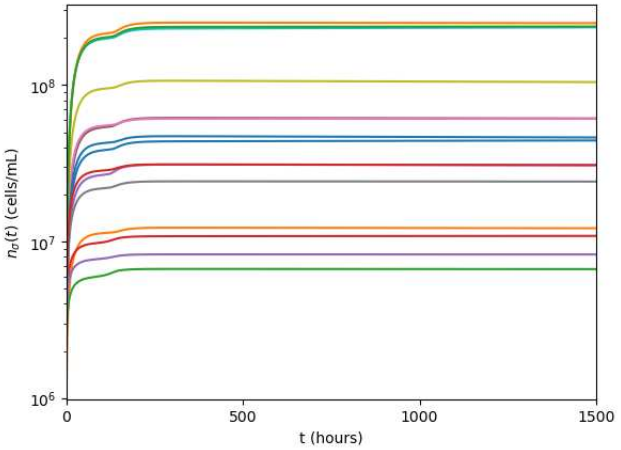

(1)

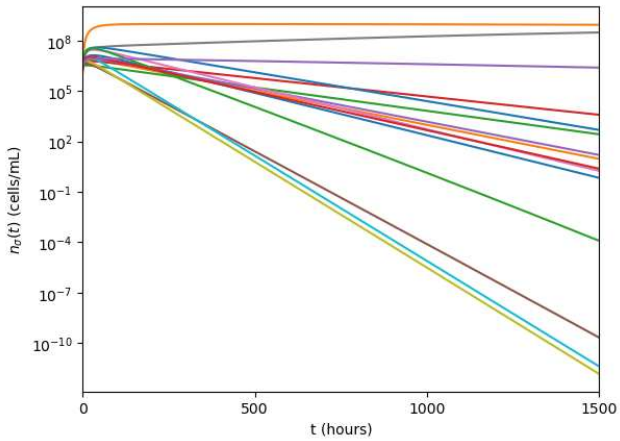

(2)

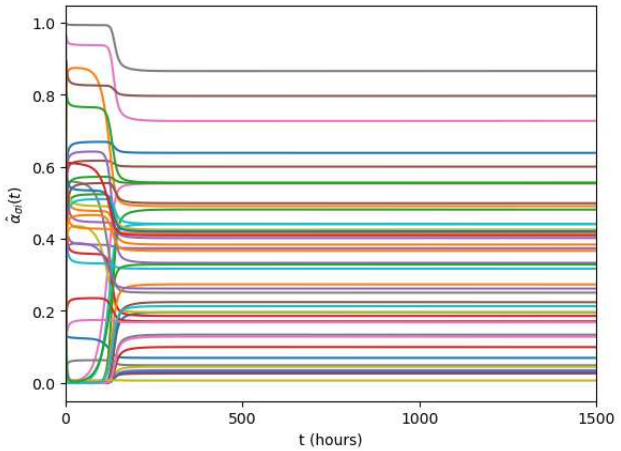

(3)

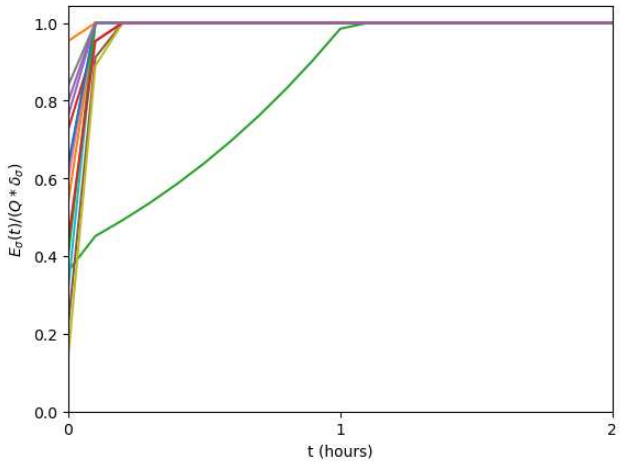

(4)

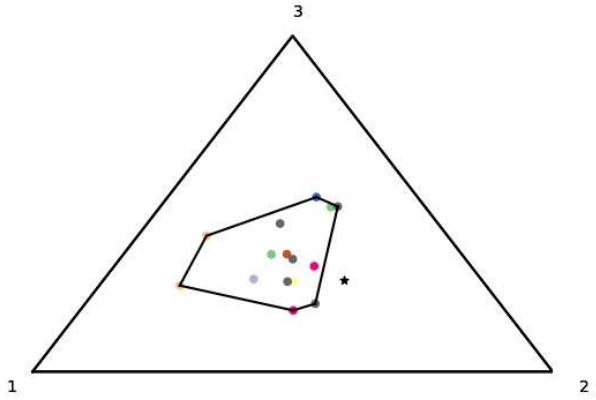

(5)

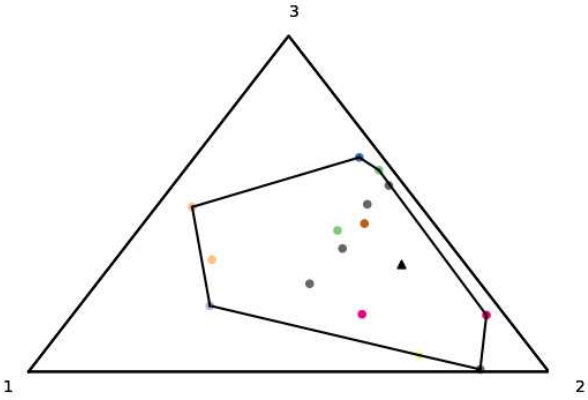

(6)

Figure 2.8: Time evolution in the Static and the Adaptive Model framework with equal degradation rates for all the species and a predominant resource value over the others. In this simulation we consider $m = 15$ species, $p = 3$ resources, $Q \in U[10^{-7}, 5 \cdot 10^{-7}]$ g of resource/cell (with U the uniform distribution), $\delta_\sigma \in U[5 \cdot 10^{-3}, 5 \cdot 10^{-2}]$ 1/h, $E_\sigma \in U[0, Q\delta_\sigma]$ g of resource/(cell $\cdot$ h), $n_\sigma(0) \in U[10^6, 5 \cdot 10^6]$ cell/mL, $c_i(0) \in U[10^{-3}, 10^{-2}]$ g of resource/mL, $k_i \in U[10^{-4}, 10^{-3}]$ g of resource/mL, $d = 4.20 \cdot 10^{-6}$ g of resource/cell, $\mu = [9000, 9000, 9000]$, $s_i \in U[10^{-3}, 10^{-2}]$ g of resource/(mL·h), $\alpha_{\sigma i}(0)$ such that $\sum_{i=1}^{p} \alpha_{\sigma i}(0) = E_\sigma(0)$. Moreover $\nu \in U[10^9, 5 \cdot 10^9]$ cell/g of resource. The resources values extracted are that such that $\nu_1 > \nu_2 \gg \nu_3$. (1) Adaptive evolution of the population's dynamics. (2) Static evolution of the population's dynamic. (3) Time evolution of the rescaled metabolic strategies. (4) Time evolution of the energy constraint. (5) Initial convex hull of the rescaled metabolic strategies and the rescaled supply rate vector (star) in the simplex. (6) Final convex hull of the rescaled metabolic strategies. All metabolic strategies have converged onto the same side, which is farthest from the less supplied resource, where lies $\tilde{\vec{s}}$ (triangle).

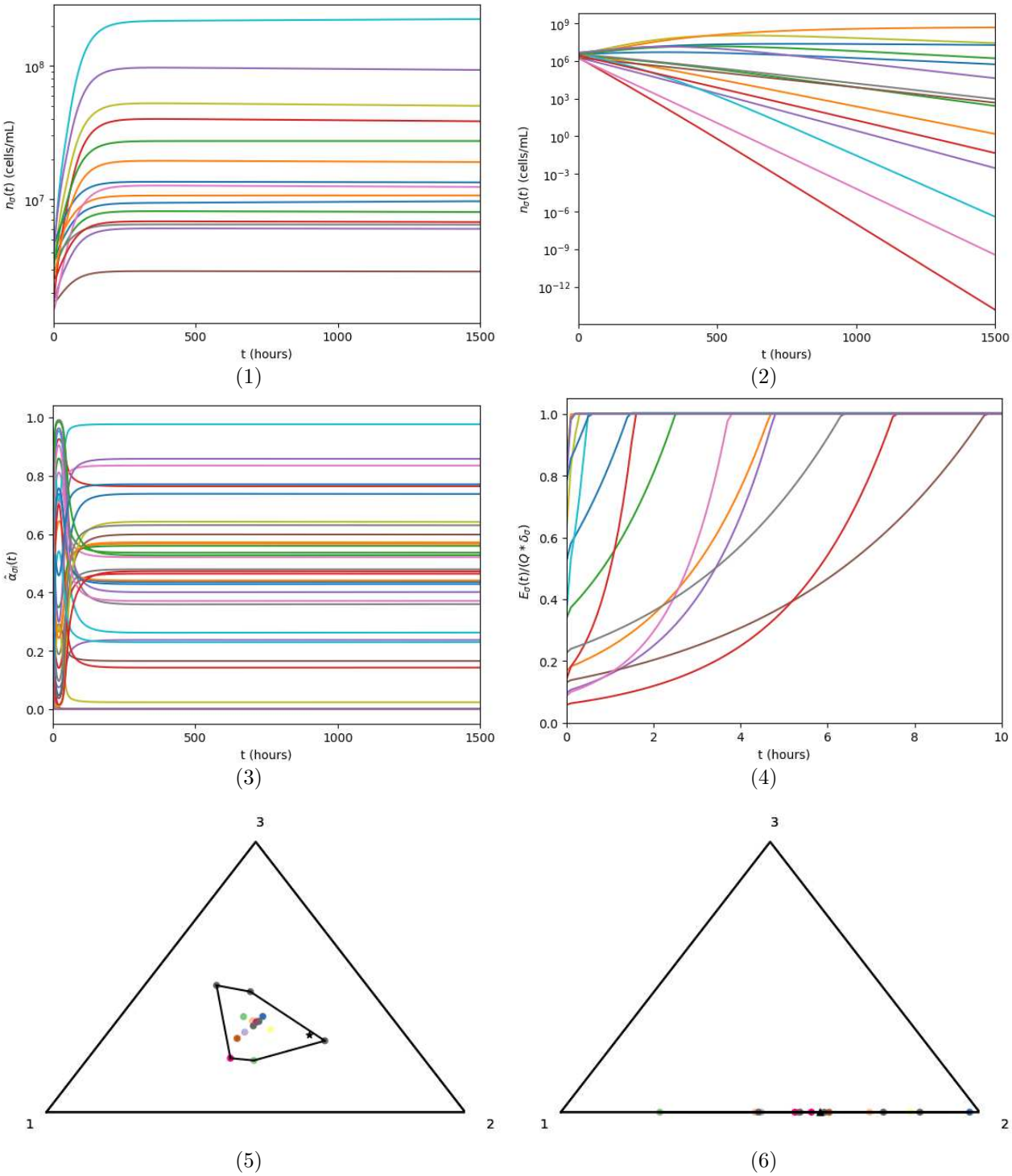

Figure 2.9: Total uptake of i-th resource for increasing value of the degradation rates. In this simulation we consider $m = 20$ species, $p = 3$ resources, $Q \in U[10^{-7}, 10^{-6}]$ g of resource/cell (with U the uniform distribution), $\delta_\sigma \in U[5 \cdot 10^{-3}, 5 \cdot 10^{-2}]$ 1/h, $E_\sigma(0) \in U[0, Q\delta_\sigma]$ g of resource/(cell $\cdot$ h), $v_i \in U[10^8, 5 \cdot 10^9$ cell/g of resource, $n_\sigma(0) \in U[10^6, 5 \cdot 10^6]$ cell/mL, $c_i(0) \in U[10^{-3}, 10^{-2}]$ g of resource/mL, $k_i \in U[10^{-4}, 10^{-3}]$ g of resource/mL, $d = 4.20 \cdot 10^{-6}$ g of resource/cell, $s_i \in U[10^{-3}, 5 \cdot 10^{-2}]$ g of resource/(mL·h), $\mu_i \in U[10^3, 5 \cdot 10^{-3}]$ and $\alpha_{\sigma i}(0)$ such that $\sum_{i=1}^{p} \alpha_{\sigma i}(0) = E_\sigma(0)$. Once the values of v_i and μ_i have been extracted from the distributions, we proceeded to order them such that $1/v_1 < ... < 1/v_p$ and $\mu_1 < ... < \mu_p$. The initial parameters and the initial conditions are kept fixed across all the simulations. The p resource is the first to be rejected from the species and then, as λ increases, only the $p - 2$ resource is used.

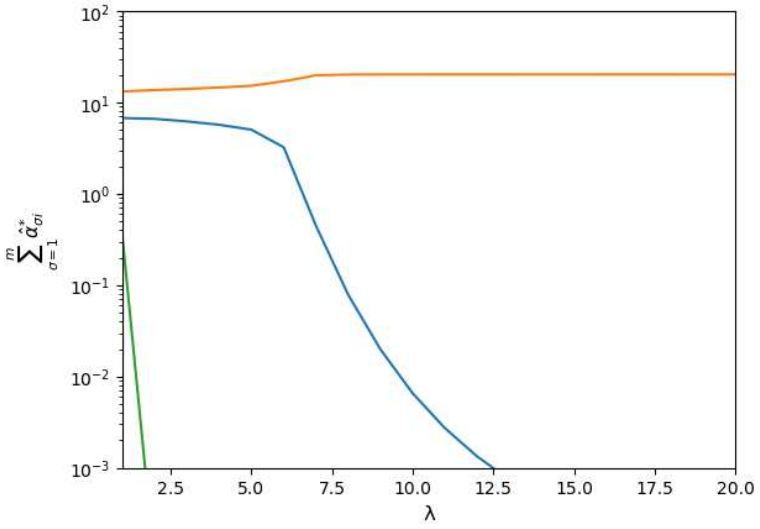

Figure 2.10: "Transition" of the Area of the Convex Hull of the rescaled metabolic strategies, where $\Delta\mu = \mu_3 - \mu_1$ is the critical parameter. The system is composed by $m = 15$ species, $p = 3$ resources. All the simulations are performed by keeping the others parameters and initial conditions fixed, once extrapolated from the following distributions. $Q \in U[10^{-7}, 5 \cdot 10^{-7}]$ g of resource/cell (with U the uniform distribution), $\delta_\sigma \in U[5 \cdot 10^{-3}, 5 \cdot 10^{-2}]$ 1/h, $E_\sigma \in U[0, Q\delta_\sigma]$ g of resource/(cell $\cdot$ h), $n_\sigma(0) \in U[10^6, 5 \cdot 10^6]$ cell/mL, $c_i(0) \in U[10^{-3}, 10^{-2}]$ g of resource/mL, $k_i \in U[10^{-4}, 10^{-3}]$ g of resource/mL, $d = 4.20 \cdot 10^{-6}$ g of resource/cell, $v_i \in U[10^9, 5 \cdot 10^9]$ cell/g of resource, $s_i \in U[10^{-3}, 10^{-2}]$ g of resource/(mL·h), $\alpha_{\sigma i}(0)$ such that $\sum_{i=1}^{p} \alpha_{\sigma i}(0) = E_\sigma(0)$. TThis figure illustrates the existence of a threshold value for the most unfavorable degradation rate, beyond which the resource is suddenly disregarded.

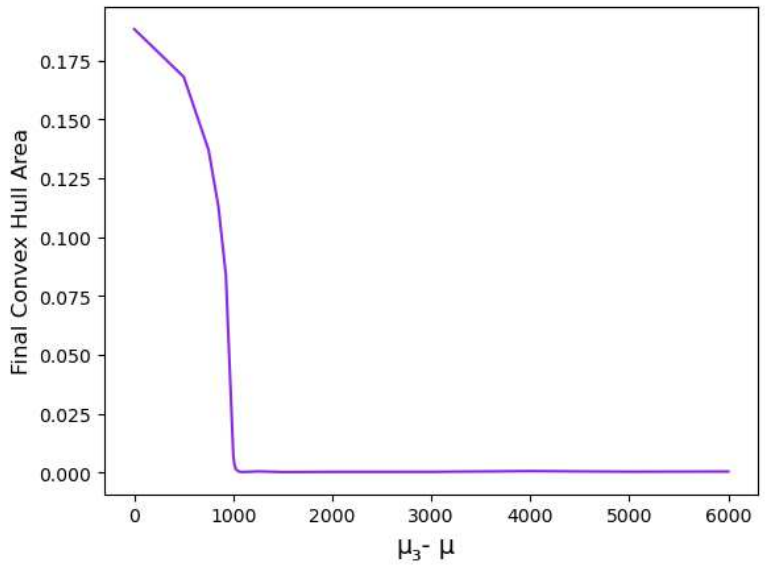

THE INTERACTIVE MODEL

In this chapter, we are going to describe the Gupta, Garlaschi, Suweis, Azaele and Maritan's Model [20], referred to thereafter as Interactive Model.

The foundational framework is once again the MacArthur's consumer-resource model, to which we include the Janzen-Connell effect (JCE), which describes the unavailability for the seedlings close to the parent trees due to the presence of the host-specific pathogens. A new term arises in the dynamic of the populations' densities, which stabilises species interactions [30], [12], [50]. This creates an inhibition of their growth and determines a threshold in the crowding of the same species [2], [3], [10]. By incorporating this additional term, it becomes possible to violate the Competition Exclusion Principle.

Considering just pathogens that are specific to each species and assuming that individuals interact only inside the same species's group, it is possible to analytically describe the coexistence region in the space of the functions where all the initial species survive. Fundamental is the role of the supply rate: the formal expression of the threshold value of $\overline{\Lambda}$ above which all the several species competing for one resource survive. It is even possible to address the validity of the CEP below the cut-off, defining a specific $\Lambda^{(l)}$ such $l < m$ species survive.

3.1 Emergence of the quadratic interaction term

In this context the equations that describe the time evolution of the system are:

$$\dot{n}_\sigma = n_\sigma \left(\sum_{i=1}^{p} v_i r_i(c_i)\ \alpha_{\sigma i}\ - \delta_\sigma \right) - n_\sigma \sum_{a=1}^{M_P} A^{(p)}_{\sigma a} p_a \tag{3.1}$$

$$\dot{c}_i = \Lambda_i \mu_i - \sum_{\sigma=1}^{m} n_\sigma \alpha_{\sigma i} r_i(c_i) - \mu_i c_i \tag{3.2}$$

$$\dot{p}_a = p_a \sum_{\rho=1}^{m} B^{(p)}_{a\rho} n_\rho - k^{(p)}_a p^2_a \tag{3.3}$$

We introduced p_a, the population of the pathogens at time t and M_P the number of different types of pathogens. In Equation 3.1 the last term contains the matrix $A^{(p)}$, which represents the degradation rate of the σ-th species due to the presence of the pathogens $a = 1, ..., M_P$. While the population of the species goes to extinction, pathogens are in a favorable situation, which is represented by the benefit matrix $B^{(p)}$ in Equation 3.3.
Given $1/k^{(p)}_a$, which is the carrying capacity for the pathogen a, the term $-k^{(p)}_a p^2_a$ represents the threshold of the growth of the pathogen's population in Equation 3.3. This is coherent with experimental observations of production of toxins from certain strains of microbes, which are harmful for other strains of the microbial community or even for them [14] [18] [16].

We notice that, in this model, it is underlined the dependence of the rate of supply of abiotic resources s_i on the degradation rates, in fact $s_i = \Lambda_i \mu_i$, where Λ_i is the carrying capacity of the i-th resource. The growth of the pathogens is characterised by a timescale which is much faster than the timescales

associated to the evolution of the species' population and the resource concentration. Straightforwardly, we assume quasi-stationarity, evaluating the stationary state of the dynamics of pathogens. Equation 3.3 becomes:

$$p_a(t) \sum_{\rho=1}^{m} B_{a\rho}^{(p)} n_\rho(t) - k_a^{(p)} p_a^2(t) = 0 \tag{3.4}$$

The instantaneous non-zero value at stationarity of the population of pathogens $p_a(t)$ for the species population $\dot{n}_\sigma$ is then:

$$p_a(t) = \frac{\sum_{\rho=1}^{m} B_{a\rho}^{(p)} n_\rho(t)}{k_a^{(p)}} \tag{3.5}$$

The solution to this equation can be expresses as a product of matrices:

$$\vec{P}(t) = [K^{(p)}]^{-1} B^{(p)} \vec{N}(t) \tag{3.6}$$

where $K^{(p)} = \text{diag}(k_1^{(p)}, ..., k_{M_P}^{(p)})$ is a diagonal matrix and $\vec{N}(t) = (n_1(t), ...n_m(t))^T$. Substituting the values of p_a in Equations 3.1, we obtain

$$\dot{n}_\sigma = n_\sigma \left(\sum_{i=1}^{p} v_i r_i \ \alpha_{\sigma i} \ - \delta_\sigma \right) - n_\sigma \sum_{a=1}^{M_P} A_{\sigma a}^{(p)} \frac{\sum_{\rho=1}^{m} B_{a\rho}^{(p)} n_\rho(t)}{k_a^{(p)}} \tag{3.7}$$

The time evolution of the species' population can be the written as:

$$\dot{n}_\sigma = n_\sigma \left(\sum_{i=1}^{p} v_i r_i \ \alpha_{\sigma i} \ - \delta_\sigma \right) - n_\sigma \sum_{\rho=1}^{m} \epsilon_{\sigma\rho} n_\rho(t) \tag{3.8}$$

if we define the epsilon term as

$$\epsilon_{\sigma\rho} \coloneqq \sum_{a=1}^{M_P} A_{\sigma a}^{(p)} \frac{B_{a\rho}^{(p)}}{k_a^{(p)}} \tag{3.9}$$

If there is a one-to-one correspondence between pathogens and species ($\sigma = \rho$), $M = M_P$ and consequently the benefit matrix $B^{(p)}$ and the degradation matrix $A^{(p)}$ becomes diagonal, which leads to the invertible matrix $E = \text{diag}(\epsilon_1, ...\epsilon_M)$ where $\epsilon_{\sigma\sigma} = \epsilon_\sigma$.
For the sake of simplicity, we set $v_i = 1 \ \forall \ i$.

The epsilon's term can arise also from introducing a spacial contribution to the dynamics of the species' population designed in the MacArthur's model to obtain:

$$\dot{n}_\sigma(\vec{x}) = n_\sigma(\vec{x}) \left(\sum_{i=1}^{p} v_i r_i(c_i(\vec{x})) \ \alpha_{\sigma i} \ - \delta_\sigma \right) - \vec{\nabla} \cdot J_{n_\sigma}(\vec{x}, t), \tag{3.10}$$

where $\vec{x}$ are the spacial degrees of freedom and the flux $J_{n_\sigma}(\vec{x}, t)$ contains in itself different ecological mechanisms: among them chemotaxis [28], crowding effects arising from competition in a local limited area and the existence of a threshold to prevent avoid overcrowding [14] [18] [16].

The derivation specifics are elaborated in Appendix B. However, at a high level, the spatial variable is discretized within a one-dimensional lattice, where each site $i \in \mathbb{Z}$ represents an area of linear size a with species' population $n_\sigma^{(i)}$ and resource concentration $c^{(i)}$. The model is able then to describe the migration of species from one area to the other due to the consumption of the resource. The main step now is to eliminate the dynamical variables $n_\sigma^{(i)}$ and $c^{(i)}$, where i corresponds to an odd position in the lattice. This coarse-graining technique could be seen also as the first step of the renormalisation group technique [9] [58]. This second approach leads to the emergence of the new carrying capacity term $\epsilon_{\sigma\rho}$, which describes the interaction of species σ with species ρ.

The matrices $\epsilon_{\sigma\rho}$ and $\alpha_{\sigma i}$ could in general be correlated. However, we are going to study a context in the presence of pathogens, so we can assume that the metabolic strategies and the interaction proportionality term are drawn from two independent distributions [41].

3.2 Coexistence given two resources

We are going to focus on the specific case of three species ($m = 3$) and two abiotic resources ($p = 2$). The case for which $\epsilon_{\sigma\rho} \to 0$ for $\sigma \neq \rho$ is analytically treatable, because the Equation 3.8 and 3.2 end up creating the following system:

$$\dot{n}_\sigma = n_\sigma \left[\sum_{i=1}^{p} \nu_i r_i \ \alpha_{\sigma i} \ - \delta_\sigma - \epsilon_\sigma n_\sigma \right] \tag{3.11}$$

$$\dot{c}_i = \Lambda_i \mu_i - \sum_{\sigma=1}^{m} n_\sigma \alpha_{\sigma i} r_i - \mu_i c_i \tag{3.12}$$

We assume that $\mu_i = \mu \ \forall \ i$.
We expect the system to evolve and to reach a stationary state characterised by $n^*_\sigma > 0 \ \forall \ \sigma$. If all the species survive (violation of CEP), then we can write $\dot{n}_\sigma = 0$ and $\dot{c}_i = 0$ for long times as:

$$\vec{N} = E^{-1}(AR\mathbb{I} - \vec{B}) \tag{3.13}$$

$$\mu(\vec{L} - \vec{\chi}) = RA^T\vec{N} \tag{3.14}$$

where $\vec{N} = (n^*_1, ..., n^*_m)^T$, $\vec{B} = (\delta_1, ..., \delta_m)^T$, $\vec{L} = (\Lambda_1, ..., \Lambda_p)^T$, $E = \text{diag}(\epsilon_1, ..., \epsilon_M)$, $\mathbb{I} = (1, ...1)^T$ is a p component vector. The A matrix is made of the metabolic strategies $\alpha_{\sigma i}$ and $R = \text{diag}[r_1(c^*_i), ..., r_p(c^*_p]$. Recalling the form of the Monod function, $c_i = \frac{k_i}{1-r_i}$.

Substituting 3.13 in 3.14 we get p coupled equations:

$$\mu(\vec{L} - \vec{\chi}) = RA^TE^{-1}AR\mathbb{I} - RA^TE^{-1}\vec{B} \tag{3.15}$$

Explicitly in the case for $m = 3$ and $p = 2$, this system can be written as:

$$r_1\left[\frac{\alpha_{21}(r_1\alpha_{21} + r_2\alpha_{22} - \beta_2)}{\epsilon_2} + \frac{\alpha_{31}(r_1\alpha_{31} + r_2\alpha_{32} - \beta_3)}{\epsilon_3} - \frac{\beta_1\alpha_{11}}{\epsilon_1} + \frac{\alpha_{11}(r_1\alpha_{11} + r_2\alpha_{12})}{\epsilon_1}\right] = \mu\left(\Lambda_1 - \frac{r_1k_1}{1-r_1}\right) \tag{3.16}$$

$$r_2\left[\frac{\alpha_{22}(r_1\alpha_{21} + r_2\alpha_{22} - \beta_2)}{\epsilon_2} + \frac{\alpha_{32}(r_1\alpha_{31} + r_2\alpha_{32} - \beta_3)}{\epsilon_3} - \frac{\beta_1\alpha_{12}}{\epsilon_1} + \frac{\alpha_{12}(r_1\alpha_{11} + r_2\alpha_{12})}{\epsilon_1}\right] = \mu\left(\Lambda_2 - \frac{r_2k_2}{1-r_2}\right) \tag{3.17}$$

Now considering the Equation 3.13, we can study the condition $(AR\mathbb{I})_\sigma > \vec{B}_\sigma \ \forall\sigma$ for which all the species survive. The condition for the violation of the Competition Exclusion principle is that the solutions $r_i(c^*_i)$ lie inside the region given by:

$$\alpha_{11}r_1\left(c^*_1\right) + \alpha_{12}r_2\left(c^*_2\right) > \beta_1 \tag{3.18}$$

$$\alpha_{21}r_1\left(c^*_1\right) + \alpha_{22}r_2\left(c^*_2\right) > \beta_2 \tag{3.19}$$

$$\alpha_{31}r_1\left(c^*_1\right) + \alpha_{32}r_2\left(c^*_2\right) > \beta_3 \tag{3.20}$$

Figure 3.2 displays the region of coexistence of three species in the presence of two resources, as described by equations 3.18, 3.19, 3.20.

3.3 Critical value $\Lambda^{(l)}$ for l surviving species given one resource

We are going to study what is the value of Λ for which all the several m initial species survive. For $p = 1$, the stationary (*) Equation 3.13 becomes $\forall\sigma$:

$$n^*_\sigma = \frac{\alpha_\sigma r\left(c^*\right) - \delta_\sigma}{\epsilon_\sigma} \tag{3.21}$$

Considering that $n^*_\sigma > 0\ \forall\sigma$, we find $r(c^*) > \frac{\delta_\sigma}{\alpha_\sigma}$.

We define the coefficients $A = \sum_{\sigma=1}^{m} \frac{\alpha_\sigma^2}{\epsilon_\sigma}$ and $B = \sum_{\sigma=1}^{m} \frac{\alpha_\sigma \delta_\sigma}{\epsilon_\sigma}$. From Equation 3.15, we can derive $r(c^*)$:

$$\begin{aligned} \mu\left(\Lambda - c^*\right) &= r^2\left(c^*\right) \sum_{\sigma=1}^{m} \frac{\alpha_\sigma^2}{\epsilon_\sigma} - r\left(c^*\right) \sum_{\sigma=1}^{m} \frac{\alpha_\sigma \delta_\sigma}{\epsilon_\sigma} \\ &= A r^2\left(c^*\right) - B r\left(c^*\right) \end{aligned} \tag{3.22}$$

Considering the form of the Monod function, we know that $r(c^*) \leq 1$, which means that $\alpha_\sigma > \delta_\sigma$ is the condition to guarantee the coexistence of all the species.
Given the fixed parameters $\{\alpha_\sigma, \delta_\sigma, \epsilon_\sigma\}$ that characterise every species in the presence of one resource and given a fixed degradation rate μ, the violation of the Competitive Exclusion Principle is observed when we vary Λ in such a way that $r(c^*) > r(\overline{c}) \coloneqq \max_\sigma\{\delta_\sigma/\alpha_\sigma\}$.

The critical value $\overline{\Lambda}$ above which we observe the coexistence of all the species is inferred from Equation 3.22.

$$\overline{\Lambda} = \frac{r(\overline{c})\left[A r(\overline{c}) - B\right]}{\mu} + \overline{c} \tag{3.23}$$

3.4 Critical value $\overline{\Lambda}$ for total coexistence given one resource

If $\Lambda < \overline{\Lambda}$, we are in the most general case in which not all the species may survive. In the presence of one resource, we are going to compute the critical value Λ^l, for the survival of l species out of the initial $m \geq l$ ones.

The metabolic strategies play a leading role in defining which species can survive or die: $n_\sigma = 0$ if $\alpha_\sigma \leq \tilde{\alpha}$. For this reason we introduce an Heaviside function $H(\alpha_\sigma - \tilde{\alpha})$ in Equation 3.21 such that $H(\alpha_\sigma \geq \tilde{\alpha}) = 1$ and $H(\alpha_\sigma \leq \tilde{\alpha}) = 0$.
The stationary state is then described by the two following equations:

$$n^*_\sigma = \frac{\alpha_\sigma \tilde{r}\left(c^*\right) - \delta_\sigma}{\epsilon_\sigma} H(\alpha_\sigma - \tilde{\alpha}) \tag{3.24}$$

where $\tilde{r}\left(c^*\right)$ is derived from Equation 3.12 in the stationary state ($\dot{c}_i = 0$):

$$\tilde{r}\left(c^*\right) = \frac{\mu\left(\Lambda - c^*\right)}{\sum_{\sigma=1}^{m} n^*_\sigma \alpha_\sigma} \tag{3.25}$$

Inserting n^*_σ from Equation 3.24 in Equation 3.23 we find

$$\mu\left(\Lambda - c^*\right) = \tilde{r}^2\left(c^*\right) \sum_{\sigma=1}^{m} \frac{\alpha_\sigma^2}{\epsilon_\sigma} H(\alpha_\sigma - \tilde{\alpha}) - \tilde{r}\left(c^*\right) \sum_{\sigma=1}^{m} \frac{\alpha_\sigma \delta_\sigma}{\epsilon_\sigma} H(\alpha_\sigma - \tilde{\alpha}) \tag{3.26}$$

We further identify the coefficients that carry the main features of the species as $\tilde{A} = \sum_{\sigma=1}^{m} \frac{\alpha_\sigma^2}{\epsilon_\sigma} H(\alpha_\sigma - \tilde{\alpha})$ and $\tilde{B} = \sum_{\sigma=1}^{m} \frac{\alpha_\sigma \delta_\sigma}{\epsilon_\sigma} H(\alpha_\sigma - \tilde{\alpha})$ so that Equation 3.25 can be written in a more compact way:

$$\mu\left(\Lambda - c^*\right) = \tilde{A}\tilde{r}^2\left(c^*\right) - \tilde{B}\tilde{r}\left(c^*\right) \tag{3.27}$$

Assuming $\delta_\sigma = 1$, from Equation 3.23, we can see that $n^*_\sigma > 0$ if

$$\begin{aligned} \tilde{r}\,(c^*) &> \alpha_l^{-1} \\ &= \tilde{r}(\overline{c}) = \max\{\alpha_\sigma^{-1} \mid 1 \leq \sigma \leq l\} \end{aligned} \tag{3.28}$$

where l is the number of surviving species starting from m initial species.

If we arrange the species in descending order in α: $\{\alpha_1, \epsilon_1; ...; \alpha_m, \epsilon_m\}$, such that the species described by α_1 and ϵ_1 has the highest α, we can identify the parameters describing the cut-off $\tilde{\alpha}$:

$$A_l^{(c)} = \sum_{j=1}^{l} \frac{\alpha_j^2}{\epsilon_j} \tag{3.29}$$

$$B_l^{(c)} = \sum_{j=1}^{l} \frac{\alpha_j \delta_j}{\epsilon_j} \tag{3.30}$$

Recalling the form of $\overline{c} = \frac{k\tilde{r}(\overline{c})}{1-\tilde{r}(\overline{c})}$, we obtain the critical supply rate for the survival of the first l species,

$$\Lambda^{(l)} = \frac{\tilde{r}\,(\overline{c})\,[A_l^{(c)}\tilde{r}\,(\overline{c}) - B_l^{(c)}]}{\mu} + \frac{k\tilde{r}\,(\overline{c})}{1-\tilde{r}\,(\overline{c})} \tag{3.31}$$

Setting by default $\Lambda^{(m+1)} = \infty$, if $\Lambda^{(l)} < \Lambda < \Lambda^{(l+1)}$ then l species survive. Note that the cut-off turns out to be $\tilde{\alpha} = \alpha_l$.

3.5 Numerical Results

In this section we present some numerical simulations describing the behaviour of the ecosystem described with the Interactive Model. Parameters and variables are evaluated in arbitrary units.

3.5.1 Supply rate in the Interactive Model

Firstly, in Figure 3.1, we highlight the role of Λ, keeping all the other parameters fixed. Using the same value of $\Lambda_1 = 3 \cdot 10^5$, we observe coexistence of the species for $\Lambda_2 = 10^6$. On the other hand species experience extinction for $\Lambda_2 = 5 \cdot 10^5$, because the solution of Equations 3.13 and 3.14 lies outside of the region designed by Equations 3.18, 3.19 and 3.20.

Furthermore, we depict the region of coexistence from Equations 3.18, 3.19 and 3.20. By leveraging the fact that we are examining a system with two resources, Figure 3.2, visually illustrates where the solutions $r_i(c_i^*)$ of Equations 3.16 and 3.17 belong to the area of complete coexistence. Upon observation, we can identify that the first panel in Figure 3.1 corresponds to a scenario within this blue region of total survival of Figure 3.2. Conversely, the less favorable conditions of Λ depicted in the second panel of Figure 3.1 make the Competitive Exclusion Principle hold, placing the system in the pink region of Figure 3.2.

Figure 3.3 provides an analysis of the temporal dynamics of a system comprising m species when a single resource is present. It emphasizes the significance of assessing Λ in predicting the overall number of species that can persist in a stationary state. Powerful theoretical predictions suggest that extinctions occur when Λ falls below a critical value, denoted as $\overline{\Lambda}$, as described in Equation 3.23. Considering an initial number of species $m > l$, the choice of $\Lambda^{(l)}$ determines the number of coexisting species, denoted as l, at the end of the process.

Figure 3.1: Time evolution of species (solid lines) and resources (dashed lines) in the Interactive Model framework, following Equations 3.13 and 3.14. In this simulation we consider the following parameters: $m = 3$ species, $p = 2$ resources, $\delta_\sigma = 1 \ \forall \ \sigma$, $\nu_i = 1$, $\mu_i = 0.001$, $k_i = 5$, $\epsilon = \text{diag}(0.001, 0.002, 0.003)$, $\alpha = \begin{pmatrix} 1.5 & 2.8 \\ 3.1 & 5.2 \\ 1.7 & 2.5 \end{pmatrix}$.
(1) Given the initial conditions $n_\sigma(0) \in U[10, 55]$, $c_i(0) \in U[50, 500]$, $\Lambda_1 = 3 \cdot 10^5$ and $\Lambda_2 = 10^6$ we observe coexistence of all the species. (2) Given the initial conditions $n_\sigma(0) \in U[40, 100]$, $c_i(0) \in U[50, 110]$, $\Lambda_1 = 3 \cdot 10^5$ and $\Lambda_2 = 5 \cdot 10^5$, two species out of three die.

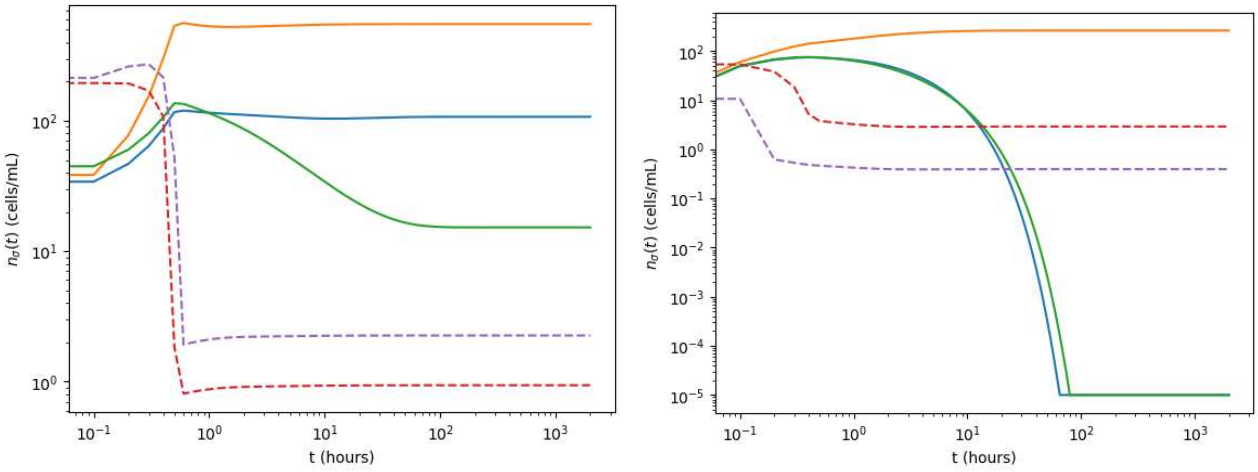

(1) (2)

Figure 3.2: Blue region of coexistence of all the initial species survive, determined by the Equations 3.18, 3.19 and 3.20. The equation of contour 3.16 (dashed curve) is evaluated for $\Lambda_1 = 3 \cdot 10^5$, common value for the two cases presented in Figure 3.1. Equation 3.17 is shown for two different values of Λ_2, i.e. $\Lambda_2 = 10^6$ (blue line) and $\Lambda_2 = 10^5$ (violet line). $\Lambda_2 = 10^6$ is the first case presented in Figure 3.1, and in fact the intersection (solution of Eqs. 3.16 and 3.17) lies inside the blue area. Whereas the intersection between Equations 3.16 and 3.18, for $\Lambda_2 = 10^5$ is inside the pink area.

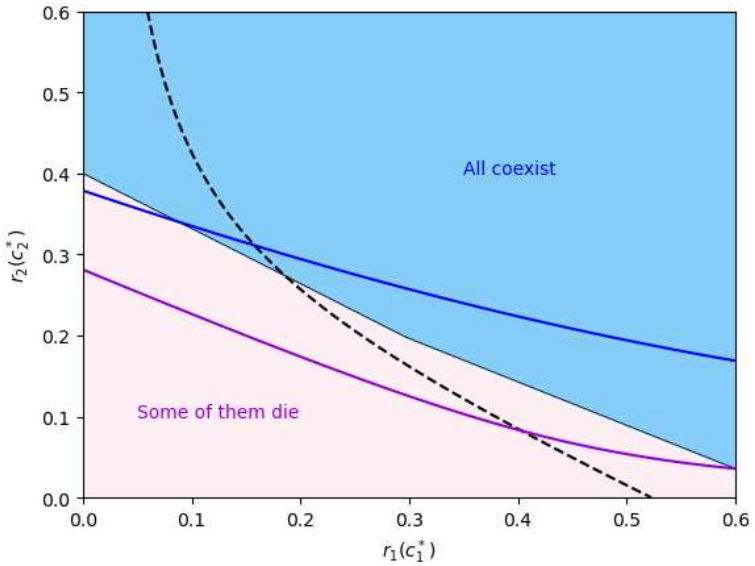

Figure 3.3: Time evolution of species competing for one nutrient in the Interactive Model framework, for growing values of Λ. The dynamics follows Equations 3.13 and 3.14. A number of l species coexist if $\Lambda^{(l)} < \Lambda < \Lambda^{(l+1)}$ with $\Lambda^{(m+1)} = \infty$. In this simulation we consider the following parameters: $m = 4$ species, $p = 1$ resources, $\delta_\sigma = 1 \ \forall \ \sigma$, $\nu_i = \nu = 1$, $\mu_i = \mu = 0.001$, $k_i = k = 5$, $\epsilon = \text{diag}(0.003, 0.0025, 0.0017, 0.0045)$, $\vec{\alpha} = (4.2, 2.5, 3.8, 4.7)$.
The initial conditions are $n_\sigma(0) = n(0) \in U[0, 10]$, $c_i(0) = c(0) \in U[0.1, 10]$. (1) For $\Lambda = 10^3$ the number of species that survive, m^*, is equal to 1. (2) For $\Lambda = 10^6$ we are in a transient situation, where $1 < m^* < m$. (3) For $\Lambda = 10^3$, all initial species coexist: $m = m^*$.

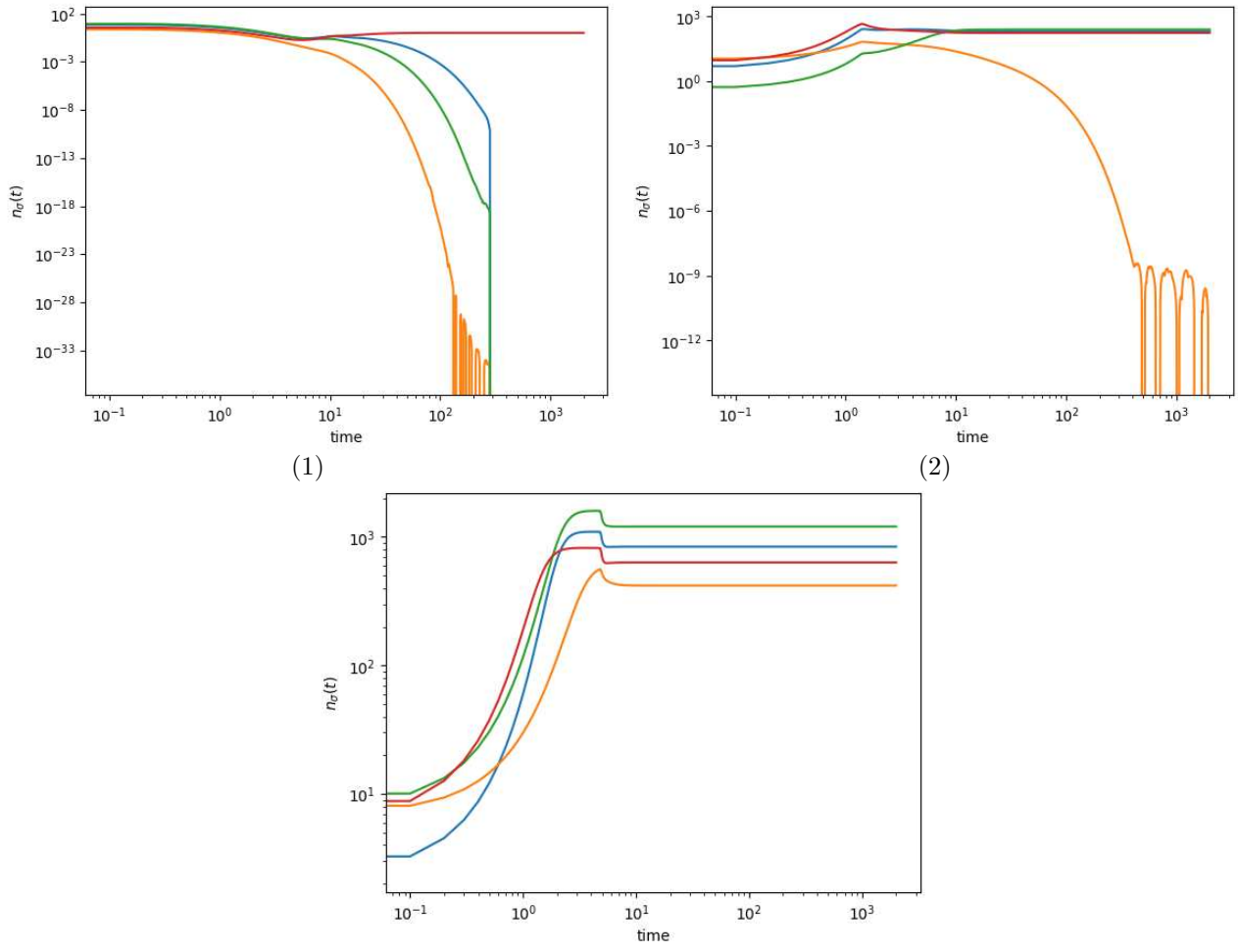

THE ADAPTIVE INTERACTIVE MODEL

The Adaptive model that we introduced previously was able to describe the violation of the Competition Exclusion Principle, succeeding where the Static Model failed, at the cost of maintaining the ratio $E^*_\sigma/\delta_\sigma = Q$ independent on the single species.

It was possible to find some justification of the independence of the Characteristic Timescale Ratio on the single species through the metabolic theory of ecology, according to which the CTR is composed of quantities that only depends on the mass of the species.
However, fluctuations in the metabolic rates and energy budgets are non negligible and it is likely that the factor Q is actually dependent on the species in nature [31] [19] [59]. In fact, starting from experimental evidence showing how proteome allocation affects microbial growth, it has been demonstrated the compartmentalization of a species' proteome into two distinct components: one responsible for housekeeping operations and the other dedicated to food metabolism. The food metabolism genome is subject to a species-specific constraint [47]. This is the reason why each species should have its own Characteristic Timescale Ratio.

It becomes necessary to create a new model, which is capable of describing a more mottled scenario. This chapter presents the Adaptive Interactive Model, that is able to incorporate the species' specific $E^*_\sigma/\delta_\sigma = Q_\sigma$. This original model takes upon itself the dynamics of the metabolic dynamics, presented in chapter 2, and the interaction quadratic term, introduced in chapter 3.

This new degree of freedom Q_σ, which determines the extinction of species in the Static and in the Interactive Model, allows to observe a violation of the CEP inside the Adaptive Interactive approach. The parameters are drawn from distributions that have been designed in a original way in this work. It is discovered all the initial species survive, even if Q_σ exhibit significant variability. Specifically, the role of the interaction term has been extensively studied, demonstrating that all species cease utilizing the most volatile resources when intra-species competition surpasses a certain threshold.

4.1 Formulation and Parameters

In this framework a ecosystem of m species, whose individuals experience interaction within the same species ($\epsilon_{\sigma\rho} \to 0$ for $\sigma \neq \rho$), competing for p resources is described by:

$$\dot{n}_\sigma = n_\sigma \left(\sum_{i=1}^{p} v_i r_i(c_i)\alpha_{\sigma i} - \delta_\sigma - \epsilon_\sigma n_\sigma \right) \tag{4.1}$$

$$\dot{c}_i = s_i(t) - \sum_{\sigma=1}^{m} n_\sigma \alpha_{\sigma i} r_i(c_i) - \mu_i c_i \tag{4.2}$$

$$\dot{\alpha}_{\sigma i} = d\delta_\sigma \, \alpha_{\sigma i} \left[v_i r_i - \frac{\theta_\sigma(\varphi(\vec{\alpha}_\sigma))}{\sum_{i=1}^{p} \alpha_{\sigma i}} \sum_{i=1}^{p} v_i r_i \, \alpha_{\sigma i} \right] \tag{4.3}$$

The maximum total resource uptake rate E^*_σ is kept fixed such that $\sum_{i=1}^{p} \alpha_{\sigma i}(t) := E_\sigma(t) \leqslant E^*_\sigma$ but choosing it from different realisations of $Q_\sigma \cdot \delta_\sigma$.

This all-embracing model is such that for:

- the adaptation velocity $d = 0$ it restores the Interactive Model
- the interaction term $\epsilon = 0$ it gives back the Adaptive Model
- $d = 0$ and $\epsilon = 0$ it reestablishes the Static Model.

This new model demonstrates a remarkable capability to prevent extinction during stationary conditions, despite introducing the dependence of the Characteristic Timescale Ratio on the single resource. A species-dependent CTR would have led to the violation of the Competition Exclusion Principle in the Adaptive Model. As seen in the previous chapters, the Adaptive Model is able to display a violation of the CEP if the Characteristic Timescale Ratio $Q = E^*_\sigma \backslash \delta_\sigma$ doesn't depend on the species' identity. On the contrary, when introducing Q_σ, $m - p$ we see extinctions at stationarity.

Making the metabolic strategies evolve according to ascent gradient descendent equation and adding the quadratic term in the equation for population's density is proven to allow all the initial species to survive, as described in Figure 4.1.

It has also been explored the ancestral model that arises just by merging the Adaptive and the Interactive Models, without relaxing the constraint on CTR. The time evolution of the system according to Equations 4.1, 4.2 and 4.3 with fixed $Q = E^*_\sigma \backslash \delta_\sigma$ is presented in Figure 4.4. This thesis work has made a significant discovery in relation to the final area of the convex hull of metabolic strategies by identifying a new "transition". This transition is under the control of the interaction term as critical parameter.

Table 4.2: Parameters used in the Adaptive Interactive Model, with their definition and the corresponding distributions that have been identified in this original work. After the metabolic strategies are drawn from the distribution, they undergo the process of normalisation $\sum_{i=1}^{p} \alpha_{\sigma i}(0) = E^*_\sigma \in U[0, Q_\sigma \delta_\sigma]$.

Parameter	**Definition**	**Distribution**
n_σ	Population density of species σ	$U[10^6, 5 \cdot 10^6]$
c_i	Density of resource i	$U[10^{-3}, 10^{-2}]$
μ_i	Degradation rate of resource i	$U[10^3, 10^4]$
δ_σ	Death rate of species σ	$U[5 \cdot 10^{-5}, 5 \cdot 10^{-3}]$
k_i	Half-saturation constant of resource i	$U[10^{-4}, 10^{-3}]$
s_i	Supply rate of resource i	$U[10^{-2}, 1]$
v_i	Conversion efficiency of resource i	$U[10^9, 5 \cdot 10^9]$
$\alpha_{\sigma i}$	Metabolic strategies	$U[10^{-11}, 10^{-10}]$
ϵ_σ	Interaction term of species σ	$U[10^{-6}, 2 \cdot 10^{-5}]$

4.2 Numerical Results

In this section, we aim to showcase the potential of the original Adaptive Interactive Model by comparing it with the Static, Interactive, and Adaptive frameworks discussed earlier. It is important to

note that all parameters and variables used in the analysis are evaluated in arbitrary units.

4.3 Adaptive Interactive model with Q_σ

As seen in the previous chapters, the Adaptive Model is able to display a violation of the CEP if the Characteristic Timescale Ratio $Q = E^*_\sigma \backslash \delta_\sigma$ doesn't depend on the species' identity. When introducing Q_σ, we see $m - p$ extinctions at stationarity. Figure 4.1 provides a visual representation on how the introduction of ϵ_σ proves to be advantageous to promote biodiversity. In the presence of Q_σ, all the species survive. In Figure 4.1, we illustrate a scenario characterized by a small variance of , showcasing the impact of the Adaptive Interactive dynamics. Beyond merely predicting the violation of the CEP, which could also be anticipated by other models given the small variance (see the Interactive Model of panel (3)), this dynamics ensures the survival of all the initial species. As shown in the right column of Figure 4.3, increasing the variance of Q_σ, the demise of species in other deterministic models would become even more severe.

Figure 4.2 shows how the dynamic of $\alpha_{\sigma i}$ changes drastically depending on the values of d and ϵ_σ. In the Adaptive Model, the metabolic strategies associated with the two resources characterized by the highest degradation rate undergo a pronounced collapse before exhibiting a subsequent upswing in their dynamics. In contrast, the Adaptive Interactive Model reveals a different behavior, where the species cease utilizing the two unfavorable resources indefinitely, while successfully sustaining themselves by relying solely on a single resource. Clearly the constant behavior of the metabolic strategies observed in both panels (1) and (2) of Figure 4.2 can be attributed to the lack of dynamics in these cases.

4.4 Variance of Q_σ in the Adaptive Interactive model

In the context of the Interactive Model, the presence of Q_σ limits the coexistence of all initial species. However, the Adaptive Interactive framework allows for the prediction of the violation of the Competitive Exclusion Principle when the variance among the elements of Q_σ is below the six order of magnitudes. However, despite the optimizing dynamics of metabolic strategies and the presence of quadratic interaction terms, extinction can still occur within a system characterized by significant variance. This is particularly evident when the values of Q_σ span several orders of magnitude, exceeding those six orders of magnitude. Figure 4.3 highlights the effectiveness of the Adaptive Interactive Model in ensuring the survival of all initial species, even in the presence of considerable variability in the energy budget of each individual species.

4.5 Interaction term in the Adaptive Interactive model with fixed Q

To be able to study methodically the role of the interaction term in this model, which is characterised by an elevated number of parameters, the Characteristic Timescale Ratio is kept fixed for all the species. For the sake of simplicity we assume also that every species is also characterised by the same $\epsilon_\sigma = \epsilon$. The value of ϵ is the only parameter that changes in the simulations, as presented in Figure 4.4. The degradation rates are such that $\mu_1 > \mu_3 > \mu_2$, thus the metabolic strategies which collapse are the ones related to the uptake of the most degrading nutrients. When intensifying the interaction among members of the same species, the convex hull area of the rescaled metabolic strategies diminishes to zero as a result of relinquishing the least favorable resource, as seen in Figure 4.5. This thesis demonstrates that as the parameter ϵ increases, the species exhibit a significant decrease in the utilization of the i-th resource with a higher μ_i. Figure 4.6 shows the "transition" that the final area of the convex hull undergoes for growing ϵ, when the dynamics of the system is described by the Adaptive Interactive model.

Figure 4.1: Time evolution of the population's density and of the metabolic strategies in the Static, Adaptive, Interactive and Adaptive Interactive Model framework. In these simulations the system is characterised by $m = 15$ species, $p = 3$ resources, $\delta_\sigma \in U[5 \cdot 10^{-3}, 5 \cdot 10^{-2}]$ (with U the uniform distribution), $v_i \in U[10^8, 5{\cdot}10^9]$, $n_\sigma(0) \in U[10^6, 5{\cdot}10^6]$, $c_i(0) \in U[10^{-3}, 10^{-2}]$, $k_i \in U[10^{-4}, 10^{-3}]$, $s_i \in U[10^{-3}, 10^{-2}]$, $Q_\sigma \in U[4{\cdot}10^{-7}, 5{\cdot}10^{-7}]$, $E_\sigma(0) \in U[0, Q_\sigma \delta_\sigma]$ and $\alpha_{\sigma i}(0)$ such that $\sum_{i=1}^{p} \alpha_{\sigma i}(0) = E_\sigma(0)$. Parameters and initial conditions are kept fixed in all the simulations. (1) Static Model with $d = 0$ and $\epsilon_\sigma = 0$, (2) Adaptive Model with $d = 4.20 \cdot 10^{-6}$ and $\epsilon_\sigma = 0$, (3) Interactive Model with $d = 0$ and $\epsilon_\sigma \in U[10^{-6}, 2 \cdot 10^{-5}]$, (4) Adaptive Interactive Model with $d = 4.20 \cdot 10^{-6}$ and $\epsilon_\sigma \in U[10^{-6}, 2 \cdot 10^{-5}]$.

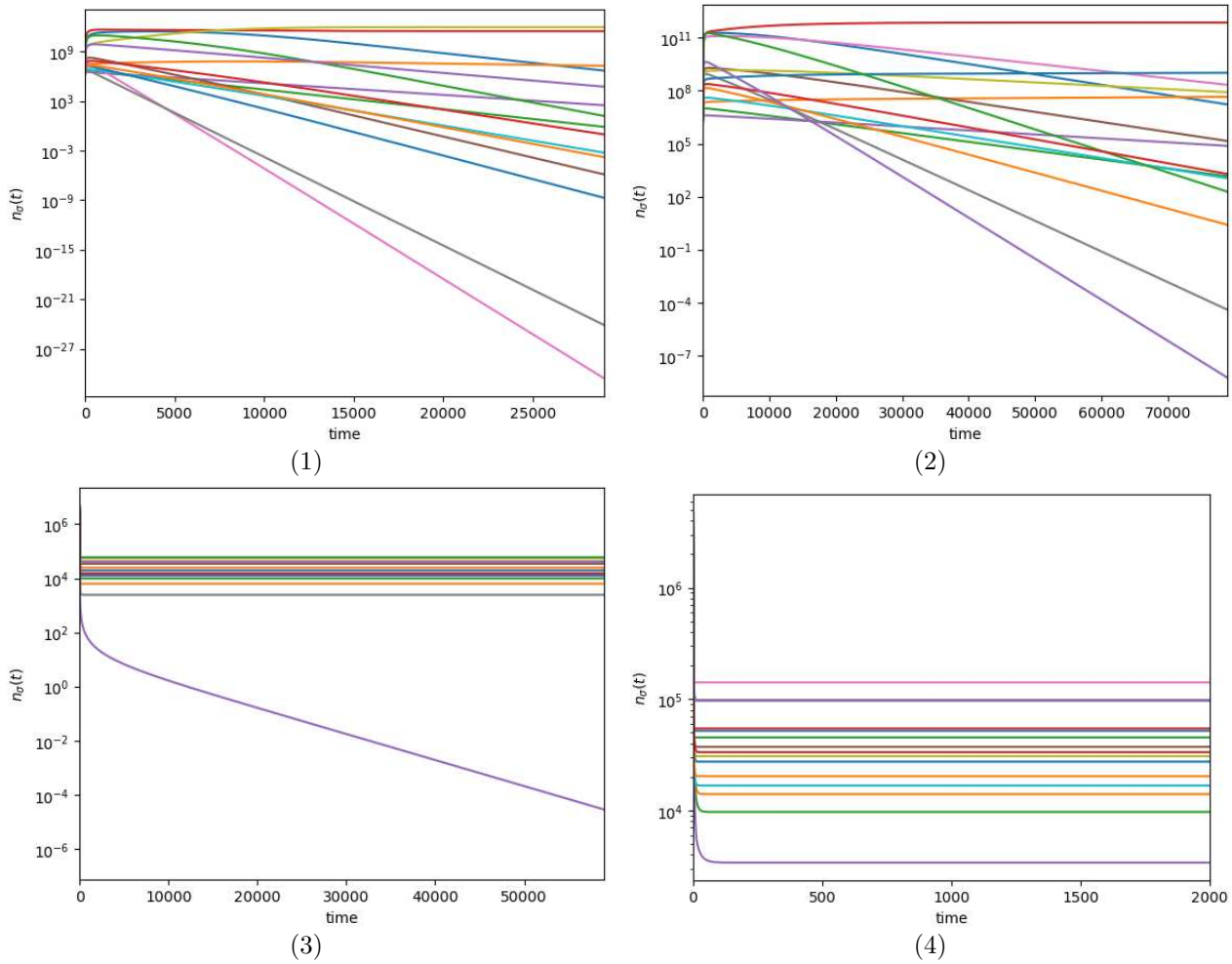

Figure 4.2: Time evolution of the rescaled metabolic strategies in the Static, Adaptive, Interactive and Adaptive Interactive Model framework, corresponding to the results presented in 4.1. (1) Static Model with $d = 0$ and $\epsilon_\sigma = 0$, (2) Adaptive Model with $d = 4.20 \cdot 10^{-6}$ and $\epsilon_\sigma = 0$, (3) Interactive Model with $d = 0$ and $\epsilon_\sigma = U[10^{-6}, 2 \cdot 10^{-5}]$, (4) Adaptive Interactive Model with $d = 4.20 \cdot 10^{-6}$ and $\epsilon_\sigma = U[10^{-6}, 2 \cdot 10^{-5}]$.

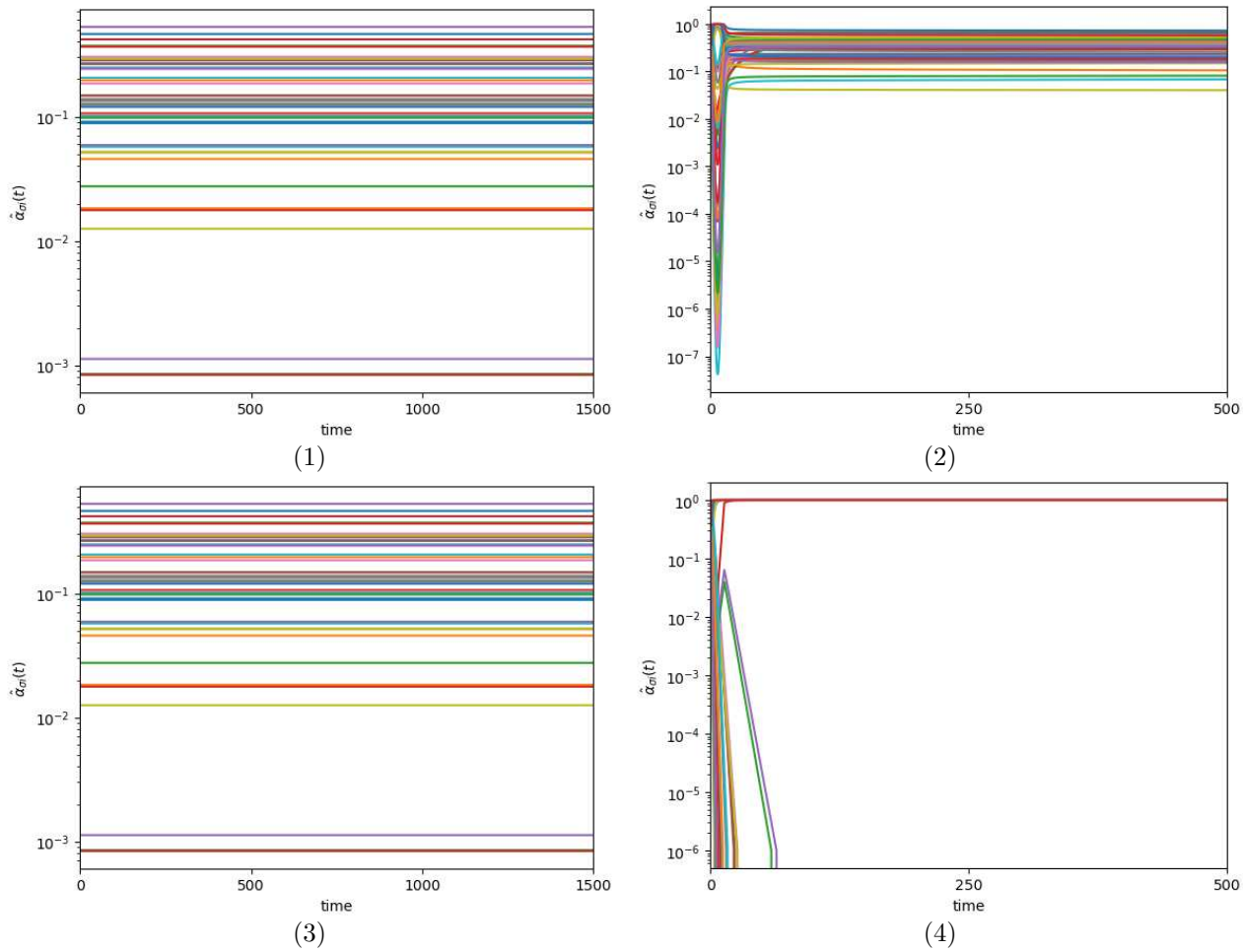

Figure 4.3: Time evolution of the population's density and of the metabolic strategies in Adaptive Interactive Model (left column) framework and in the Interactive Model (right column) for different values of the variance of the elements of Q_σ. In these simulations the system is characterised by $m = 15$ species, $p = 3$ resources, $\delta_\sigma \in U[5 \cdot 10^{-3}, 5 \cdot 10^{-2}]$ (with U the uniform distribution), $v_i \in U[10^8, 5 \cdot 10^9]$, $n_\sigma(0) \in U[10^6, 5 \cdot 10^6]$, $c_i(0) \in U[10^{-3}, 10^{-2}]$, $k_i \in U[10^{-4}, 10^{-3}]$, $s_i \in U[10^{-3}, 10^{-2}]$, $E_\sigma(0) \in U[0, Q_\sigma \delta_\sigma]$ and $\alpha_{\sigma i}(0)$ such that $\sum_{i=1}^{p} \alpha_{\sigma i}(0) = E_\sigma(0)$. In the left column $\epsilon_\sigma = U[10^{-6}, 2 \cdot 10^{-5}]$, in the right column $\epsilon_\sigma = 0$. (1)-(2): $Q_\sigma \in U[10^{-7}, 9 \cdot 10^{-5}]$, (3)-(4): $Q_\sigma \in U[10^{-7}, 5 \cdot 10^{-3}]$, (5)-(6): $Q_\sigma \in U[10^{-7}, 5 \cdot 10^{-1}]$: within such a huge variance extinctions appear despite the Adaptive Interactive dynamics.

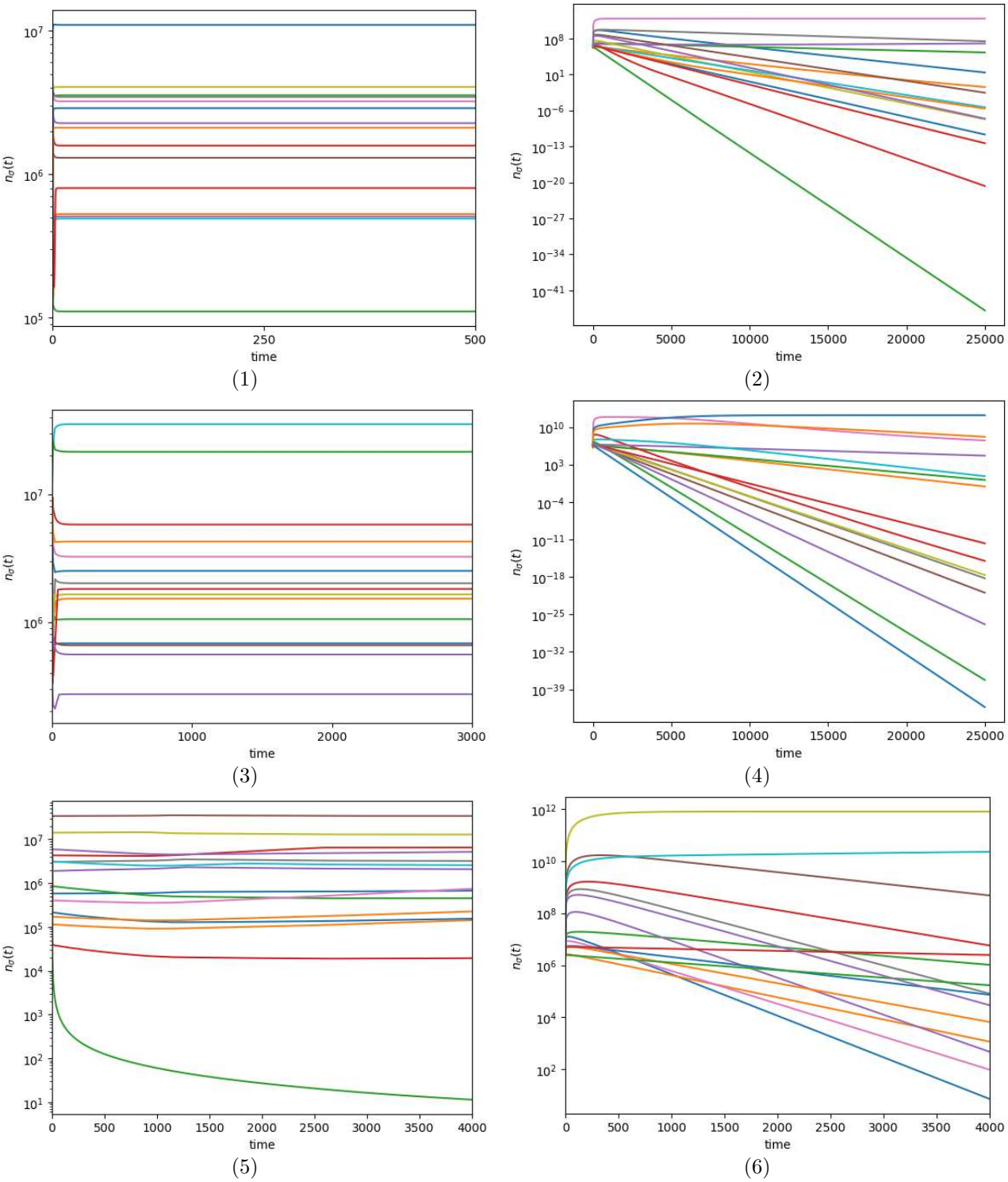

Figure 4.4: Time Evolution of the rescaled metabolic strategies over time for different values of $\epsilon_\sigma = \epsilon$ in the Adaptive Interactive Model framework with fixed Q. In these simulations we consider $m = 15$ species, $p = 3$ resources, $\delta_\sigma \in U[5 \cdot 10^{-3}, 5 \cdot 10^{-2}]$ (with U the uniform distribution), $v_i \in U[10^9, 5 \cdot 10^9$, $\mu_i \in U[10^3, 10^4$, $n_\sigma(0) \in U[10^6, 5 \cdot 10^6]$, $c_i(0) \in U[10^{-3}, 10^{-2}]$, $k_i \in U[10^{-4}, 10^{-3}]$, $s_i \in U[10^{-3}, 10^{-2}]$, $Q \in U[4 \cdot 10^{-7}, 5 \cdot 10^{-7}]$, $E_\sigma(0) \in U[0, Q\delta_\sigma]$ and $\alpha_{\sigma i}(0)$ such that $\sum_{i=1}^{p} \alpha_{\sigma i}(0) = E_\sigma(0)$. Parameters and initial conditions are kept fixed in all the simulations, only ϵ changes: (1) $\epsilon = 1.40 \cdot 10^{-9}$ (2) $\epsilon = 1.47 \cdot 10^{-9}$ (3) $\epsilon = 1.48 \cdot 10^{-9}$ (4) $\epsilon = 1.50 \cdot 10^{-9}$ (5) $\epsilon = 1.55 \cdot 10^{-9}$. Due to the fact that $\mu_1 > \mu_3 > \mu_2$, the metabolic strategies collapsing are the ones related to the uptake of the first nutrient.

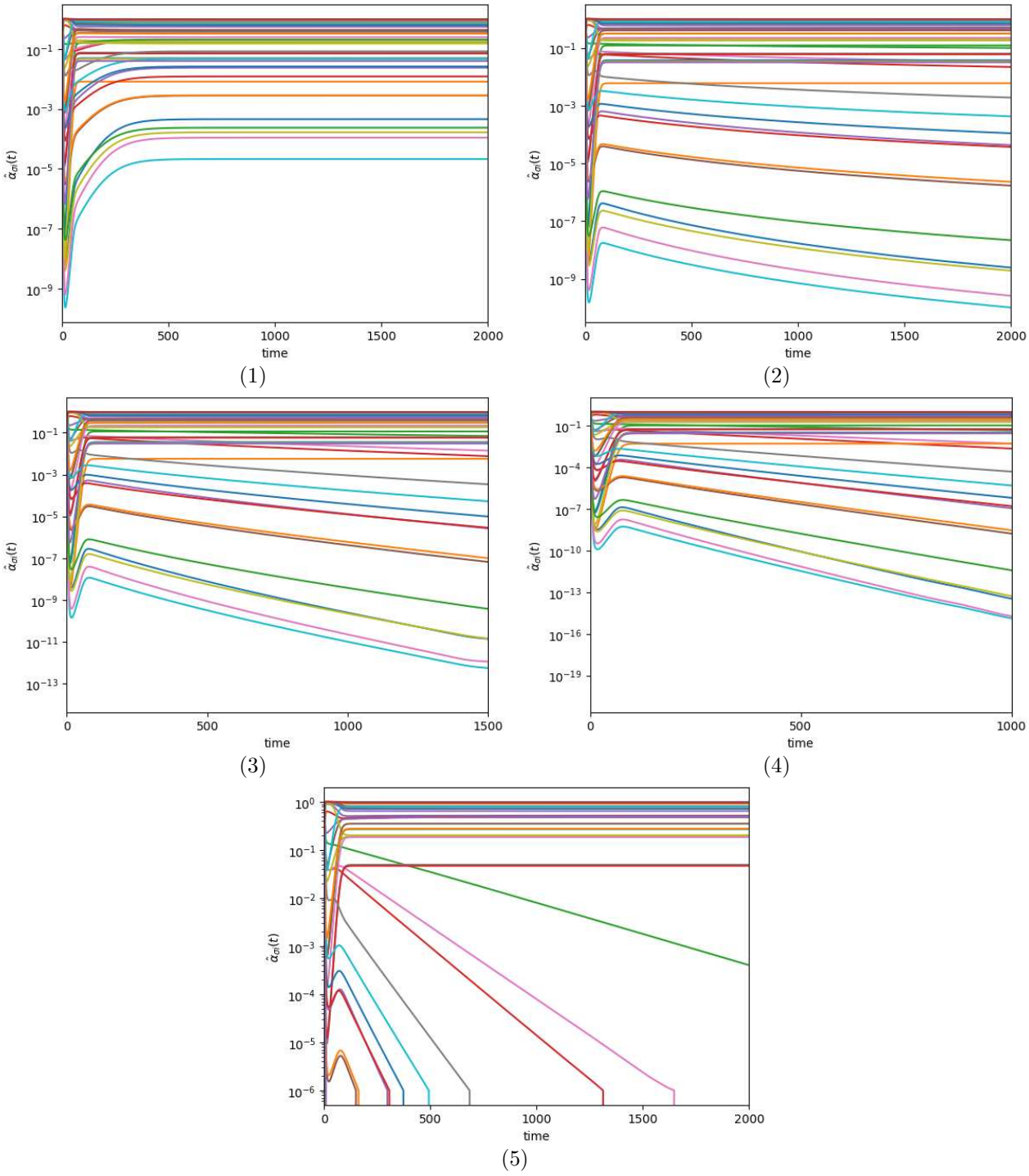

Figure 4.5: Convex hull of the rescaled metabolic startegies, which evolve over time for different values of $\epsilon_\sigma = \epsilon$ in the Adaptive Interactive Model framework with fixed Q. The system presented is the same of Figure 4.4. (1) Initial convex hull, which remains consistent across all simulations, as all the parameters are maintained fixed after being extracted from the distributions presented in Figure 4.2. In the simplex the rescaled supply vector of the nutrients $\overrightarrow{\hat{s}}$ is depicted with a star. (2)-(6): Final convex hull corresponding the stationary state of their time evolution presented in Figure 4.2, for different values of $\epsilon_\sigma = \epsilon$. The stationary rescaled supply vector of the nutrients $\overrightarrow{\tilde{s}}$ is represented by the blue triangle. As $\mu_1 > \mu_3 > \mu_2$, the metabolic strategies migrate towards the opposite side of the vertex corresponding to the first resource: (2) $\epsilon = 1.40 \cdot 10^{-9}$, (3) $\epsilon = 1.47 \cdot 10^{-9}$, (4) $\epsilon = 1.48 \cdot 10^{-9}$, (5) $\epsilon = 1.50 \cdot 10^{-9}$, (6) $\epsilon = 1.55 \cdot 10^{-9}$.

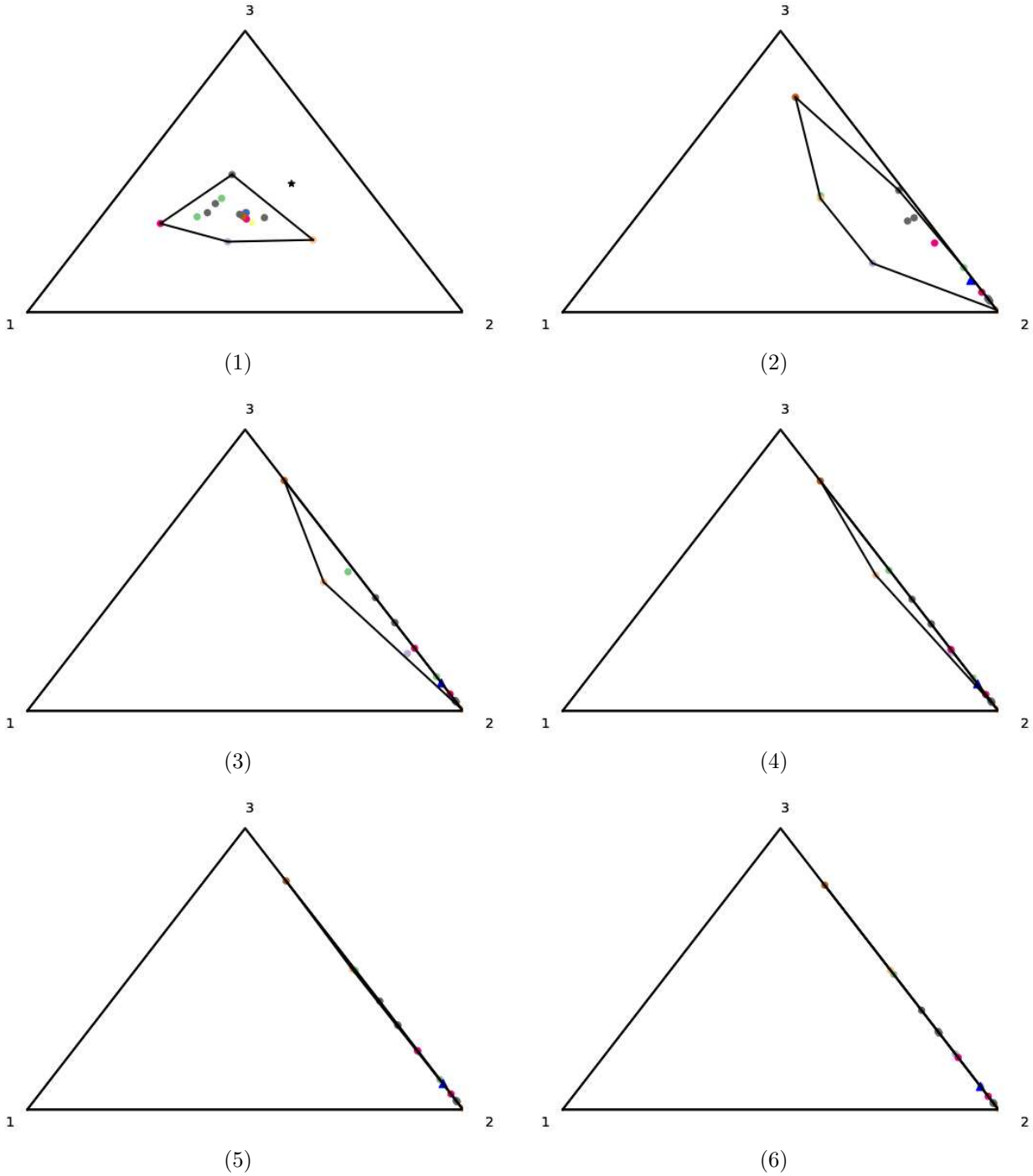

Figure 4.6: "Transition" of the final area of the Convex Hull of the rescaled metabolic strategies, where $\epsilon_\sigma = \epsilon \cdot 10^9$ is the critical parameter. All the simulations are performed by keeping the others parameters and initial conditions fixed, as shown in Figures 4.4 and 4.5.

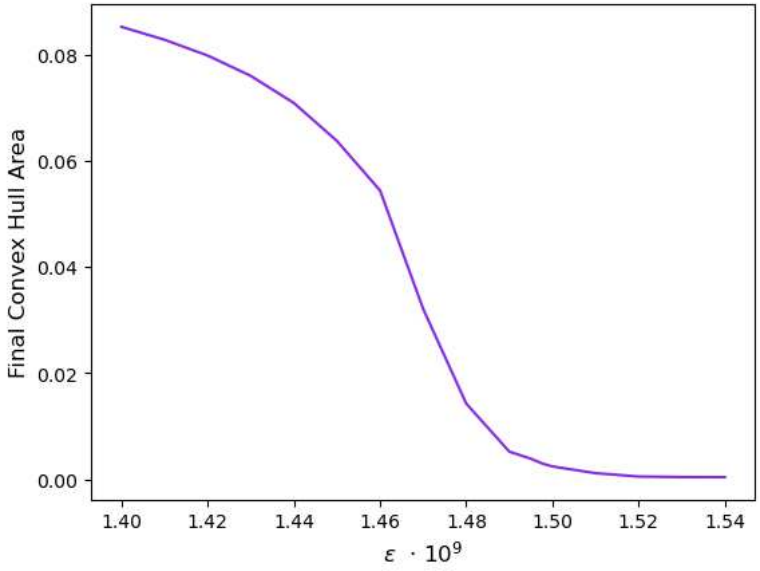

THE STOCHASTIC MODEL

Most ecological research has focused on identifying deterministic mechanisms that stabilize communities and generate equilibrium species compositions. While the deterministic approach has been successful in developing ecological concepts and theories, its applicability to real systems is challenging due to its emphasis on species-specific interactions. In order to overcome these limitations, MacArthur and Wilson [40] emphasized the role of stochastic processes as key drivers of species diversity.

The incorporation of stochasticity into ecological dynamics has been achieved through various approaches, with a major focus on demographic random fluctuations in population dynamics, particularly through processes such as stochastic death-immigration processes. The role of stochasticity fluctuations in resource supply rates and species mortality rates has also been studied [48]. However those stochastic ingredients usually enter just on the species' densities or resources' concentrations dynamics.

In this chapter, we present a novel approach to incorporate stochasticity into the time evolution of metabolic strategies. Starting from the Static Model, we elevate the metabolic strategies to the status of dynamical variables and propose a new formulation that takes into account the inherent stochastic nature of these strategies in time. We achieve this by introducing a colored noise term that exhibits temporal autocorrelation, meaning that the current values of the noise depend on all previous history, i.e. it is not a Markov process.

The evolution of metabolic strategies in our model is governed by two components: a deterministic part that accounts for deterministic processes and interactions, that would lead metabolic strategies to a linear behaviour over time, and an Ornstein-Uhlenbeck noise component. This noise component introduces random fluctuations that exhibit temporal correlation, reflecting the influence of past states on the current state of the system.

This approach introduces an annealed dynamics that goes beyond traditional deterministic models and provides a more comprehensive understanding of the dynamics of metabolic strategies and their impact on community dynamics.

The Stochastic model is described by Equations 5.1 to 5.4. These equations capture the dynamics of population density and resource concentration, which resemble the form of Equations 1.43 and 1.44. However, it is important to note that the Stochastic model is not static. Unlike the MacArthur's Model, the metabolic strategies are no longer treated as fixed parameters. Instead, they are dynamic variables whose time evolution is governed by both deterministic and fluctuating factors.

The deterministic component of the metabolic strategies equation is composed of two main terms. The first $\overline{\alpha}_i$ represents the minimum metabolic rates of the species for that respective resources. The second term is the species-dependent $\sigma\Delta_i$, which accounts for the species-specific adjustments to a certain nutrient. When considering two closely related metabolic strategies, denoted as α_σ and $\alpha_{\sigma+1}$, for the same resource, a difference of Δ is assumed between them. Specifically, in the consumption of the i-th resource, the metabolic strategy $\alpha_{\sigma i}$ of species σ differs by a factor of $\sigma\Delta_i$ from the baseline metabolic strategy $\overline{\alpha}_i$.
The stochastic part of Equation 5.3 is regulated by the parameter Σ which acts on the noise $\eta_{\sigma i}$. The colored noise $\eta_{\sigma i}$ is generated from a white noise via the Ornstein-Uhlenbeck process of Equation 5.4.

$$dn_\sigma = n_\sigma \left(\sum_{i=1}^{p} v_i r_i \; d\alpha_{\sigma i} \; - \delta_\sigma dt \right) \tag{5.1}$$

$$dc_i = s_i \; dt - \sum_{\sigma=1}^{m} n_\sigma d\alpha_{\sigma i} r_i - \mu_i c_i \; dt \tag{5.2}$$

$$d\alpha_{\sigma i} = (\overline{\alpha}_i + \sigma\Delta_i) \;\; dt \;\; + \;\; \Sigma \; d\eta_{\sigma i} \tag{5.3}$$

$$d\eta_{\sigma i} = -\frac{\eta_{\sigma i}}{\tau} dt + \frac{\sqrt{2D}}{\tau} dW_{\sigma i} \tag{5.4}$$

where τ is the correlation time of the noise, which allows to define the noise intensity as:

$$D = \frac{1 + 2\tau}{2} \tag{5.5}$$

$W_{\sigma i}$ is the white noise of zero mean and amplitude D:

$$\langle W_{\sigma i}(t) \rangle = 0 \tag{5.6}$$

$$\langle W_{\sigma i}(t) W_{\sigma' i'}(t') \rangle = D \delta_{\sigma\sigma'} \delta_{ii'} \delta(t - t') \tag{5.7}$$

The colored fluctuation process, presented in Equation 5.4, introduces a random variation which is temporally correlated, creating a smoother and more realistic representation of noise.

The Ornstein-Uhlenbeck process is characterized by the attractor $-\frac{\eta_{\sigma i}}{\tau}$ towards which the color tends to move over time. The variance $\frac{\sqrt{2D}}{\tau}$ controls the amount of random fluctuation in the color values. A higher diffusion parameter leads to greater variability and stronger fluctuations, while a lower diffusion parameter results in smoother and less pronounced variations.

The time-correlated noise $\eta_{\sigma i}$ are Ornstein-Uhlenbeck processes which are uncorrelated among them:

$$\langle \eta_{\sigma i}(t) \rangle = 0 \tag{5.8}$$

and with different autocorrelation times:

$$\begin{aligned} \langle \eta_{\sigma i}(t) \; \eta_{\sigma' i'}(t') \rangle \; &= \delta_{\sigma\sigma'} \delta_{ii'} \frac{D}{\tau} e^{-|t-t'|/\tau} = \delta_{\sigma\sigma'} \delta_{ii'} \frac{1 + 2\tau}{2\tau} e^{-|t-t'|/\tau} \\ &= \delta_{\sigma\sigma'} \delta_{ii'} \begin{cases} \delta(t - t') & \tau \downarrow 0 \\ \\ 1 & \tau \uparrow \infty \end{cases} \end{aligned} \tag{5.9}$$

To derive the exponential decay of the auto-correlation time functions, we start considering the Equation 5.4, for the Ornstein-Uhlenbeck process with just one species and one resource:

$$\frac{d\eta(t)}{dt} = -\gamma \; \eta(t) + A \; W(t) \tag{5.10}$$

where $\gamma = 1/\tau$ and $A = \sqrt{2D}/\tau$ with the initial condition $\eta(t = 0) = \eta_0$.

Integrating the Equation 5.6 gives formally

$$\eta(t) = \eta_0 e^{-\gamma t} + \int_0^t e^{-\gamma(t-s)} A\ W(s) ds \tag{5.11}$$

Averaging over several independent realisation of the stochastic term keeping the same initial condition $\eta(t=0) = \eta_0$, we get the mean solution over time

$$\langle \eta(t) \rangle_{\eta_0} = \left\langle \eta_0 e^{-\gamma t} \right\rangle_{\eta_0} + \langle \int_0^t e^{-\gamma(t-s)} A\ W(s)\ ds \rangle_{\eta_0} \tag{5.12}$$

The Gaussian noise has zero mean $\langle W(t) \rangle_{\eta_0} = 0$, so we obtain

$$\langle \eta(t) \rangle_{\eta_0} = \eta_0 e^{-\gamma t} \tag{5.13}$$

The autocorrelation function can be

$$\langle \eta(t_1)\, \eta(t_2) \rangle_{\eta_0} = \eta_0^2 e^{-\gamma(t_1+t_2)} + \int_0^{t_1} ds_1 \int_0^{t_2} ds_2 e^{-\gamma(t_1-s_1)} e^{-\gamma(t_2-s_2)} A^2 \langle W(s_1)\, W(s_2) \rangle \tag{5.14}$$

The auto-correlation function present in the r.h.s is given by the properties of the Gaussian noise: $\langle W(s_1)\, W(s_2) \rangle = \delta(s_1 - s_2)$. The second term with the double integral can be simplified as it follows:

$$\begin{aligned}
\int_0^{t_1} ds_1 \int_0^{t_2} ds_2 e^{-\gamma(s_1+s_2)} \delta(s_1 - s_2) &= \int_0^{\infty} ds_1 \int_0^{\infty} ds_2\ e^{\gamma(s_1+s_2)} \theta(t_1 - s_1)\, \theta(t_2 - s_2)\, \delta(s_1 - s_2) \\
&= \int_0^{\infty} ds_1\ e^{2\gamma s_1} \underbrace{\theta(t_1 - s_1)\, \sigma(t_2 - s_1)}_{\theta(\min(t_1,t_2) - s_2)} \\
&= \int_0^{\min(t_1,t_2)} ds_1\ e^{2\gamma s_1} \\
&= \frac{1}{2\gamma}(e^{2\gamma \min(t_1,t_2)} - 1)
\end{aligned} \tag{5.15}$$

Considering the identity $t_1 + t_2 - 2\min(t_1, t_2) =_1 -t_2 \mid$ and inserting Equation 5.15 in Equation 5.14, we get

$$\langle \eta(t_1)\, \eta(t_2) \rangle_{\eta_0} = \eta_0^2\ e^{-\gamma(t_1+t_2)} + \frac{A^2}{2\gamma} \left(e^{-\gamma|t_1 - t_2|} - e^{-\gamma(t_1+t_2)} \right) \tag{5.16}$$

For $t_1, t_2 \gg 1$, stationary states are characterized by time scales which are much larger than the characteristic time $1/\tau$, giving

$$\langle \eta(t_1)\, \eta(t_2) \rangle_{\eta_0} = \frac{A^2}{2\gamma} e^{-\gamma|t_1 - t_2|} \tag{5.17}$$

Considering the relation $\frac{A^2}{2\gamma} = \frac{D}{\tau}$, we can recover the autocorrelation function described in Equation (5.9). This autocorrelation function is independent of the initial condition η_0 and only depends on the time interval $|t_1 - t_2|$.

In the presence of multiple species, denoted by $\sigma = 1, \ldots, m$, and multiple resources, denoted by $i = 1, \ldots, p$, the decaying exponential term derived earlier is multiplied by the Kronecker delta terms $\delta_{\sigma\sigma'}$ and $\delta_{ii'}$. This implies that the autocorrelation function for each species and resource is independent of the other species and resources. In the limit $\tau \to 0$, the effect of memory or persistence in the color noise diminishes. The system becomes highly responsive to immediate changes, and correlations between consecutive samples approach zero. Consequently, the noise appears more random and resembles the uncorrelated and constant power characteristics of white noise, as can be seen in Figure 5.1

Figure 5.1: Time evolution of the color noise $\eta_{\sigma i}$ according to Equation 5.4, with $dW_{\sigma i} \sim \mathcal{N}(0, dt)$ and the correlation time of the noise being (1) $\tau = 0.1$ (white gaussian limit) (2) $\tau = 10$ (3) $\tau = 100$.

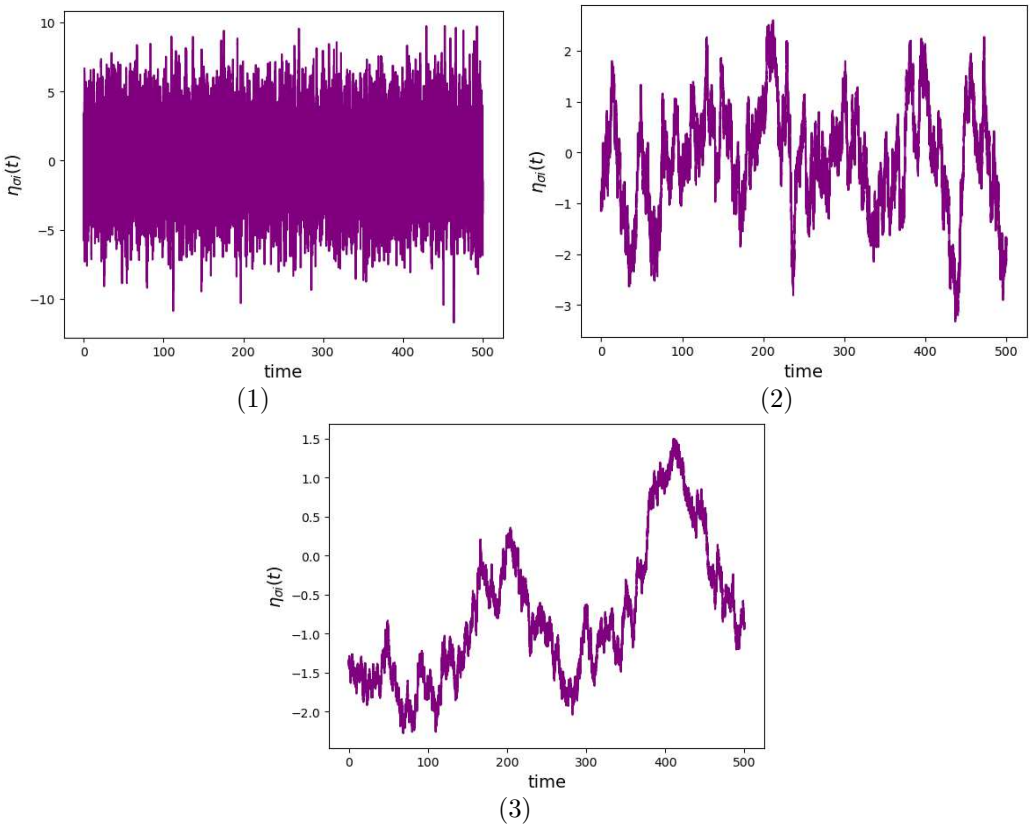

Introducing the colored noise described by Equation 5.3 into the time evolution equations for the populations' density, Equation 5.1, and the resources' concentration, Equation 5.2, we obtain

$$dn_\sigma = n_\sigma \left(\sum_{i=1}^{p} v_i r_i \ (\overline{\alpha}_i + \sigma\Delta_i) - \delta_\sigma \right) dt + n_\sigma \sum_{i=1}^{p} v_i r_i \ \Sigma \ d\eta_{\sigma i} \tag{5.18}$$

$$dc_i = \left(s_i - \mu_i c_i \ + \ \sum_{\sigma=1}^{m} n_\sigma r_i \ (\overline{\alpha}_i + \sigma\Delta_i) \right) dt \ - \sum_{\sigma=1}^{m} n_\sigma r_i \ \Sigma \ d\eta_{\sigma i} \tag{5.19}$$

The stochastic dynamics of metabolic strategies enable the coexistence of all initial species, as demonstrated in Figure 5.2. Indeed, in the absence of the stochastic component, we would encounter the known scenario of the Static Model, with each species adopting distinct metabolic strategies that would inevitably lead to the Competition Exclusion Principle, limiting the coexistence of species.

5.1 Shannon Entropy to measure coexistence

Our primary focus is on understanding the interplay between the variability of metabolic strategies and the strength of annealed noise, specifically in relation to the characteristic time. We aim to determine a quantitative parameter that can effectively capture the number of species that survive at stationarity.

To address this question, we seek a robust measure that accounts for the abundance of species in the ecosystem.

One commonly used parameter to estimate the population status of species at stationarity is the fraction of surviving individuals. This parameter compares the number of different individuals present at

stationarity with the initial community size. In that sense, deterministic models often utilize visual analysis of the model's output to detect potential extinctions. Visual examination of population dynamics can offer valuable insights into the behavior of species populations and their vulnerability to extinction. In stochastic frameworks, it becomes crucial to have a formal indicator that can quantitatively determine the coexistence of multiple species. In this regard, we propose using Shannon Entropy as a measure of the species survival within an ecosystem. The Shannon entropy is a mathematical measure used to quantify the amount of information or uncertainty in a random variable or probability distribution. It provides a measure of the average information content or disorder within a set of data. Instead of employing subjective criteria, such as considering a species dead when its population density falls below a certain threshold, we have opted to utilize Shannon entropy as our chosen metric. This approach offers several advantages, including reduced bias and a standardized measure commonly employed in Statistical Mechanics to evaluate the accessible states of a system. In this specific ecological context, we use the Shannon entropy as quantitative assessment of how much the system is biodiverse.

The Shannon entropy of the ecosystem at a certain time t is defined as:

$$S = -\sum_{i=1}^{m} P_i(t) log(P_i(t)) \tag{5.20}$$

where

$$P_i(t) = \frac{n_i(t)}{\sum_{i=1}^{m} n_i(t)} \tag{5.21}$$

represents the probability of the i-th species within the community at a given time. The calculation of probability and Shannon entropy involves summation over all species present in the community. The underlying assumption for accurately evaluating the quantitative value of Shannon entropy is having knowledge of the number of species present at the beginning.

The Shannon entropy value ranges from 0 to $log(m)$, where m is the total number of initial species. A value of 0 indicates a community with only one species, while a higher value signifies greater diversity among species. If the Shannon entropy $S(t^*)$ of the ecosystem displays the value of $log(m)$, it suggests that all the species within that community are coexisting at time $t = t^*$. This observation indicates a violation of the Competition Exclusion Principle.

5.2 Numerical Results

In the presence of stochasticity, it is crucial to accurately account for the actual presence of species in the ecosystem. The occurrence of species disappearing and reappearing intermittently would be entirely unphysical. Therefore, to address this issue, the population densities are plotted on a logarithmic scale in the following simulations. Parameters and variables are evaluated in arbitrary units.

5.2.1 Characteristic time τ in the Stochastic Model

As the characteristic time scale τ increases, cyclic patterns in the population dynamics of the species begin to emerge. When τ is small, all the species exhibit similar behavior: the populations of different species tend to fluctuate together, showing a more synchronized pattern. However, as τ grows, the width of the population fluctuations increases, and the time span between periods of high population and low population becomes larger. These extended periods of population dominance indicate a higher degree of asynchrony among the species, with some populations experiencing favorable conditions while others face more challenging environments. Distinct cycles of population growth and decline become more and more visible increasing the characteristic time τ as shown in Figure 5.2.

The population of each species is individually re-evaluated in Figure 5.2 to emphasize the increasing magnitude of fluctuations and the prolonged periods during which one population flourishes while

Figure 5.2: Time evolution of the populations' density according to 5.7. The system simulated is characterised by $m = 15$ species, $p = 1$ resources, $\delta_\sigma = 1$, $v_i = v = 1$, $n_\sigma(0) \in U[0.5, 1.5]$, $c_i(0) = c(0) \in U[0.5, 1.5]$, $k_i = k = 5$, $s_i = s \in U[30, 40]$, $\overline{\alpha}_i = \overline{\alpha} = 5$, $\Delta = 1$, $\Sigma = 5$, $dW_{\sigma i} \sim \mathcal{N}(0, dt)$ and the correlation time of the noise being (1) $\tau = 0.01$ (white Gaussian limit) (2) $\tau = 0.1$ (3) $\tau = 1$ (4) $\tau = 10$.

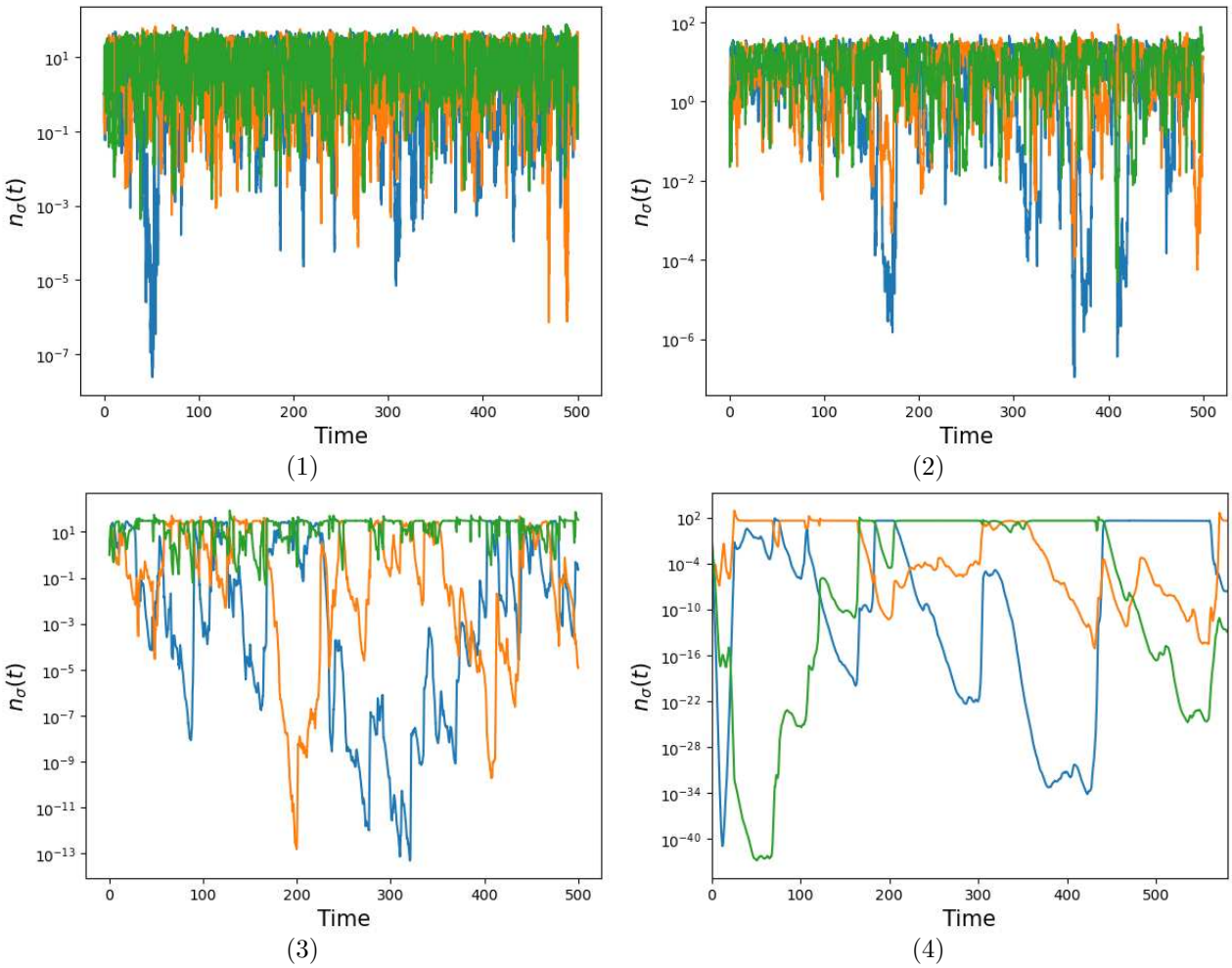

others experience significantly lower values. If the metabolic strategies were constant over time, we would expect $m - 1$ species to die in the presence of only one resource. However, in the stochastic framework, if the metabolic strategies remain nearly constant on timescales of the order of τ, we would expect one species to consistently survive while the remaining $m-1$ species approach zero more closely as τ increases. When the metabolic strategies change after a time interval of τ, the species with the strongest fitness advantage shift, leading to the survival of a different species. Statistically, we anticipate that each species will experience a period where it is the fittest over a time interval of approximately $m\tau$. This cyclic nature, along with the survival of most species, is observed due to these dynamics.

The emergence of such temporal cyclical dynamics highlights the importance of considering the interplay between the characteristic time scale and the population dynamics in understanding the overall ecosystem behavior.

In this context, the analysis is extended to highly biodiverse systems where the number of species exceeds by far the number of available resources. In these conditions, we have chosen to rescale Equations 5.1, 5.2, 5.3, and 5.4 to facilitate the comparative analysis between these ecosystems. By multiplying the supply rate by m, dividing the deterministic part of the metabolic strategies' dynamics by $\frac{1}{m}$, and the stochastic part by $\frac{1}{\sqrt{m}}$, the equations are transformed as follows:

$$dn_\sigma = n_\sigma \left(\sum_{i=1}^{p} v_i r_i \; d\alpha_{\sigma i} \; - \delta_\sigma dt \right) \tag{5.22}$$

$$dc_i = m s_i \; dt - \sum_{\sigma=1}^{m} n_\sigma d\alpha_{\sigma i} r_i - \mu_i c_i \; dt \tag{5.23}$$

$$d\alpha_{\sigma i} = \frac{1}{m} \left(\overline{\alpha}_i + \sigma \Delta_i \right) \; dt \; + \frac{1}{\sqrt{m}} \; \Sigma \; d\eta_{\sigma i} \tag{5.24}$$

$$d\eta_{\sigma i} = -\frac{\eta_{\sigma i}}{\tau} dt + \frac{\sqrt{2D}}{\tau} dW_{\sigma i} \tag{5.25}$$

This is the standard method to have a correctly defined limit $m \to \infty$, which allows to properly compare different ecosystems, guaranteeing a more consistent analysis in the subsequent steps.

The dynamics of the metabolic strategies exhibits the distinctive characteristic of having an intrinsic variability in the deterministic components. This is represented by the scattering of $\alpha_{\sigma i}$ values in relation to the α_{1i} values associated with the first resource. In addition to the inherent "quenched" Δ variation, the strength Σ of the annealed noise greatly impacts the dynamics. Therefore, it becomes particularly interesting to investigate how species coexist in relation to the ratio between these two sources of variation. Figure 5.4 represents exactly the Shannon entropy depending on the values of Δ/Σ and τ. For each combination of parameters Δ/Σ and τ, multiple iterations are conducted. In each experiment, the mean probability $\overline{P}_i$ is calculated over a significant time interval to obtain the Shannon Entropy $S = -\sum_{i=1}^{m} \overline{P}_i log(\overline{P}_i)$ for that specific experiment. By averaging the Shannon Entropy values obtained from all these experiments, we obtain the mean Shannon Entropy $\overline{S}_{|\Delta/\Sigma,\tau}$ for that particular combination of Δ/σ and τ. To visualize these biodiversity measures, we can use a color plot, where the color intensity represents the magnitude of the mean Shannon Entropy. The color spectrum used in the plot ranges from violet to yellow, representing different ecological scenarios. The violet color indicates the complete extinction of all species, while the yellow color represents the complete coexistence of all initial species. The transition between these extremes is depicted by colors that lie in between, representing intermediate situations. By observing the color variations in the plot, it becomes evident how the system transitions from a state of high biodiversity to intermediate regimes where several species face the risk of extinction. This is the case both for $m = 7$ and $m = 14$ species.

To better illustrate the transition between the high biodiversity region and the intermediate region, Figure 5.5 depicts the behavior of the mean Shannon Entropy $\overline{S}_{|\Delta/\Sigma,\text{fixed}\tau}$ (averaged over multiple iterations) at a fixed τ. As shown in Figure 5.2, the characteristic time τ influences the dynamics in terms of population cycles, but it does not affect the overall survival of species. Therefore, when the Δ/Σ ratio is held constant and τ is varied, we observe a symmetric pattern in the color plot of Figure 5.4. This implies that any chosen value of the characteristic time would yield a similar pattern in Figure 5.5. The mean Shannon Entropy starts from the highest possible value accessible for that number of species and then decreases to reach a plateau.

To investigate the dynamics further, the time for each iteration has been multiplied by a factor of ten. In Figure 5.6, three distinct regions can be observed: a highly biodiverse region, an intermediate region, and a low biodiversity region, particularly when Δ becomes significantly larger than Σ. The comparison between Figure 5.7 and Figure 5.5 demonstrates that the values of Shannon Entropy exhibit a higher standard deviation, and notably, the plateau of the mean Shannon Entropy decreases when the iteration time is greater (Figure 5.7).

A potential avenue for future research involves exploring the role of the limit as τ approaches infinity in the extinction of the initial species.

Figure 5.3: Separate time evolution of the populations' density according to 5.7. The system simulated is the same as in 5.2 for (1) $\tau = 0.01$ (white Gaussian limit), (2) $\tau = 0.1$, (3) $\tau = 1$ (4) $\tau = 10$.

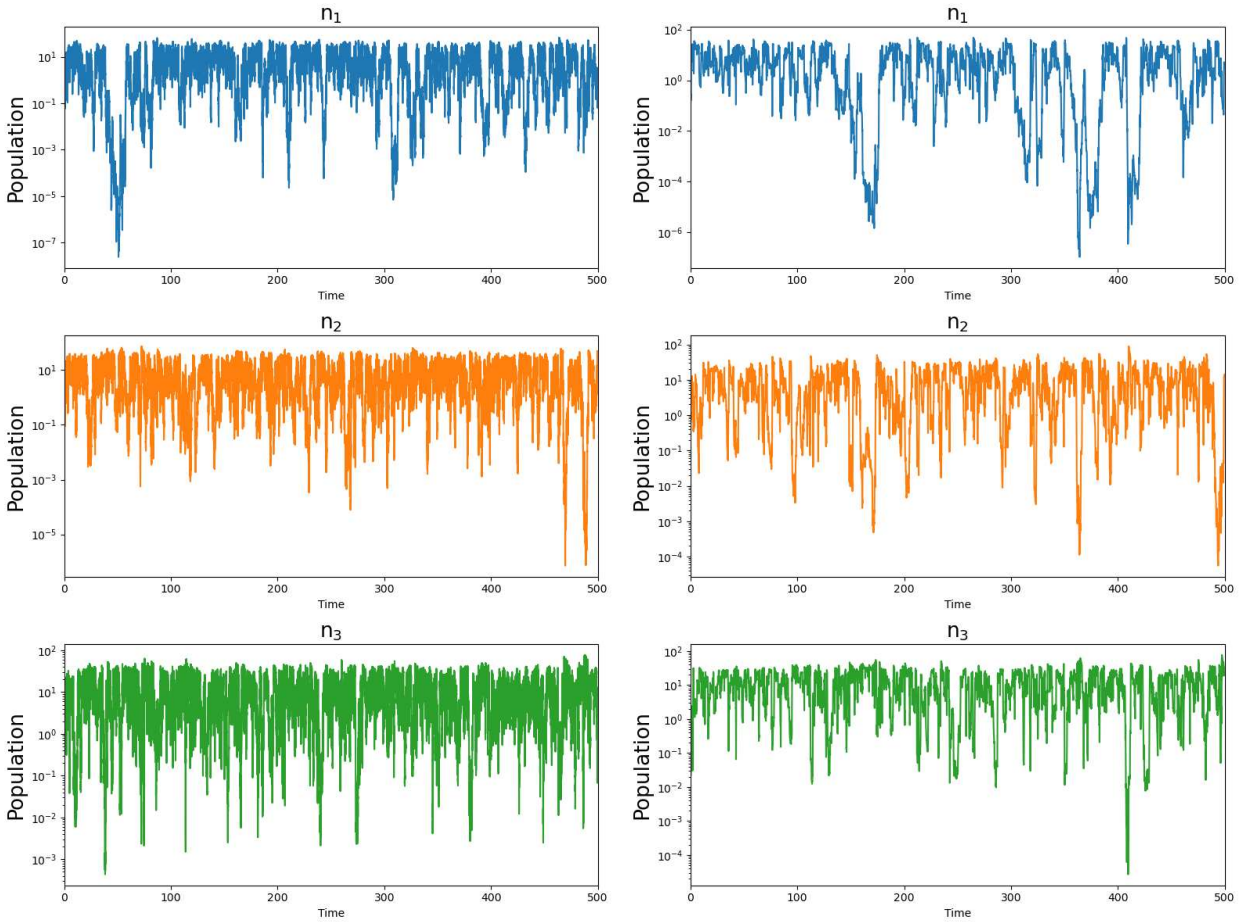

(1) (2)

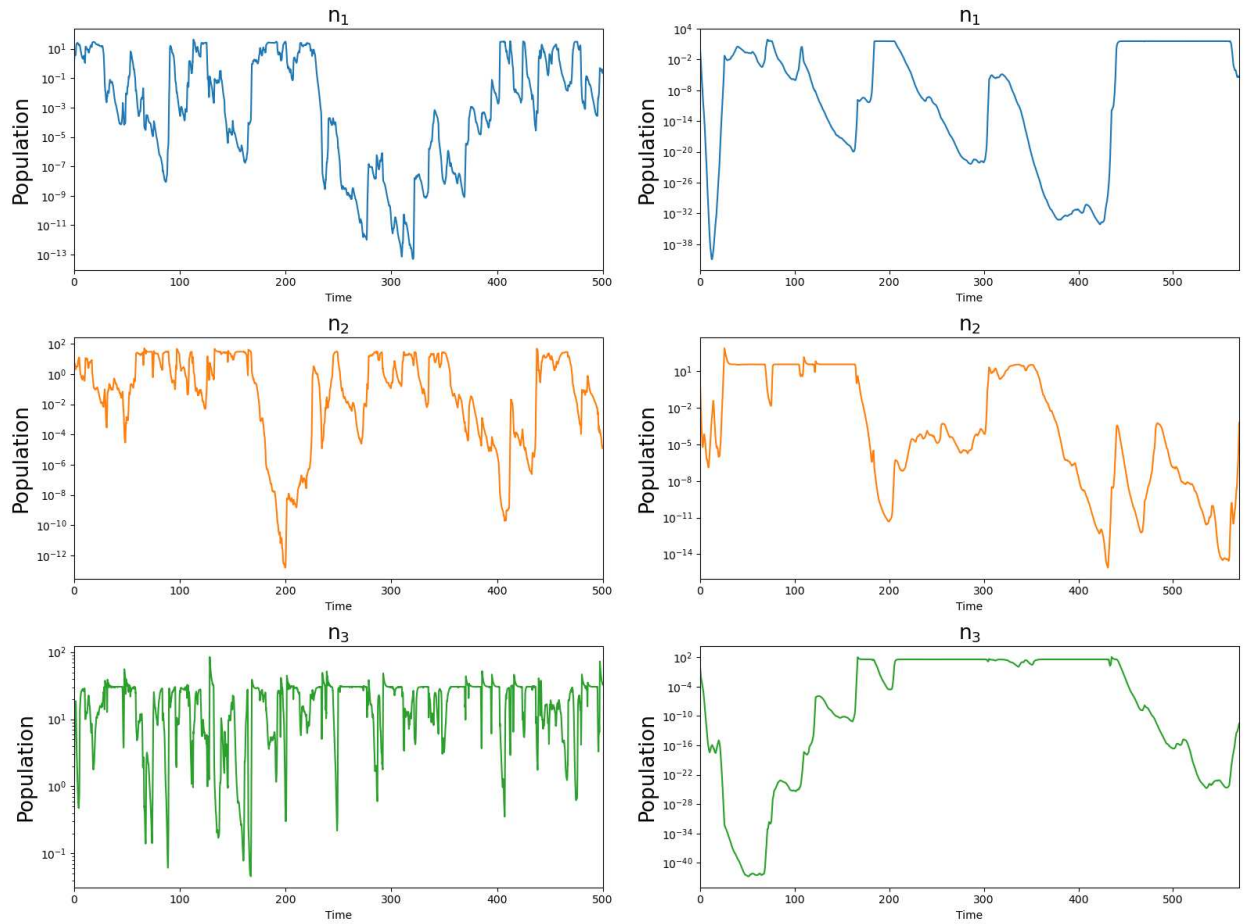

(3) (4)

Figure 5.4: Color Plot of Shannon Entropy for different values of Δ/Σ as the characteristic time τ increases. The color spectrum ranges from violet, indicating the complete extinction of all species, to yellow, representing the complete coexistence of all initial species. Intermediate situations are depicted by colors between the two extremes. The simulations are performed in a system $p = 1$ resource, $\delta_\sigma = 1$, $v_i = v = 1$, $n_\sigma(0) \in U[0.5, 1.5]$, $c_i(0) = c(0) \in U[0.5, 1.5]$, $k_i = k = 5$, $s_i = s \in U[30, 40]$, $\overline{\alpha}_i = \overline{\alpha} = 5$, $dW_{\sigma i} \sim \mathcal{N}(0, dt)$, $\Sigma = 0.5$. For each combinations of the variables $\Delta \in [1, 10]$ and $\tau \in [0.1, 20.1]$ we have performed 60 different iterations. The number of species is (1) $m = 7$ and (2) $m = 14$ species.

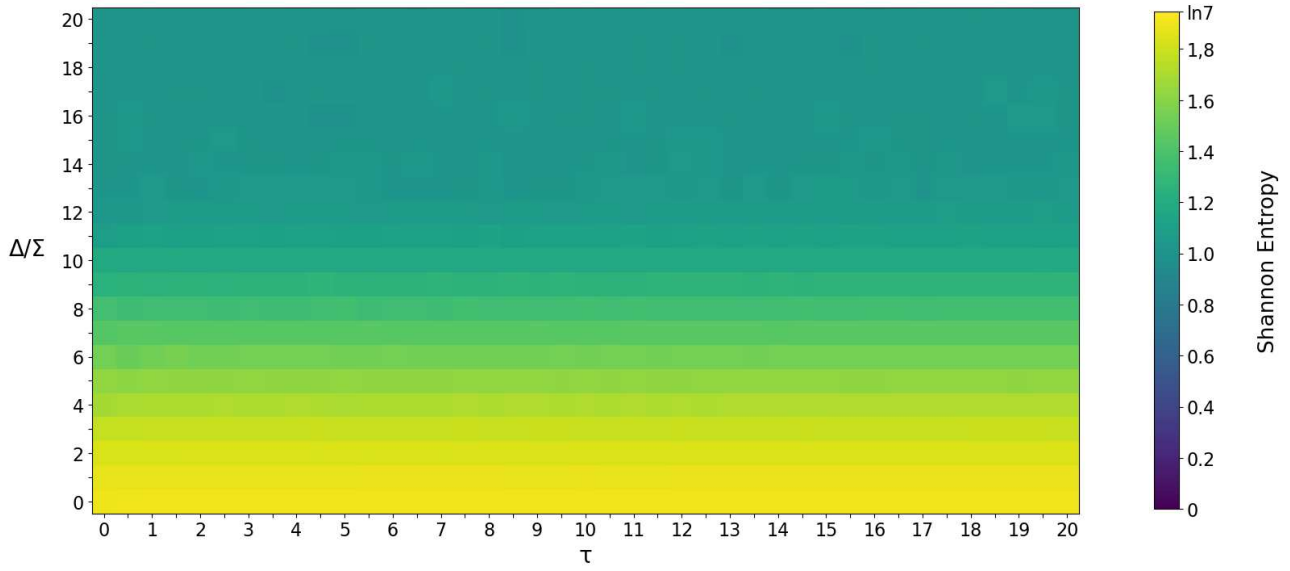

(1)

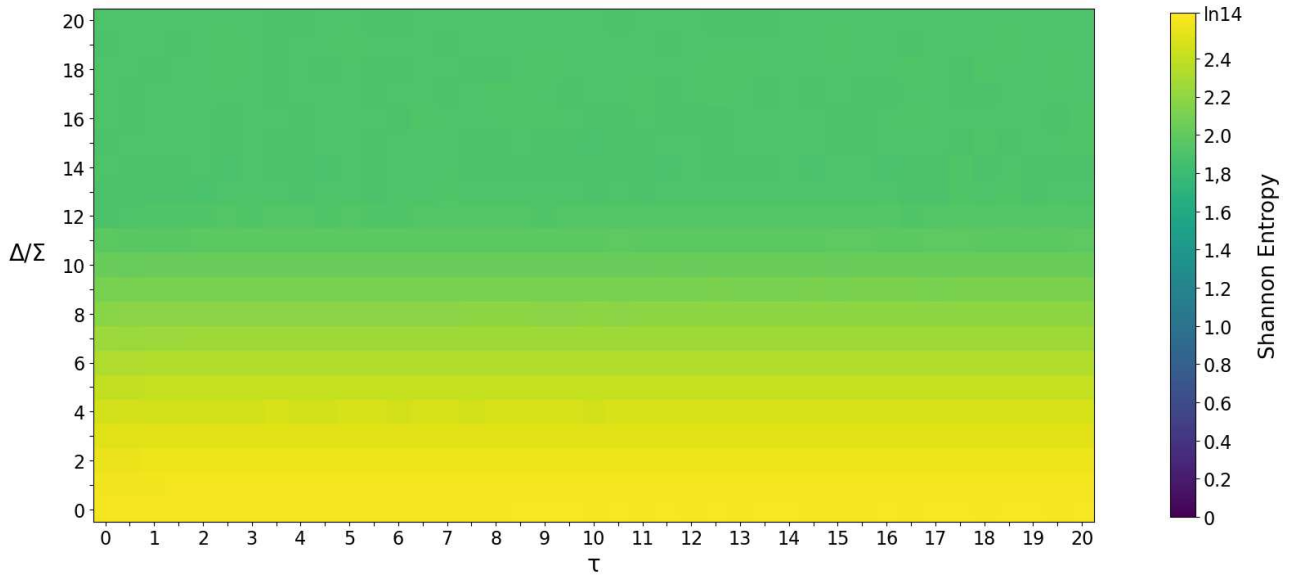

(2)

Figure 5.5: Average Shannon Entropy for different values of Δ/Σ at a characteristic time $\tau = 10$. For each value of the ratio Δ/Σ we have realised 60 iterations. For each sample the standard deviation from the mean value is represented by the error bar. The simulations are performed in the same system of Figure 5.4 with $p = 1$ resource, $\delta_\sigma = 1$, $v_i = v = 1$, $n_\sigma(0) \in U[0.5, 1.5]$, $c_i(0) = c(0) \in U[0.5, 1.5]$, $k_i = k = 5$, $s_i = s \in U[30, 40]$, $\overline{\alpha}_i = \overline{\alpha} = 5$, $dW_{\sigma i} \sim \mathcal{N}(0, dt)$, $\Sigma = 0.5$. The system has (1) $m = 7$ and (2) $m = 14$ species.

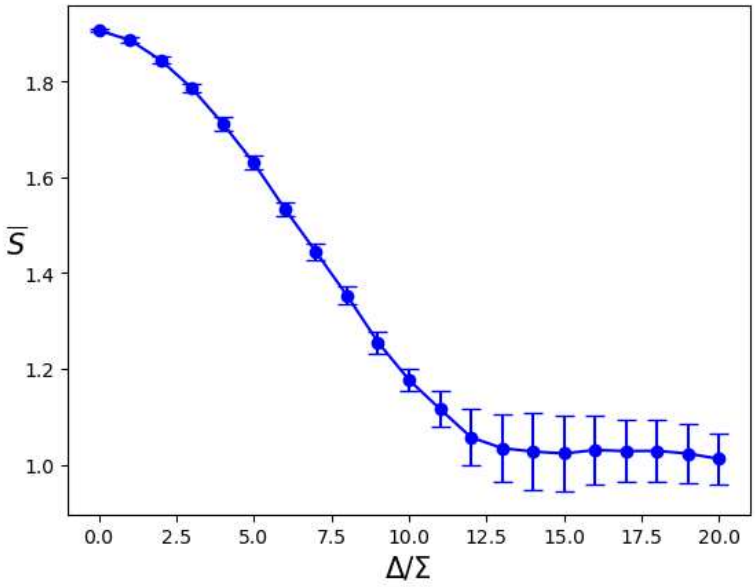

(1)

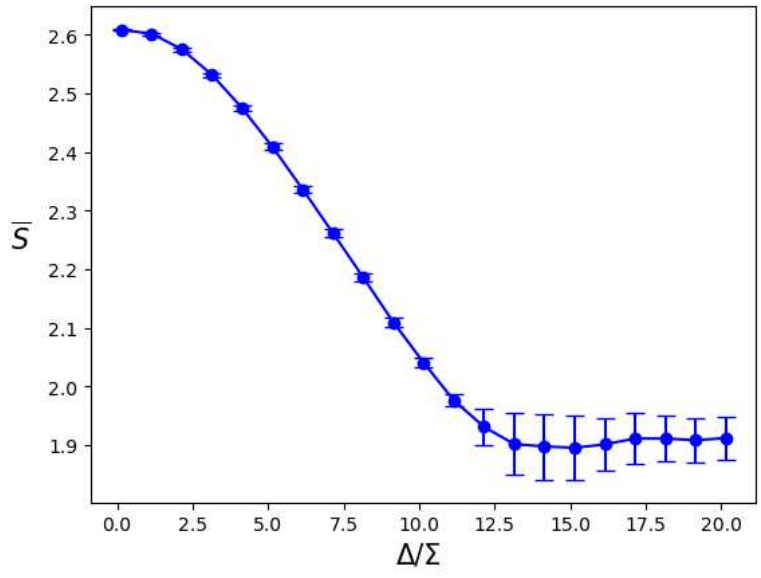

(2)

Figure 5.6: Color Plot of Shannon Entropy for different values of Δ/Σ as the characteristic time τ grows. The iteration time is increased by a factor ten compared to Figure 5.4. The color spectrum ranges from violet, indicating the complete extinction of all species, to yellow, representing the complete coexistence of all initial species. Intermediate situations are depicted by colors between the two extremes. The simulations are performed in a system $p = 1$ resource, $\delta_\sigma = 1$, $v_i = v = 1$, $n_\sigma(0) \in U[0.5, 1.5]$, $c_i(0) = c(0) \in U[0.5, 1.5]$, $k_i = k = 5$, $s_i = s \in U[30, 40]$, $\overline{\alpha}_i = \overline{\alpha} = 5$, $dW_{\sigma i} \sim \mathcal{N}(0, dt)$, $\Sigma = 0.5$. For each combinations of the variables $\Delta \in [1, 10]$ and $\tau \in [0.1, 20.1]$ we have performed 60 different iterations. The number of species is (1) $m = 7$ and (2) $m = 14$ species.

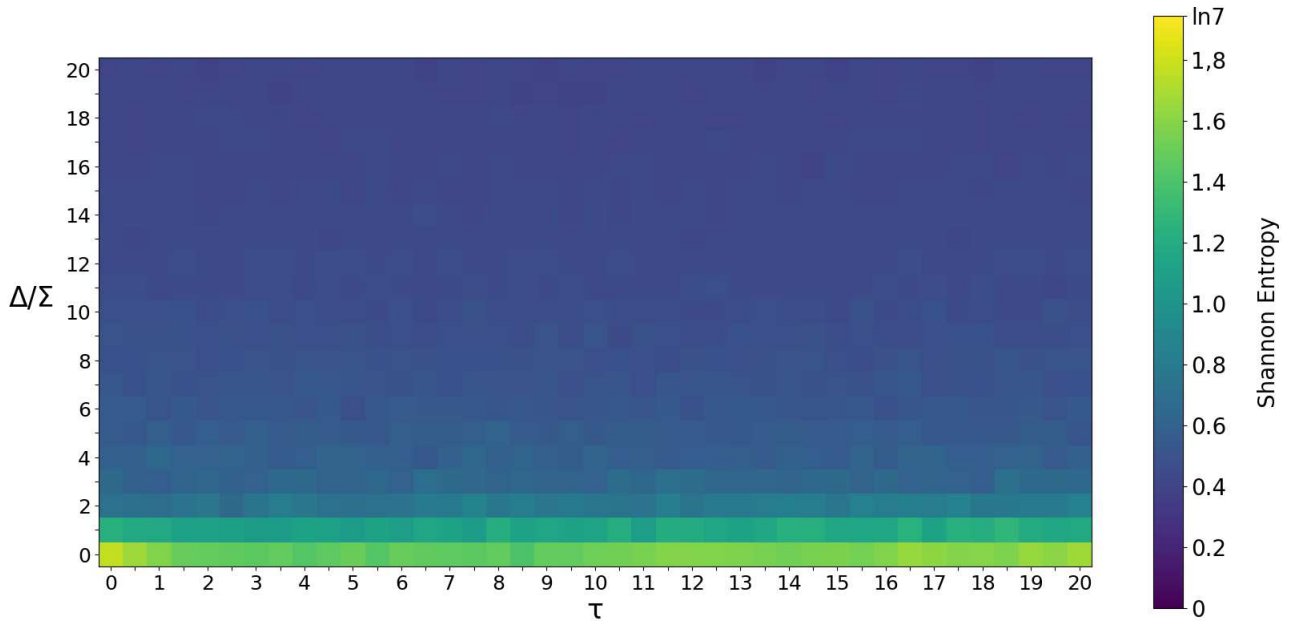

(1)

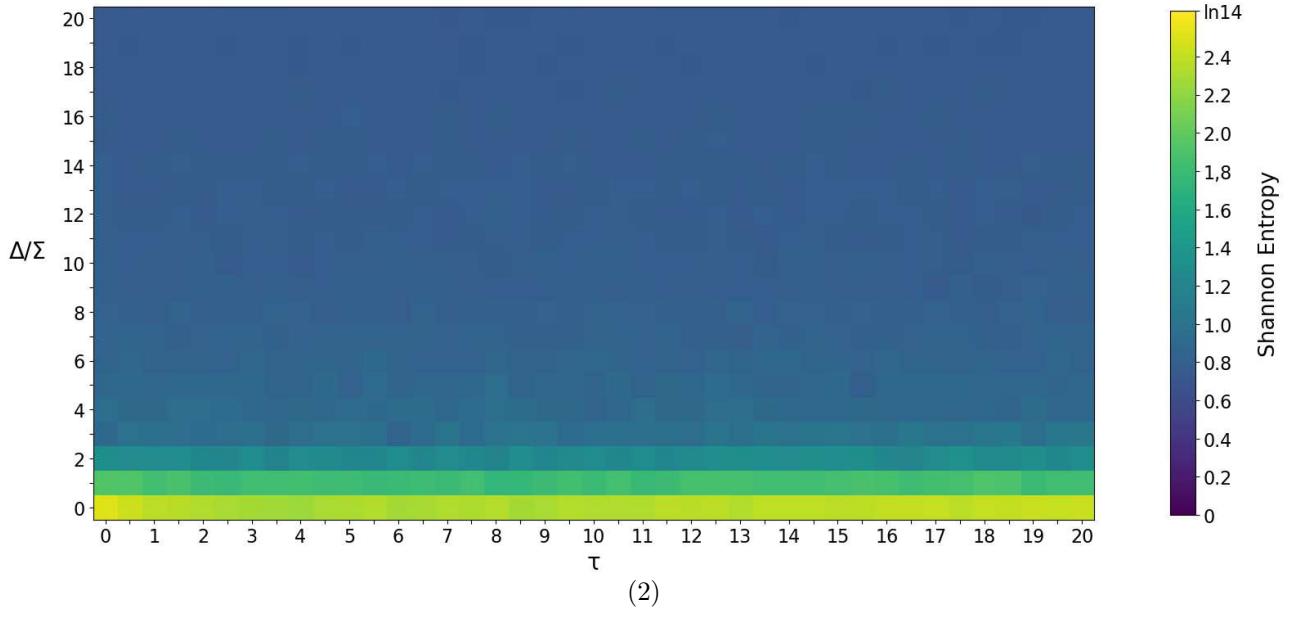

(2)

Figure 5.7: Average Shannon Entropy for different values of Δ/Σ at a characteristic time $\tau = 10$. For each value of the ratio Δ/Σ we have realised 60 iterations. The iteration time has increased by a factor ten compared to Figure 5.4. For each sample the standard deviation from the mean value is represented by the error bar. The simulations are performed in the same system of Figure 5.4 with $p = 1$ resource, $\delta_\sigma = 1$, $v_i = v = 1$, $n_\sigma(0) \in U[0.5, 1.5]$, $c_i(0) = c(0) \in U[0.5, 1.5]$, $k_i = k = 5$, $s_i = s \in U[30, 40]$, $\overline{\alpha}_i = \overline{\alpha} = 5$, $dW_{\sigma i} \sim \mathcal{N}(0, dt)$, $\Sigma = 0.5$. The system has (1) $m = 7$ and (2) $m = 14$ species.

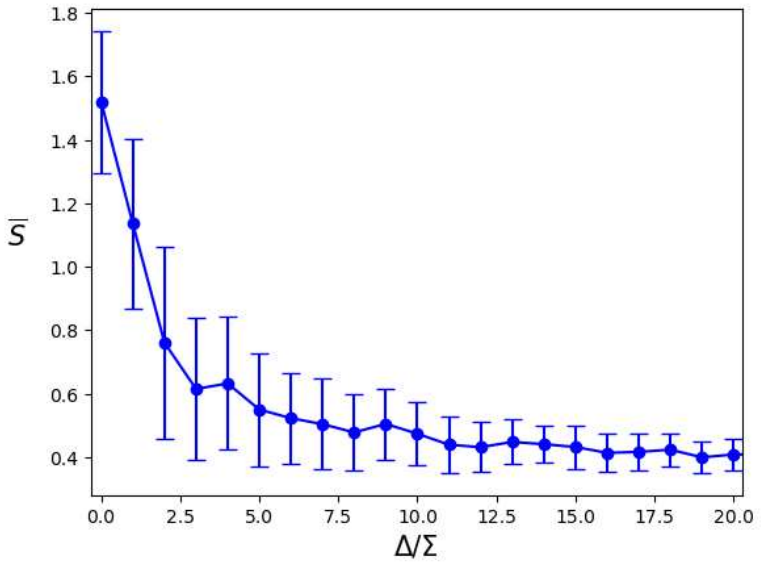

(1)

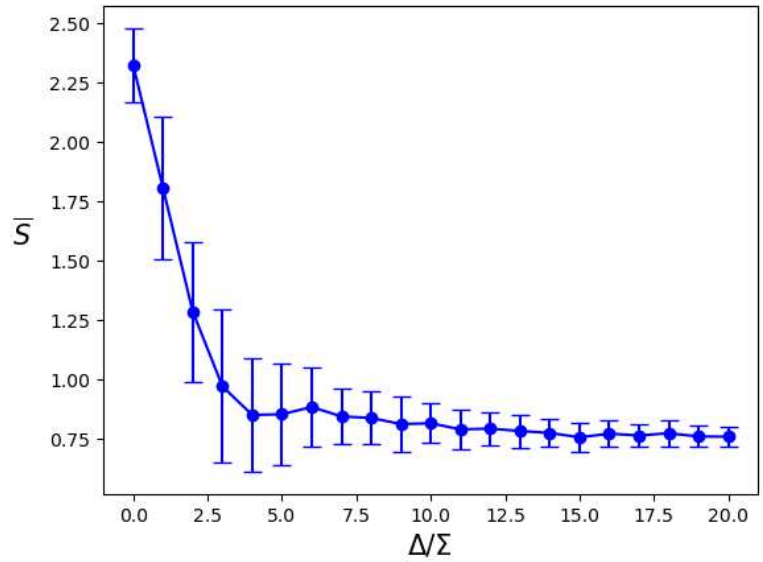

(2)

CONCLUSIONS

"Role of dynamic metabolic strategies in species coexistence patterns" is a master thesis in Physics of Complex Systems, which addresses the ecological population dynamics of different species competing for multiple nutrients, beginning from the MacArthur's consumer-resource model and adding progressively new insightful terms that enable to describe more closely the high level of diversity of microbial communities, in particular the coexistence of several species in a pool of few resources. The central focus of this study has been on the metabolic strategies, which define the consumption rates at which species σ uptake resource i and convert it into biomass.

The first main result of this thesis is the creation of the Adaptive Interactive Model, which not only is able to describe analytically and numerically the time evolution of m different species uptaking p resources from the environment, whose individuals experience intraspecies interactions, but also it enables to explain the violation of the well known Competitive Exclusion Principle (CEP) at stationarity.

The core feature of this model is represented by the promotion of the metabolic strategies to dynamical variables to maximize the growth rate of each species, while ensuring a maximum energy constraint. The first fundamental parameter is the velocity of the dynamic metabolic adaptation and optimisation. The interaction term is the other peculiar characteristic of this formulation. This new parameter emerges in ecosystems where spatial effects are non-negligible, and it originally takes in account intraspecies and interspecies interactions. This thesis focuses on the interplay between individuals belonging to the same species, because this case is analytically treatable.

Initially, a comprehensive analysis of the individual effects of each term is conducted by alternately studying the effects of the velocity adaptation and the interaction term.

Firstly, the Adaptive Interactive Model has been analytically studied for null adaptation velocity and null interactive term. This Static framework imposes the maximum total uptake rate to be species dependent at the cost of introducing a dependence of it on the death rate of each species, in accordance with the metabolic theory of ecology. If this condition is not met, CEP holds. The steady state that enables the coexistence of an arbitrary number of species is non-empty, i.e. the supply rate is inside the convex hull of the metabolic strategies, if the Characteristic Timescale Ratio (CTR), defined as the ratio between the maximum energy budget of each species and the death rate of each species, does not depend on the identity of the species.

Secondly, the Adaptive Interactive Model has been analytically studied for a null interaction term. Starting from this point onward, metabolic strategies have their own dynamics to optimise the fitness of each species, and thus their matrix $m \times p$ evolves in time thanks to a non-null adaptation velocity. The time evolution of the metabolic strategies is obtained trough a constrained optimisation approach. The role of various parameters associated with the resources has been thoroughly investigated. This dynamic framework demonstrates its capability to support species coexistence, even when the system faces drastic conditions, such as environmental variability or the presence of unfavorable resources. Significant emphasis has been placed on comprehending the crucial role of resource degradation in this ecological dynamics. A significant finding of this thesis is that once the degradation rate of a resource surpasses a certain threshold, there is an immediate and complete cessation of resource metabolism

by the species. Many questions regarding the dynamics of metabolic strategies remain unanswered, indicating the need for further analytical investigations.

Table 5.3: Synthetic description of the main features of the different deterministic models analysed in this thesis. Note how the Adaptive Interactive Model's flexibility is able to violate the Competition Exclusion Principle, even in presence of the species-dependent Characteristic Timescale Ratios (CTR). The energy constraint is $E = Q\delta_\sigma$ for the Static Model, $E_\sigma(0) \in U[0, Q\delta_\sigma]$ for the Adaptive Model and $E_\sigma(0) \in U[0, Q_\sigma\delta_\sigma]$ for the Adaptive Interactive Model. The column related the metabolic strategies are stationarity is a qualitative description of their behaviour and the parameters determining it.

MODEL	**d**	$\boldsymbol{\epsilon}$	$\boldsymbol{\alpha_{\sigma i}(t_i)}$	$\boldsymbol{\alpha_{\sigma i}(t_f)}$	**CTR**	**CEP**
MAC ARTHUR	\	\	random	constant	\	YES
STATIC (fine-tuned: $\delta_\sigma = \delta\ \forall\sigma$ and $\vec{s}$ in the convex hull of $\vec{\alpha}_\sigma$)	\	\	$\sum_{i=1}^{p} \alpha_{\sigma i} = E\ \forall\sigma$	constant	\	NO
STATIC	\	\	$\sum_{i=1}^{p} \alpha_{\sigma i} = E\ \forall\sigma$	constant	\	YES
ADAPTIVE (with Q fixed)	$4,20 \cdot 10^6$	\	$\sum_{i=1}^{p} \alpha_{\sigma i}(0) = E_\sigma(0)$	μ_i, $1/\nu_i \to$ regime or collapse	Q	NO
ADAPTIVE (with Q_σ)	$4,20 \cdot 10^6$	\	$\sum_{i=1}^{p} \alpha_{\sigma i}(0) = E_\sigma(0)$	μ_i, $1/\nu_i \to$ regime or collapse	Q_σ	YES
INTERACTIVE	\	$\vec{\epsilon}_\sigma$	random	constant	\	NO
ADAPTIVE INTERACTIVE	$4,20 \cdot 10^6$	$\vec{\epsilon}_\sigma$	$\sum_{i=1}^{p} \alpha_{\sigma i}(0) = E_\sigma(0)$	ϵ_σ, μ_i, $1/\nu_i \to$ regime or collapse	Q_σ	NO

Third, the Adaptive Interactive Model with null adaptation velocity allows to study the role of the spacial contributions to the dynamics with static metabolic strategies. The interaction term is formally derived considering the quasi-static dynamics of the pathogens, alongside with the ones of the species and resources, to describe the Janzen-Connel effect. Considering just species-specific pathogens and assuming only intra-species interactions, it is possible to analytically describe the coexistence region in the space of the Monod functions where all the initial species survive. Once again, the supply rate plays a fundamental role: its threshold value, which determines whether the Competition Exclusion Principle is violated or upheld, is analytically derived. It is even possible to address the validity of the CEP below this threshold, by predicting the corresponding supply rate required for a specific number of species to die.

Finally, the innovative Adaptive Interactive Model absorbs the dynamic of the metabolic strategies, through the adaptation velocity and the quadratic competitive interaction term. Contrary on the previous models, this new formulation enables to better model evidences showing that in nature the Characteristic Timescale Ratio depends on the species. This new degree of freedom, which determines the extinction of species in the Static and in the Interactive Model, allows to observe a violation of the CEP inside the Adaptive Interactive approach. The parameters are drawn from distributions that have been designed in a original way in this work.

As the interaction term increases, the uptake of the unfavorable nutrient with the highest degradation rate experiences a sharp decrease across all species. Interestingly, a new transition is observed, where all components of the metabolic strategies related to that resource become null when the interaction term surpasses a certain threshold. Despite the considerable variance among the species-dependent values of the CTR, spanning multiple orders of magnitude, the new model demonstrates robustness, ensuring the survival of all initial species in the stationary state.

To conclude, table 5.3 presents a comprehensive qualitative overview of all the deterministic models studied in this thesis.

The second main result of this thesis is the introduction of the Stochastic Model. The study of the temporal evolution of metabolic strategies, which combines a deterministic and a stochastic term, represents an innovative development in the field of population dynamics. It has been shown that introducing annealed noise into the dynamics of metabolic strategies can greatly enhance species coexistence and promote biodiversity. Moreover, for sufficiently long characteristic times of the fluctuations, demographic cycles become apparent. During these cycles, species appear to experience a period of low population size followed by a subsequent recovery and resurgence to high values. The relationship between the variance of deterministic values of metabolic strategies and the strength of noise in relation to the characteristic time provides insights into high, intermediate, and low biodiversity regimes: this study is still in its preliminary stages, so further investigations and implementations are necessary to deepen our understanding. However, the dynamics of metabolic strategies in the Stochastic Model can be considered more effective than that in the Adaptive Interactive Model, as it predicts coexistence of initial species with fewer constraints.

Overall, this thesis rolls out the original Adaptive Innovative Model, its formal description and computational parameters, which permit to describe why a large number of species can coexist in the presence of few resources. The role of the metabolic strategies, their adaptation velocity, the degradation rates, the characteristic timescale ratio, the supply rate and the interaction terms has been methodically explored in details in the deterministic model.
Ultimately, the thesis introduces a Stochastic Model, creating a more comprehensive and complete representation of the ecosystem studied when it is subjected to time correlated fluctuations. The questions related to the Competition Exclusion Principle and, in particular, to the Paradox of the Plankton can not be considered solve as a comprehensive biodiversity's theory has not be formulated yet. However, it has been demonstrated that a dynamic, even a stochastic one, on the metabolic strategies plays a crucial role in facilitating coexistence and biodiversity.

APPENDIX

A Angular Behaviour of the Metabolic Strategies in the Adaptive Non-Degradative model with constant supply rate

In this section of the Appendix, we present the study of a system with $p = 2$ resources, whose corresponding $p-1$ dimensional simplex is a line. By studying the dynamics of the metabolic strategies within the simplex, each species is represented by an arrow, which provides information about the proportion of investment allocated by the species in metabolizing the first and the second resource.

Firstly, for a given $m = 10$, a series of simulations were conducted to investigate the distribution of arrow directions, which represent the proportions of effort exerted by species in metabolizing different resources. This analysis of the directions aims to identify any patterns or regularities in the angular probability distribution. Within the same number of species, no common behaviour was found in dividing the energy budget among the different species. The same enquire is performed scaling with much greater number of species ($m = 20, 30, 40, 50, 60, 70$ are the cases examined) allowing to discard the hypothesis of some regularities in the frequency of the proportions with which species choice to metabolize one or the other nutrient. No regularities have been detected simulating the system several time with the same number of species, and no arising behaviour has been noticed at higher values of m. Some of the simulations performed are presented in Figure A.1

Secondly, the correlation between the initial and the final stationary direction of the metabolic strategies has been enquired. By comparing the initial and final angles that correspond to different species, representing the initial and final proportions of their choice in utilizing either of the two resources, it became evident that the dynamics of time evolution play a crucial role in energy management. Analyzing the changes in the angles allows us to gain insights into how species adapt their energy allocation strategies over time. The comparison revealed that the initial proportions of resource utilization were not determinative of the final outcomes. Instead, the species exhibited dynamic shifts in their energy management patterns as the system evolved. This method has been implemented on multiple realizations of the system while keeping the number of species constant. Figure A.2 displays a selection of simulations conducted within the range of $m = 10, 20, 30, 40, 50, 60, 70$, which was explored during the analysis. In the left and central columns, the direction and intensity of the initial and final metabolic strategies, respectively, have been presented. In the right column, the plot shows the relationship between the final angles and the initial angles, which are determined by the metabolic strategies' vectors. The blue points that lie on the bisector visually correspond to species whose energy distribution between the two resources remains fixed throughout the entire time evolution. However, upon inspection of Figure A.2, it becomes evident that there is no systematic energy distribution pattern among the species.This visualisation leads to discard any peculiar correlation between the initial and the final proportions in up-taking the two species. Due to the dynamics occurring in the system, the species don't exhibit a stable allocation of energy between the resources. Further inquiries are necessary to comprehend the analytical conditions under which the final angles align with the initial angles.

Figure A.1: Simplex of the stationary rescaled metabolic strategies for different values of m. In these simulations we consider $p = 2$ resources, $Q \in U[10^{-7}, 5 \cdot 10^{-5}]$ g of resource/cell (with U the uniform distribution), $\delta_\sigma \in U[5 \cdot 10^{-3}, 5 \cdot 10^{-2}]$ 1/h, $E_\sigma(0) \in U[0, Q\delta_\sigma]$ g of resource/(cell $\cdot$ h), $v_i \in U[10^8, 5 \cdot 10^9$ cell/g of resource, $n_\sigma(0) \in U[10^6, 5 \cdot 10^6]$ cell/mL, $c_i(0) \in U[10^{-3}, 10^{-2}]$ g of resource/mL, $k_i \in U[10^{-4}, 10^{-3}]$ g of resource/mL, $d = 4.20 \cdot 10^{-6}$ g of resource/cell, $s_i \in U[10^3, 5 \cdot 10^{-2}]$ g of resource/(mL·h) and $\alpha_{\sigma i}(0)$ such that $\sum_{i=1}^{p} \alpha_{\sigma i}(0) = E_\sigma(0)$. The simplex is shown for (1) m=20 (2) m=40 and (3) m=60: no regularities in the corresponding angular probability distributions are found.

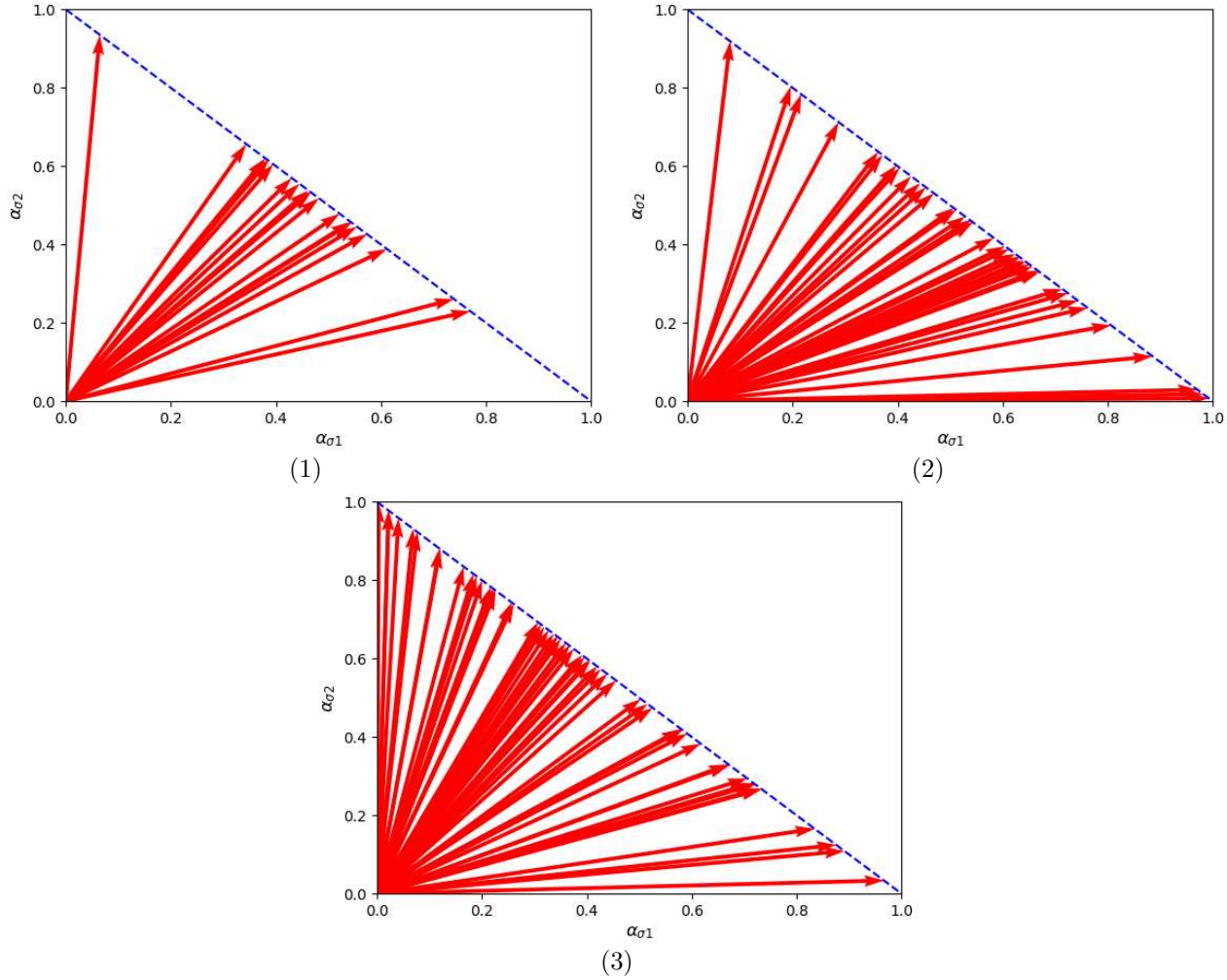

Figure A.2: Initial directions (left column) and Final directions of the rescaled metabolic strategies (central column) and Initial Angles vs Final Angles (right column) for (1) m=30, (2) m=50, (3) m=70. The parameters and the initial conditions are the ones introduced in Figure A.1. The red line in the right column represents the bisector. No recurrent pattern of blue points lying on this line has been found. The time evolution of the system leads to a changing energy distribution among the two resources for the species.

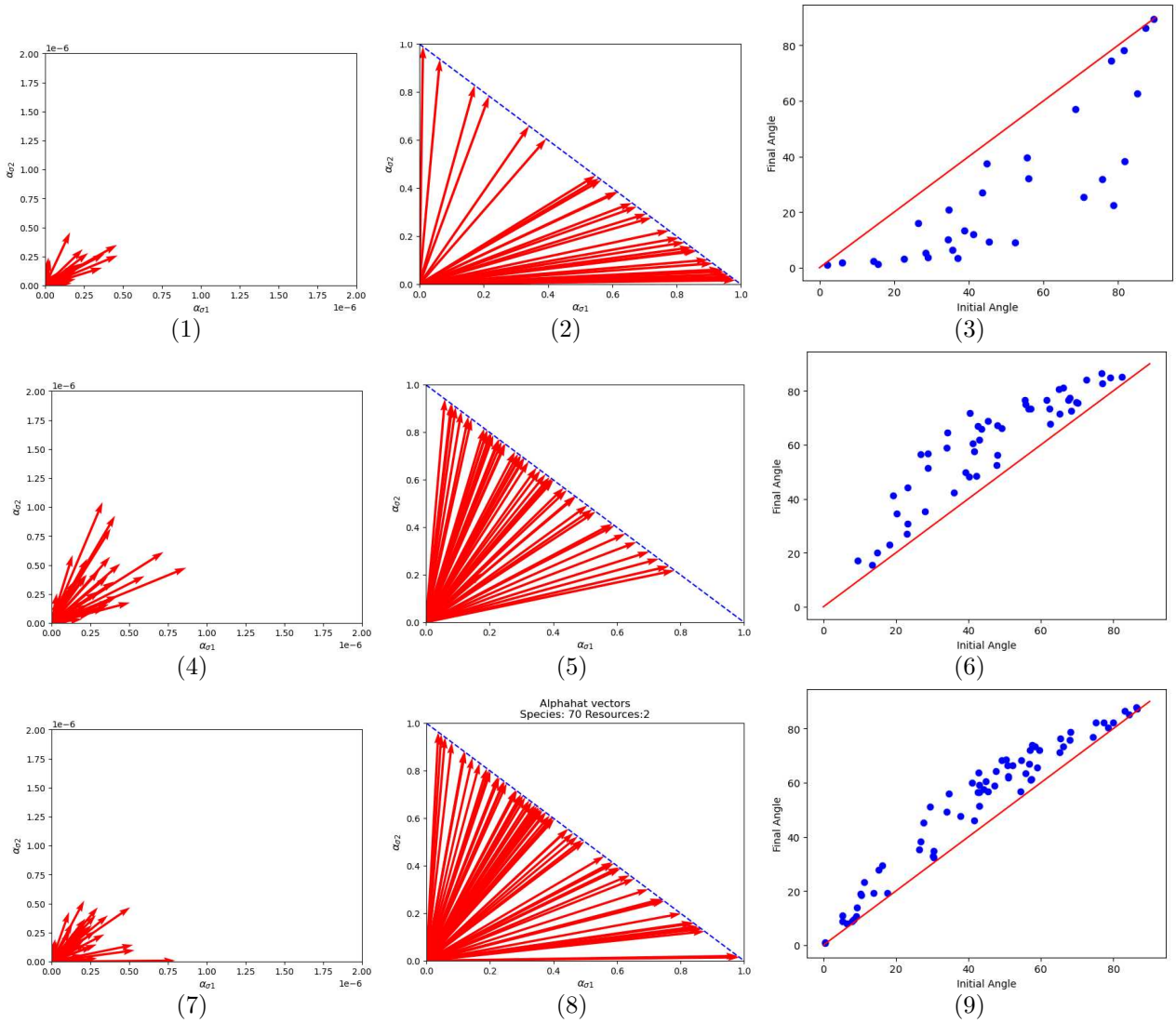

B Emergence of the interaction quadratic term in the Interactive Model

In the chapter dedicated to the Interactive Model, we described the emergence of the carrying capacity via Janzen-Connel effect. In this section of the Appendix, we provide a detailed derivation that justifies the inclusion of the quadratic term in the model. We achieve this by employing coarse-graining techniques on a consumer-resource model that incorporates the effects of diffusive motion and foraging or chemotactic strategies. This complete calculation leads to the same result of inducing the quadratic competitive interaction term, $\sum_\rho \epsilon_{\sigma\rho} n_\sigma n_\rho$ that presented in the main text.

The starting point is a MacArthur's model, where several species compete for only one resource. To include spatial contributions in the dynamics, we add flux-terms expressed as

$$J_{n_\sigma}(x,t) = -\left(A_{1,\sigma} + A_{2,\sigma} c(x,t) - \sum_\rho K_{\sigma\rho} n_\rho(x,t)\right) \nabla n_\sigma(x,t) + A_{3,\sigma} n_\sigma(x,t) \nabla c(x,t) \tag{B.1}$$

$A_{1,\sigma}, A_{2,\sigma}, A_{3,\sigma}$ and $K_{\sigma\rho}$ are constants in time. The terms proportional to $A_{i,\sigma}$ in the flux capture the movement dynamics and interactions within the system. Additionally, the contributions denoted by $K_{\sigma\rho}$ arise from incorporating mechanisms that prevent local overcrowding. In microbial communities, certain strains are known to modify their environment by producing harmful toxins, which can adversely affect other strains and even themselves.

The equations governing the time evolution of populations' density and of the resource concentration are:

$$\dot{n}_\sigma(x,t) = n(x,t)\left(\alpha_\sigma c(x,t) - \beta_\sigma\right) - \nabla J_{n_\sigma}(x,t) \tag{B.2}$$

$$\dot{c}(x,t) = s - \mu c(x,t) - c(x,t) \sum_\rho \alpha_\rho n_\rho(x,t) \tag{B.3}$$

The Monod function has been substituted by with $c(x,t)$, which is its leading order in its Taylor expansion for small c.

Substituting J_{n_σ} from Equation B.1 in Equations B.2 and B.3 we obtain

$$\begin{aligned}\dot{n}_\sigma(x,t) = n(x,t)\left(\alpha_\sigma c(x,t) - \beta\right) + \left(A_{1,\sigma} + A_{2,\sigma} c(x,t) - \sum_\rho K_{\sigma\rho} n_\rho(x,t)\right) \nabla^2 n_\sigma(x,t) - A_{3,\sigma} n_\sigma(x,t) \nabla^2 c(x,t) \\ + \left(A_{2,\sigma} - A_{3,\sigma}\right) \nabla n_\sigma(x,t) \cdot \nabla c(x,t) - \sum_\rho K_{\sigma\rho} \nabla n_\sigma(x,t) \cdot \nabla n_\rho(x,t)\end{aligned} \tag{B.4}$$

$$\dot{c}(x,t) = s - \mu c(x,t) - c(x,t) \sum_\rho \alpha_\rho n_\rho(x,t) \tag{B.5}$$

We explore a scenario where the spatial variable is discretized on a one-dimensional lattice. In this setup, each i site, represents a patch of size a and is associated with populations $n_\sigma^{(i)}$ and a resource concentration $c^{(i)}$. It's important to note that the superscripts now indicate spatial positions.

$$\begin{aligned}\dot{n}_\sigma^{(i)}(t) = n_\sigma^{(i)}(t)\left[\alpha c^{(i)}(t) - \beta\right] + \left[A_1 + A_2 c^{(i)}(t)\right]\left[n_\sigma^{(i+1)}(t) + n_\sigma^{(i-1)}(t) - 2n_\sigma^{(i)}(t)\right] + \\ - A_3 n_\sigma^{(i)}(t)\left[c^{(i+1)}(t) + c^{(i-1)}(t) - 2c^{(i)}(t)\right] + (A_2 - A_3)\left[n_\sigma^{(i+1)}(t) - n_\sigma^{(i)}(t)\right]\left[c^{(i+1)}(t) - c^{(i)}(t)\right] \\ - \sum_\rho K_{\sigma\rho}\left[n_\sigma^{(i-1)}(t)n_\rho^{(i)}(t) - n_\sigma^{(i)}(t)n_\rho^{(i)}(t) + n_\sigma^{(i+1)}(t)n_\rho^{(i+1)}(t) - n_\sigma^{(i)}(t)n_\rho^{(i+1)}(t)\right]\end{aligned} \tag{B.6}$$

$$\dot{c}^{(i)}(t) = s - \mu c^{(i)}(t) - c^{(i)}(t)\sum_\rho \alpha_\rho n_\rho^{(i)}(t) \tag{B.7}$$

The lattice site is labeled by $i \in \mathbb{Z}$. Due to the consumption of the resource, the species migrate from one patch to another.

The coarse-graining procedure involves removing the dynamical variables $n_\sigma^{(i)}$ and $c^{(i)}$ for odd positions, while retaining the variables for even positions. This calculation can be illustrated by considering a scenario where a single species of consumers colonizes two adjacent sites/patches $i = 1, 2$ with periodic boundary conditions. We can forget about the subscript for species population as we are going to consider just one specie.

In the next steps,the following substitution is needed in the non-linear terms:

$$n_\sigma^{(i)} \longrightarrow \delta n_\sigma^{(i)} \tag{B.8}$$

Equations B.6 and B.7 become

$$\begin{aligned}\dot{n}^{(1)} &= n^{(1)}\left(\alpha c^{(1)} - \beta\right) + 2A_1\left(n^{(2)} - n^{(1)}\right) + \delta\,(A_2 - A_3)\left(n^{(2)}c^{(2)} - n^{(1)}c^{(1)}\right) \\ &= +\delta\,(A_2 + A_3)\left(n^{(2)}c^{(1)} - n^{(1)}c^{(2)}\right) - \delta^2 K\left(n^{(2)}n^{(2)} - n^{(1)}n^{(1)}\right)\end{aligned} \tag{B.9}$$

$$\begin{aligned}\dot{n}^{(2)} &= n^{(2)}\left(\alpha c^{(2)} - \beta\right) + 2A_1\left(n^{(1)} - n^{(2)}\right) + \delta\,(A_2 - A_3)\left(n^{(1)}c^{(1)} - n^{(2)}c^{(2)}\right) \\ &= +\delta\,(A_2 + A_3)\left(n^{(1)}c^{(2)} - n^{(2)}c^{(1)}\right) - \delta^2 K\left(n^{(1)}n^{(1)} - n^{(2)}n^{(2)}\right)\end{aligned} \tag{B.10}$$

$$\dot{c}^{(1)} = s - \mu c^{(1)} - \delta\alpha n^{(1)}c^{(1)} \tag{B.11}$$

$$\dot{c}^{(2)} = s - \mu c^{(2)} - \delta\alpha n_2 c^{(2)} \tag{B.12}$$

We recall the definitions of the Laplace transform and its inverse:

$$\tilde{\Omega}(\omega) = \mathcal{L}[\Omega(t)](\omega) = \int_0^{+\infty} dt e^{-\omega t}\Omega(t), \tag{B.13}$$

$$\Omega(t) = \mathcal{L}^{-1}[\tilde{\Omega}(\omega)](t) = \frac{1}{2\pi i}\lim_{\gamma\to\infty}\int_{a-i\gamma}^{a+i\gamma} d\omega e^{\omega t}\tilde{\Omega}(\omega) \tag{B.14}$$

a is defined so that all singularities of $\tilde{\Omega}(\omega)$ belong the region $\mathrm{Re}(\omega) < a$

The definition of Laplace transform applied to Equations B.9, B.10, B.11 and B.12, starting from the initial conditions of the system $n_i(0)$ and $c_i(0)$, gives

$$\omega\tilde{n}^{(1)}(\omega) - n^{(1)}(0) = -\beta\tilde{n}^{(1)}(\omega) + \delta\alpha\tilde{n}^{(1)}(\omega) * \tilde{c}^{(1)}(\omega) + 2A_1\left(\tilde{n}^{(2)}(\omega) - \tilde{n}^{(1)}(\omega)\right) + \delta\left(A_2 - A_3\right)\left(\tilde{n}^{(2)}(\omega) * \tilde{c}^{(2)}(\omega) + -\tilde{n}^{(1)}(\omega) * \tilde{c}^{(1)}(\omega)\right) + \delta\left(A_2 + A_3\right)\left(\tilde{n}^{(2)}(\omega) * \tilde{c}^{(1)}(\omega) - \tilde{n}^{(1)}(\omega) * \tilde{c}^{(2)}(\omega)\right) - \delta^2 K\left(\tilde{n}^{(2)}(\omega) * \tilde{n}^{(2)}(\omega) - \tilde{n}^{(1)}(\omega) * \tilde{n}^{(1)}(\omega)\right) \tag{B.15}$$

$$\omega\tilde{n}^{(2)}(\omega) - n^{(2)}(0) = -\beta\tilde{n}^{(2)}(\omega) + \delta\alpha\tilde{n}^{(2)}(\omega) * \tilde{c}^{(2)}(\omega) + 2A_1\left(\tilde{n}^{(1)}(\omega) - \tilde{n}^{(2)}(\omega)\right) + \delta\left(A_2 - A_3\right)\left(\tilde{n}^{(1)}(\omega) * \tilde{c}^{(1)}(\omega) + -\tilde{n}^{(2)}(\omega) * \tilde{c}^{(2)}(\omega)\right) + \delta\left(A_2 + A_3\right)\left(\tilde{n}^{(1)}(\omega) * \tilde{c}^{(2)}(\omega) - \tilde{n}^{(2)}(\omega) * \tilde{c}^{(1)}(\omega)\right) - \delta^2 K\left(\tilde{n}^{(1)}(\omega) * \tilde{n}^{(1)}(\omega) - \tilde{n}^{(2)}(\omega) * \tilde{n}^{(2)}(\omega)\right) \tag{B.16}$$

$$\omega\tilde{c}^{(1)}(\omega) - c^{(1)}(0) = \tilde{s}(\omega) - \mu\tilde{c}^{(1)}(\omega) - \delta\alpha\tilde{n}^{(1)}(\omega) * \tilde{c}^{(1)}(\omega) \tag{B.17}$$

$$\omega\tilde{c}^{(2)}(\omega) - c^{(2)}(0) = \tilde{s}(\omega) - \mu\tilde{c}^{(2)}(\omega) - \delta\alpha\tilde{n}^{(2)}(\omega) * \tilde{c}^{(2)}(\omega) \tag{B.18}$$

The symbol $*$ indicates the convolution of the functions in the complex plane defined as

$$\mathcal{L}\left[n^{(2)}(t)c^{(1)}(t)\right](\omega) = \tilde{n}^{(2)}(\omega) * \tilde{c}^{(1)}(\omega) = \frac{1}{2\pi i}\lim_{\gamma\to\infty}\int_{a-i\gamma}^{a+i\gamma} d\omega'\tilde{n}^{(2)}(\omega')\, c^{(1)}(\omega - \omega') \tag{B.19}$$

Equations B.15,B.16,B.17 and B.18 become respectively

$$\left(\omega + \beta + 2A_1\right)\tilde{n}^{(1)}(\omega) = n^{(1)}(0) + 2A_1\tilde{n}^{(2)}(\omega) + \delta\left\{\alpha\tilde{n}^{(1)}(\omega) * \tilde{c}^{(1)}(\omega) + \left(A_2 - A_3\right)\left(\tilde{n}^{(2)}(\omega) * \tilde{c}^{(2)}(\omega) + -\tilde{n}^{(1)}(\omega) * \tilde{c}^{(1)}(\omega)\right) + \left(A_2 + A_3\right)\left(\tilde{n}^{(2)}(\omega) * \tilde{c}^{(1)}(\omega) - \tilde{n}^{(1)}(\omega) * \tilde{c}^{(2)}(\omega)\right)\right\} - \delta^2 K\left(\tilde{n}^{(2)}(\omega) * \tilde{n}^{(2)}(\omega) - \tilde{n}^{(1)}(\omega) * \tilde{n}^{(1)}(\omega)\right) \tag{B.20}$$

$$\left(\omega + \beta + 2A_1\right)\tilde{n}^{(2)}(\omega) = n^{(2)}(0) + 2A_1\tilde{n}^{(1)}(\omega) + \delta\left\{\alpha\tilde{n}^{(2)}(\omega) * \tilde{c}^{(2)}(\omega) + \left(A_2 - A_3\right)\left(\tilde{n}^{(1)}(\omega) * \tilde{c}^{(1)}(\omega) + -\tilde{n}^{(2)}(\omega) * \tilde{c}^{(2)}(\omega)\right) + \left(A_2 + A_3\right)\left(\tilde{n}^{(1)}(\omega) * \tilde{c}^{(2)}(\omega) - \tilde{n}^{(2)}(\omega) * \tilde{c}^{(1)}(\omega)\right)\right\} - \delta^2 K\left(\tilde{n}^{(1)}(\omega) * \tilde{n}^{(1)}(\omega) - \tilde{n}^{(2)}(\omega) * \tilde{n}^{(2)}(\omega)\right) \tag{B.21}$$

$$\left(\omega + \mu\right)\tilde{c}^{(1)}(\omega) = c^{(1)}(0) + \tilde{s}(\omega) - \delta\alpha\tilde{n}^{(1)}(\omega) * \tilde{c}^{(1)}(\omega) \tag{B.22}$$

$$\left(\omega + \mu\right)\tilde{c}^{(2)}(\omega) = c^{(2)}(0) + \tilde{s}(\omega) - \delta\alpha\tilde{n}^{(2)}(\omega) * \tilde{c}^{(2)}(\omega) \tag{B.23}$$

We carry a perturbative approach out using δ as the expansion parameter to express $\tilde{n}^{(1)}(\omega)$ and $\tilde{c}^{(1)}(\omega)$ in terms of $\tilde{n}^{(2)}(\omega)$ and $\tilde{c}^{(2)}(\omega)$ up to second order in δ. We obtain the expressions (omitted here for brevity), which then are substituted into B.21. This effectively removes the dynamics of patch 1.

$$
\begin{aligned}
\omega\tilde{n}^{(2)}(\omega) - n_2(0) = &-\left(\beta + 2A_1 - \frac{4A_1^2}{\omega+\beta+2A_1}\right)\tilde{n}^{(2)}(\omega) + \delta\left\{\left(\alpha - A_2 + A_3 + \frac{2A_1\,(A_2+A_3)}{\omega+\beta+2A_1}\right)\tilde{n}^{(2)}(\omega) * \tilde{c}^{(2)}(\omega) + \right.\\
&+ \frac{2A_1\,(A_2+A_3)}{\omega+\beta+2A_1}\left(\frac{\tilde{s}(\omega)}{\omega+\mu}\right) * \tilde{n}^{(2)}(\omega) + \frac{4A_1^2\,(\alpha - A_2 + A_3)}{\omega+\beta+2A_1}\left(\frac{\tilde{n}^{(2)}(\omega)}{\omega+\beta+2A_1}\right) * \left(\frac{\tilde{s}(\omega)}{\omega+\mu}\right) +\\
&- \frac{4A_1^2\,(A_2+A_3)}{\omega+\beta+2A_1}\left(\frac{\tilde{n}^{(2)}(\omega)}{\omega+\beta+2A_1}\right) * \tilde{c}^{(2)}(\omega) + 2A_1\,(A_2+A_3)\,\tilde{c}^{(2)}(\omega) * \left(\frac{\tilde{n}^{(2)}(\omega)}{\omega+\beta+2A_1}\right) +\\
&\left.- (A_2+A_3)\,\tilde{n}^{(2)}(\omega) * \left(\frac{\tilde{s}(\omega)}{\omega+\mu}\right) + 2A_1\,(A_2 - A_3)\left(\frac{\tilde{s}(\omega)}{\omega+\mu}\right) * \left(\frac{\tilde{n}^{(2)}(\omega)}{\omega+\beta+2A_1}\right)\right\} +\\
&+ \delta^2\left\{\frac{8A_1^3\alpha\,(\alpha - A_2 + A_3)}{\omega+\beta+2A_1}\left[\left(\frac{\tilde{n}^{(2)}(\omega)}{\omega+\beta+2A_1}\right) * \left(\frac{\left(\frac{\tilde{n}^{(2)}(\omega)}{\omega+\beta+2A_1}\right) * \left(\frac{\tilde{s}(\omega)}{\omega+\mu}\right)}{\omega+\mu}\right)\right] +\right.\\
&- \frac{2A_1\,(A_2 - A_3)\,(A_2+A_3)}{\omega+\beta+2A_1}\left[\left(\frac{\tilde{n}^{(2)}(\omega) * \tilde{c}^{(2)}(\omega)}{\omega+\beta+2A_1}\right) * \tilde{c}^{(2)}(\omega)\right] +\\
&- \frac{4A_1^2\alpha\,(A_2+A_3)}{\omega+\beta+2A_1}\left[\left(\frac{\left(\frac{\tilde{s}(\omega)}{\omega+\mu}\right) * \left(\frac{\tilde{n}^{(2)}(\omega)}{\omega+\beta+2A_1}\right)}{\omega+\mu}\right) * \tilde{n}^{(2)}(\omega)\right] +\\
&+ \frac{4A_1^2\,(\alpha - A_2 + A_3)^2}{\omega+\beta+2A_1}\left[\left(\frac{\tilde{s}(\omega)}{\omega+\mu}\right) * \left(\frac{\left(\frac{\tilde{s}(\omega)}{\omega+\mu}\right) * \left(\frac{\tilde{n}^{(2)}(\omega)}{\omega+\beta+2A_1}\right)}{\omega+\beta+2A_1}\right)\right] +\\
&+ \frac{2A_1\,(A_2 - A_3)\,(\alpha - A_2 + A_3)}{\omega+\beta+2A_1}\left[\left(\frac{\tilde{s}(\omega)}{\omega+\mu}\right) * \left(\frac{\tilde{n}^{(2)}(\omega) * \tilde{c}^{(2)}(\omega)}{\omega+\beta+2A_1}\right)\right] +\\
&+ \frac{2A_1\,(A_2+A_3)\,(\alpha - A_2 + A_3)}{\omega+\beta+2A_1}\left[\left(\frac{\tilde{s}(\omega)}{\omega+\mu}\right) * \left(\frac{\tilde{n}^{(2)}(\omega) * \left(\frac{\tilde{s}(\omega)}{\omega+\mu}\right)}{\omega+\beta+2A_1}\right)\right] +\\
&- \frac{4A_1^2\,(A_2+A_3)\,(\alpha - A_2 + A_3)}{\omega+\beta+2A_1}\left[\left(\frac{\tilde{s}(\omega)}{\omega+\mu}\right) * \left(\frac{\tilde{c}^{(2)}(\omega) * \left(\frac{\tilde{n}^{(2)}(\omega) * \tilde{c}^{(2)}(\omega)}{\omega+\beta+2A_1}\right)}{\omega+\beta+2A_1}\right)\right] +\\
&- \frac{4A_1^2\,(A_2+A_3)\,(\alpha - A_2 + A_3)}{\omega+\beta+2A_1}\left[\tilde{c}^{(2)}(\omega) * \left(\frac{\left(\frac{\tilde{s}(\omega)}{\omega+\mu}\right) * \left(\frac{\tilde{n}^{(2)}(\omega) * \tilde{c}^{(2)}(\omega)}{\omega+\beta+2A_1}\right)}{\omega+\beta+2A_1}\right)\right] +\\
&- \frac{2A_1\,(A_2+A_3)^2}{\omega+\beta+2A_1}\left[\tilde{c}^{(2)}(\omega) * \left(\frac{\tilde{n}^{(2)}(\omega) * \left(\frac{\tilde{s}(\omega)}{\omega+\mu}\right)}{\omega+\beta+2A_1}\right)\right] +\\
&+ \frac{4A_1^2\,(A_2+A_3)^2}{\omega+\beta+2A_1}\left[\tilde{c}^{(2)}(\omega) * \left(\frac{\tilde{c}^{(2)}(\omega) * \left(\frac{\tilde{n}^{(2)}(\omega)}{\omega+\beta+2A_1}\right)}{\omega+\beta+2A_1}\right)\right] +\\
&+ 2A_1\alpha\,(A_2+A_3)\left[\tilde{n}^{(2)}(\omega) * \left(\frac{\left(\frac{\tilde{s}(\omega)}{\omega+\mu}\right) * \left(\frac{\tilde{n}^{(2)}(\omega)}{\omega+\beta+2A_1}\right)}{\omega+\mu}\right)\right] +\\
&+ 2A_1\,(A_2+A_3)\,(\alpha - A_2 + A_3)\left[\tilde{c}^{(2)}(\omega) * \left(\frac{\left(\frac{\tilde{s}(\omega)}{\omega+\mu}\right) * \left(\frac{\tilde{n}^{(2)}(\omega)}{\omega+\beta+2A_1}\right)}{\omega+\mu}\right)\right] +\\
&+ (A_2+A_3)\,(A_2 - A_3)\left[\tilde{c}^{(2)}(\omega) * \left(\frac{\tilde{n}^{(2)}(\omega) * \tilde{c}^{(2)}(\omega)}{\omega+\beta+2A_1}\right)\right] +
\end{aligned}
$$

$$
\begin{aligned}
&+ (A_2 + A_3)^2 \left[\tilde{c}^{(2)}(\omega) * \left(\frac{\tilde{n}^{(2)}(\omega) * \left(\frac{\tilde{s}(\omega)}{\omega+\mu} \right)}{\omega + \beta + 2A_1} \right) \right] + \\
&- 2A_1 (A_2 + A_3)^2 \left[\tilde{c}^{(2)}(\omega) * \left(\frac{\tilde{c}^{(2)}(\omega) * \left(\frac{\tilde{n}^{(2)}(\omega)}{\omega+\beta+2A_1} \right)}{\omega + \beta + 2A_1} \right) \right] + \\
&- 4A_1^2 \alpha (A_2 - A_3) \left[\left(\frac{\tilde{n}^{(2)}(\omega)}{\omega + \beta + 2A_1} \right) * \left(\frac{\left(\frac{\tilde{s}(\omega)}{\omega+\mu} \right) * \left(\frac{\tilde{n}^{(2)}(\omega)}{\omega+\beta+2A_1} \right)}{\omega + \mu} \right) \right] + \\
&+ 2A_1 (A_2 - A_3) (\alpha - A_2 + A_3) \left[\left(\frac{\tilde{s}(\omega)}{\omega + \mu} \right) * \left(\frac{\left(\frac{\tilde{s}(\omega)}{\omega+\mu} \right) * \left(\frac{\tilde{n}^{(2)}(\omega)}{\omega+\beta+2A_1} \right)}{\omega + \mu} \right) \right] + \\
&+ (A_2 - A_3)^2 \left[\left(\frac{\tilde{s}(\omega)}{\omega + \mu} \right) * \left(\frac{\tilde{n}^{(2)}(\omega) * \tilde{c}^{(2)}(\omega)}{\omega + \beta + 2A_1} \right) \right] + \\
&+ (A_2 - A_3) (A_2 + A_3) \left[\left(\frac{\tilde{s}(\omega)}{\omega + \mu} \right) * \left(\frac{\tilde{n}^{(2)}(\omega) * \left(\frac{\tilde{s}(\omega)}{\omega+\mu} \right)}{\omega + \beta + 2A_1} \right) \right] + \\
&- 2A_1 (A_2 - A_3) (A_2 + A_3) \left[\left(\frac{\tilde{s}(\omega)}{\omega + \mu} \right) * \left(\frac{\tilde{c}^{(2)}(\omega) * \left(\frac{\tilde{n}^{(2)}(\omega)}{\omega+\beta+2A_1} \right)}{\omega + \beta + 2A_1} \right) \right] + \\
&- K \left[\tilde{n}^{(2)}(\omega) * \tilde{n}^{(2)}(\omega) - 4A_1^2 \left(\frac{\tilde{n}^{(2)}(\omega)}{\omega + \beta + 2A_1} \right) * \left(\frac{\tilde{n}^{(2)}(\omega)}{\omega + \beta + 2A_1} \right) \right] \Bigg\} + O\left(\delta^3\right)
\end{aligned}
\tag{B.24}
$$

The inverse Laplace transform of $\tilde{n}^{(2)}(\omega)/(\omega + \omega_0)$, with $\beta + 2A_1 \equiv \omega_0 > 0$ can be calculated using the integration by parts when $t \gg \omega_0^{-1}$, because in the limit for infinite time, $\dot{n}^{(2)}$ and $\dot{c}^{(2)}$ are negligible.

$$
\begin{aligned}
\mathcal{L}^{-1} \left[\frac{\tilde{n}^{(2)}(\omega)}{\omega + \omega_0} \right](t) &= \int_0^t dt' n^{(2)}(t')\, e^{-\omega_0 (t-t')} \\
&= \frac{1}{\omega_0} \left(n^{(2)}(t) - n^{(2)}(0) e^{-t\omega_0} - \int_0^t dt' \dot{n}^{(2)}(t')\, e^{-\omega_0 (t-t')} \right) \\
&\approx \frac{n^{(2)}(t)}{\omega_0}
\end{aligned}
\tag{B.25}
$$

This reasoning can be iterated in all the elements containing $\dot{n}^{(2)}$ and $\dot{c}^{(2)}$ in Equation B.24. We introduce a parameter τ which multiplies the time derivatives in Equations B.9,B.10,B.11 and B.12. Consequently we get theEquation B.24 where all ω 's are multiplied by τ except for the ω which are the arguments of the functions $\tilde{n}^{(2)}(\omega), \tilde{c}^{(2)}(\omega)$ and $\tilde{s}(\omega)$. We define $\tilde{n}^{(2)}(\omega)$ as

$$
\tilde{n}'^{(2)}(\omega) \equiv \left[1 + \left(\frac{2A_1}{\beta + 2A_1} \right)^2 \right] \tilde{n}^{(2)}(\omega), \tag{B.26}
$$

For τ approaching zero, we obtain

$$
\tau \dot{n}'(t) = n'(t) (\alpha'[c(t)] c(t) - \beta') - \epsilon' n'^2(t)
$$

with

$$\beta' = \left(C_1 + \delta s C_2 + \delta^2 s^2 C_3\right)\left[1 + \left(\frac{2A_1}{\beta + 2A_1}\right)^2\right]^{-1} + O(\tau\delta) \tag{B.27}$$

$$\alpha'[c(t)] = \left(\delta C_4 + \delta^2 s C_5 + \delta^2 C_6 c(t)\right)\left[1 + \left(\frac{2A_1}{\beta + 2A_1}\right)^2\right]^{-1} + O(\tau\delta) \tag{B.28}$$

$$\epsilon' = \delta^2 \left(sC_7 + C_8\right)\left[1 + \left(\frac{2A_1}{\beta + 2A_1}\right)^2\right]^{-2} + O\left(\tau\delta^2\right) \tag{B.29}$$

where

$$C_1 = \beta\left(\frac{\beta + 4A_1}{\beta + 2A_1}\right) \tag{B.30}$$

$$C_2 = -\frac{1}{\mu}\left(\frac{4A_1A_2}{\beta + 2A_1} + \frac{4A_1^2\left(\alpha - A_2 + A_3\right)}{\left(\beta + 2A_1\right)} - \left(A_2 + A_3\right)\right) \tag{B.31}$$

$$C_3 = -\frac{1}{\mu^2\left(\beta + 2A_1\right)}\left(\frac{4A_1^2\left(\alpha - A_2 + A_3\right)^2}{\left(\beta + 2A_1\right)^2} + \frac{4A_1A_2\left(\alpha - A_2 + A_3\right)}{\beta + 2A_1} + A_2^2 - A_3^2\right) \tag{B.32}$$

$$C_4 = \left(\alpha - A_2 + A_3 + \frac{4A_1A_2}{\beta + 2A_1} - \frac{4A_1^2\left(A_2 + A_3\right)}{\left(\beta + 2A_1\right)^2}\right) \tag{B.33}$$

$$C_5 = \frac{2}{\mu\left(\beta + 2A_1\right)}\left(-\frac{4A_1^2\left(\alpha - A_2 + A_3\right)\left(A_2 + A_3\right)}{\left(\beta + 2A_1\right)^2} + A_2^2 + A_3^2 + \frac{2A_1A_2\left(\alpha - 2A_2\right)}{\beta + 2A_1}\right) \tag{B.34}$$

$$C_6 = \frac{1}{\beta + 2A_1}\left(-\frac{4A_1A_2\left(A_2 + A_3\right)}{\beta + 2A_1} + \frac{4A_1^2\left(A_2 + A_3\right)^2}{\left(\beta + 2A_1\right)^2} + A_2^2 - A_3^2\right) \tag{B.35}$$

$$C_7 = \frac{2A_1\alpha}{\mu^2\left(\beta + 2A_1\right)}\left(\frac{4A_1^2\left(\alpha - A_2 + A_3\right)}{\left(\beta + 2A_1\right)^2} + \frac{4A_1A_2}{\beta + 2A_1} - \left(A_2 + A_3\right)\right) \tag{B.36}$$

$$C_8 = K\left(1 - \frac{4A_1^2}{\left(\beta + 2A_1\right)^2}\right) \tag{B.37}$$

The coarse-graining procedure leads to the emergence of a carrying capacity term. This effect can be attributed to the "renormalization" of the growth term, which now takes the form of an expansion in both the resource concentration c and the resource supply s. Furthermore, the term ϵ' corresponds to the desired contribution that establishes the carrying capacity in the effective model. Thus, the coarse-graining process provides a mechanism for the emergence of carrying capacity in the system's dynamics, as described by Equations 3.11 and 3.12.

The above derivation can be reiterated considering several species metabolising one resource. Again for τ negligible, it is important to define

$$\tilde{n}'_\sigma(\omega) \equiv \left[1 + \left(\frac{2A_{1,\sigma}}{\beta_\sigma + 2A_{1,\sigma}}\right)^2\right]\tilde{n}_\sigma(\omega) \tag{B.38}$$

to obtain

$$\tau\dot{n}'_\sigma(t) = n'_\sigma(t)\left(\alpha'_\sigma[c(t)]c(t) - \beta'_\sigma\right) - \sum_\rho \epsilon'_{\sigma\rho} n'_\sigma(t) n'_\rho(t) \tag{B.39}$$

which now is defined through

$$\beta'_\sigma = \left(C_{1,\sigma} + \delta s C_{2,\sigma} + \delta^2 s^2 C_{3,\sigma}\right)\left[1 + \left(\frac{2A_{1,\sigma}}{\beta_\sigma + 2A_{1,\sigma}}\right)^2\right]^{-1} + O(\tau\delta) \tag{B.40}$$

$$\alpha'_\sigma[c(t)] = \left(\delta C_{4,\sigma} + \delta^2 s C_{5,\sigma} + \delta^2 C_{6,\sigma} c(t)\right)\left[1 + \left(\frac{2A_{1,\sigma}}{\beta_\sigma + 2A_{1,\sigma}}\right)^2\right]^{-1} + O(\tau\delta) \tag{B.41}$$

$$\epsilon'_{\sigma\rho} = \delta^2\left(s C_{7,\sigma\rho} + C_{8,\sigma\rho}\right)\left[1 + \left(\frac{2A_{1,\sigma}}{\beta_\sigma + 2A_{1,\sigma}}\right)^2\right]^{-1}\left[1 + \left(\frac{2A_{1,\rho}}{\beta_\rho + 2A_{1,\rho}}\right)^2\right]^{-1} + O\left(\tau\delta^2\right) \tag{B.42}$$

where the C terms are

$$C_{1,\sigma} = \beta_\sigma\left(\frac{\beta_\sigma + 4A_{1,\sigma}}{\beta_\sigma + 2A_{1,\sigma}}\right) \tag{B.43}$$

$$C_{2,\sigma} = -\frac{1}{\mu}\left(\frac{4A_{1,\sigma}A_{2,\sigma}}{\left(\beta_\sigma + 2A_{1,\sigma}\right)} + \frac{4A_{1,\sigma}^2\left(\alpha_\sigma - A_{2,\sigma} + A_{3,\sigma}\right)}{\left(\beta_\sigma + 2A_{1,\sigma}\right)^2} - \left(A_{2,\sigma} + A_{3,\sigma}\right)\right) \tag{B.44}$$

$$C_{3,\sigma} = -\frac{1}{\mu^2\left(\beta_\sigma + 2A_{1,\sigma}\right)}\left(\frac{4A_{1,\sigma}^2\left(\alpha_\sigma - A_{2,\sigma} + A_{3,\sigma}\right)^2}{\left(\beta_\sigma + 2A_{1,\sigma}\right)^2} + \frac{4A_{1,\sigma}A_{2,\sigma}\left(\alpha_\sigma - A_{2,\sigma} + A_{3,\sigma}\right)}{\beta_\sigma + 2A_{1,\sigma}} + A_{2,\sigma}^2 - A_{3,\sigma}^2\right) \tag{B.45}$$

$$C_{4,\sigma} = \left(\alpha_\sigma - A_{2,\sigma} + A_{3,\sigma} + \frac{4A_{1,\sigma}A_{2,\sigma}}{\beta_\sigma + 2A_{1,\sigma}} - \frac{4A_{1,\sigma}^2\left(A_{2,\sigma} + A_{3,\sigma}\right)}{\left(\beta_\sigma + 2A_{1,\sigma}\right)^2}\right) \tag{B.46}$$

$$C_{5,\sigma} = \frac{2}{\mu\left(\beta_\sigma + 2A_{1,\sigma}\right)}\left(-\frac{4A_{1,\sigma}^2\left(\alpha_\sigma - A_{2,\sigma} + A_{3,\sigma}\right)\left(A_{2,\sigma} + A_{3,\sigma}\right)}{\left(\beta_\sigma + 2A_{2,\sigma}\right)^2} + A_{2,\sigma}^2 + A_{3,\sigma}^2 + \frac{2A_{1,\sigma}A_{2,\sigma}\left(\alpha_\sigma - 2A_{2,\sigma}\right)}{\beta_\sigma + 2A_{1,\sigma}}\right) \tag{B.47}$$

$$C_{6,\sigma} = \frac{1}{\beta_\sigma + 2A_{1,\sigma}}\left(-\frac{4A_{1,\sigma}A_{2,\sigma}\left(A_{2,\sigma} + A_{3,\sigma}\right)}{\beta_\sigma + 2A_{1,\sigma}} + \frac{4A_{1,\sigma}^2\left(A_{2,\sigma} + A_{3,\sigma}\right)^2}{\left(\beta_\sigma + 2A_{1,\sigma}\right)^2} + A_{2,\sigma}^2 - A_{3,\sigma}^2\right) \tag{B.48}$$

$$C_{7,\sigma\rho} = \frac{2A_{1,\rho}\alpha_\rho}{\mu^2\left(\beta_\rho + 2A_{1,\rho}\right)}\left(\frac{4A_{1,\sigma}^2\left(\alpha_\sigma - A_{2,\sigma} + A_{3,\sigma}\right)}{\left(\beta_\sigma + 2A_{1,\sigma}\right)^2} + \frac{4A_{1,\sigma}A_{2,\sigma}\alpha_\sigma}{\beta_\sigma + 2A_{1,\sigma}} - \left(A_{2,\sigma} + A_{3,\sigma}\right)\right) \tag{B.49}$$

$$C_{8,\sigma\rho} = K_{\sigma\rho}\left(1 - \frac{2A_{1,\sigma}}{\beta_\sigma + 2A_{1,\sigma}}\right)\left(1 + \frac{2A_{1,\rho}}{\beta_\rho + 2A_{1,\rho}}\right) \tag{B.50}$$

The matrix $\epsilon'_{\sigma\rho}$ is defined by the sum of two matrices proportional to $C_{7,\sigma\rho}$ and $C_{8,\sigma\rho}$, as described in Equation B.42. These matrices usually are considered to be independent as referring to not connected spatial ecological mechanisms. This observation is consistent with the reasoning presented in [41] regarding random ecological systems. For these reasons we have always used the assumption that the elements of the matrix of the metabolic strategies α 's and the entries of the matrix ϵ are independent random variables.

BIBLIOGRAPHY

[1] R.A. ARMSTRONG, R. McGEHEE, *Competitive exclusion*, Am. Nat. 115, (1980), pp. 151.

[2] R. BAGCHI, T. SWINFIELD, R.E. GALLERY, O.T. LEWIS, S. GRIPENBERG, L. NARAYAN, R.P. FRECKLETON, *Testing the Janzen-Connell mechanism: Pathogens cause overcompensating density dependence in a tropical tree*, Ecol. Lett. 13, (2010), pp. 1262.

[3] R. BAGCHI, R.E. GALLERY, S. GRIPENBERG, S. J. GURR, L. NARAYAN, C.E. ADDIS, R.P. FRECKLETON, O.T. LEWIS, *Pathogens and insect herbivores drive rainforest plant diversity and composition*, Nature (London) 506, (2014), pp. 85.

[4] Q.K. BEG, A. VAZQUEZ, J. ERNST, M.A. DE MENEZES, Z. BAR-JOSEPH, A-L. BARABASI, et al, *Intracellular crowding defines the mode and sequence of substrate uptake by Escherichia coli and constrains its metabolic activity*, Proceedings of the National Academy of Sciences, (2007), pp. 104(31): 12663–12668.

[5] S. BOULINEAU, F. TOSTEVIN, D.J. KIVIET, P.R. TEN WOLDE, P. NGHE, S. J. TANS, *Single-Cell Dynamics Reveals Sustained Growth during Diauxic Shifts*, PLOS ONE, (2013), 8(4): 1–9.

[6] R.A. CAETANO, Y. ISPOLATOV, M. DOEBELI, *Evolution of diversity in metabolic strategies*, bioRxiv 2020–10, (2021).

[7] P. CERMENO, I.G. TEIXEIRA, M. BRANCO F.G. FIGUEIRAS, E. MARANON, *Sampling the limits of species richness in marine phytoplankton communities*, Journal of Plankton Research, 36 (2014), pp. 1135–1139.

[8] P. CHESSON, *Macarthur's consumer-resource model*, Theor. Popul. Biol. 37, (1990), pp. 26.

[9] P. CHESSON, *Mechanisms of maintenance of species diversity*, Annu. Rev. Ecol. Syst. 31, (2000), pp. 343.

[10] D.A. CLARK, D.B. CLARK, *Spacing dynamics of a tropical rain forest tree: Evaluation of the Janzen-Connell model*, Am. Nat. 124, (1984), pp. 769.

[11] P. COLET, R. TORAL, *Stochastic Numerical Methods*, Wiley-VCH, (2016).

[12] J.H. CONNELL, *On the role of natural enemies in preventing competitive exclusion in some marine animals and in rain forest trees*, in Dynamics of Populations, edited by P. J. Den Boer and G. Gradwell, PUDOC, Wageningen, (1971).

[13] L. FANT, I. MACOCCO, J. GRILLI, *Eco-evolutionary dynamics lead to functionally robust and redundant communities*, bioRxiv, (2021).

[14] L. GARCÍA-BAYONA, L.E. COMSTOCK, *Bacterial antagonism in host-associated microbial communities*, Science, (2018), pp. 361(6408).

[15] S.E. GEORGE, C.J. COSTENBADER, T. MELTON, *Diauxic Growth in Azotobacter Vinelandii*, Journal of Bacteriology, (1985), pp. 164(2):866–871.

[16] A. GIOMETTO, D.R. NELSON, A.W. MURRAY, *Antagonism between killer yeast strains as an experimental model for biological nucleation dynamics*, bioRxiv, (2020).

[17] R. GONCALVES, *Bacterial Growth in the Presence of Several Resources*, Instituto Gulbenkian de Ciencia de Lisboa, (2019).

[18] E.T. GRANATO, T.A. MEILLER-LEGRAND, K.R. FOSTER, *The evolution and ecology of bacterial warfare*, Current biology, (2019), pp. 29.

[19] A. GIOMETTO, F. ALTERMATT, F. CARRARA, A. MARITAN, A. RINALDO, *Scaling body size fluctuations*, Proceedings of the National Academy of Sciences of the United States of America, (2013).

[20] D. GUPTA, S. GARLASCHI, S. SUWEIS, S. AZAELE, A. MARITAN, *Effective Resource Competition Model for Species Coexistence*, Physical Review Letter 127, 208101 (2021).

[21] G. HARDIN, *The competitive exclusion principle*. Science 131, (1960), pp. 1292.

[22] P. HÄUNGGI, P. JUNG, *Colored Noise in Dynamical Systems*, Advances in Chemical Physics, Volume LXXXIX, Edited by I. Prigogine and Stuart A.Rice (1994).

[23] A. HENING, D.H. NGUYEN, *The competitive exclusion principle in stochastic environments*, J. Math. Biol. 80, (2020), pp. 1323.

[24] J. HOFB AUER, K. SIGMUND, *Evolutionary Games and Population Dynamics*, Cambridge University Press, (1998).

[25] J. HUISMAN, F. J. WEISSING, *Biodiversity of plankton by species oscillations and chaos*. Nature (London) 402, (1999), pp. 407.

[26] G.E. HUTCHINSON, *Homage to Santa Rosalia or Why Are There So Many Kinds of Animals?*, The American Naturalist, Vol. 93, No. 870, (1959).

[27] G.E. HUTCHINSON, *The paradox of the plankton*. Am. Nat. 95, (1961), pp. 137.

[28] E.F. KELLER, L.A. SEGEL, *Model for chemotaxis*, J. Theor.Biol. 30, (1971), pp. 225.

[29] D.S. KOMPALA, D. RAMKRISHNA, N.B. JANSEN, G.T. TSAO, *Investigation of bacterial growth on mixed substrates: Experimental evaluation of cybernetic models*, Biotechnology and Bioengineering, (1986), pp. 28 (7):1044–1055.

[30] D.H. JANZEN, *Herbivores and the number of tree species in tropical forests*. Am. Nat. 104, (1970), pp. 501.

[31] F.A. LABRA, P.A. MARQUET, F. BOZINOVIC, *Scaling metabolic rate fluctuations*, Proceedings of the National Academy of Sciences of the United States of America, (2007), 104(26):10900–10903.

[32] I.H. LEE, A.G. FREDRICKSON, H.M. TSUCHIYA, *Diauxic Growth of Propionibacterium shermanii*, Applied Microbiology, (1974), pp. 28(5):831–835.

[33] R.E. LENSKI, M.R. ROSE, S.C. SIMPSON, S.C. TADLER, *Long-Term Experimental Evolution in Escherichia coli. I. Adaptation and Divergence During 2,000 Generations*, The American Naturalist, (1991), pp. 138(6):1315–1341.

[34] E. LITCHMAN, C.A. KLAUSMEIER, *Trait-Based Community Ecology of Phytoplankton*, Annual Review of Ecology, Evolution, and Systematics, 39 (2008), pp. 615–639.

[35] E. LITCHMAN, C.A. KLAUSMEIER, *Annu. Rev. Ecol. Evol.Syst.* 39, (2008), pp. 615.

[36] W.F. LOOMIS, B. MAGASANIK, *Glucose-lactose diauxie in Escherichia coli*, Journal of Bacteriology, (1967), pp. 93(4):1397–1401.

[37] R. LIU, G. LIU *Complex dynamics of a stochastic uni-directional consumer-resource mutualism system* Ecological Complexity Volume 48, (2021), 100965.

[38] R. MACARTHUR, *Species packing, and what competition minimizes*. Proc. Natl. Acad. Sci. U.S.A. 64, (1969), pp. 1369.

[39] R. MACARTHUR, R. LEVINS, *Competition, habitat selection, and character displacement in a patchy environment*. Proc. Natl. Acad. Sci. U.S.A. 51, (1964), pp. 1207.

[40] R. MACARTHUR, E. WILSON, *The theory of island biogeography*, Princeton University Press, Princeton, (1967).

[41] R.M. MAY, *Will a large complex system be stable?* Nature, (1972), pp. 238(5346).

[42] J. MONOD, *Recherches sur la croissance des cultures bactériennes*, Hermann Cie, Paris (1942).

[43] J. MONOD, *The growth of bacterial cultures*. Annual Review of Microbiology, (1949), pp. 3(1):371–394.

[44] A.M. NEW, B. CERULUS, S.K. GOVERS, G. PEREZ-SAMPER, B. ZHU, S. BOOGMANS, et al, *Different Levels of Cataolite Repression Optimize Growth in Stable and Variable Environments*. PLOS Biology, (2014), pp. 12(1):1–22.

[45] H.A. ORR, *Fitness and its role in evolutionary genetics*. Nature Review Genetics, (2009), pp. 10:531–539.

[46] L. PACCIANI-MORI, A. GIOMETTO, S. SUWEIS, A. MARITAN, *Dynamic metabolic adaptation can promote species coexistence in competitive microbial communities*, PLoS Comput. Biol. 16, (2020).

[47] L. PACCIANI-MORI,S. SUWEIS, A. MARITAN, A. GIOMETTO, *Constrained proteome allocation affects coexistence in models of competitive microbial communities*, The ISME Journal volume 15, (2021), pp. 1458–1477.

[48] A. POSFAI, T. TAILLEFUMIER, N.S. WINGREEN, *Metabolic Trade-Offs Promote Diversity in a Model Ecosystem*. Phys. Rev. Lett. 118, (2017), pp. 028103.

[49] S. ROY, J. CHATTOPADHYAY, *The stability of ecosystems: A brief overview of the paradox of enrichment*. J. Biosci. 32, (2007), pp. 421.

[50] E.W. SCHUPP, *The Janzen-Connell model for tropical tree diversity: Population implications and the importance of spatial scale*. Am. Nat. 140, (1992), pp. 526.

[51] S. SHALEV-SHWARTZ, S. BEN-DAVID, *Understanding Machine Learning from Theory to Algorithms*, Cambridge University Press, (2014).

[52] N. SHORESH, M. HEGRENESS, R. KISHONY, *Proc. Natl. Acad. Sci. U.S.A.* 105, (2008), pp. 12365.

[53] H.L. SMITH, P. WALTMAN, *The Theory of the Chemostat: Dynamics of Microbial Competition*, Cambridge University Press, Cambridge, (1995), Vol. 13.

[54] A. SOLOPOVA, J. VAN GESTEL, F.J. WEISSING, H. BACHMANN, B. TEUSINK, J. KOK, et al, *Bet-hedging during bacterial diauxic shift*. Proceedings of the National Academy of Sciences, (2014), pp. 111(20):7427–743.

[55] D. TILMAN *Resource Competition and Community Structure*, Monographs in Population Biology, 17,Princeton University Press, (1982).

[56] P. TURCHIN, *Complex Population Dynamics: A Theoretical/Empirical Synthesis*, Series: MPB-35 Monographs in Population Biology, Princeton University Pres, (2003).

[57] G.E. UHLENBECK, L. S. ORNSTEIN, *On the theory of the Brownian Motion*. Phys. Rev. 36, (1930), pp. 823.

[58] T.L.S. VINCENT, D. SCHEEL, J. S. BROWN, T. L. VINCENT, *Trade-offs and coexistence in consumer-resource models: It all depends on what and where you eat.* Am. Nat. 148, (1996), pp. 1038.

[59] S. ZAOLI, A. GIOMETTO, E. MARAÑÓN, S. ESCRIG, A. MEIBOM, A. AHLUWALIA, et al, *Generalized size scaling of metabolic rates based on single-cell measurements with freshwater phytoplankton.* Proceedings of the National Academy of Sciences of the United States of America, (2019), pp. 116(35):17323–17329.

[60] Statistical Mechanics of Complex Systems Course Notes of Prof. Maritan, University of Padova, (2021).

[61] Qualitative Life Science Course Notes of Prof. Suweis, University of Padova, (2021).